

Yajie Ruan

**Interference Cancellation Techniques
for Multiple-Line Transmission
in Modern DSL Systems**



Cuvillier Verlag Göttingen
Internationaler wissenschaftlicher Fachverlag



Interference Cancellation Techniques for Multiple-Line Transmission in Modern DSL Systems





Interference Cancellation Techniques for Multiple-Line Transmission in Modern DSL Systems

Vom Promotionsausschuss der
Technischen Universität Hamburg-Harburg
zur Erlangung des akademischen Grades
Doktor-Ingenieurin (Dr.-Ing.)
genehmigte Dissertation

von
Yajie Ruan

aus
Nanjing, China

2014



Bibliografische Information der Deutschen Nationalbibliothek

Die Deutsche Nationalbibliothek verzeichnet diese Publikation in der Deutschen Nationalbibliografie; detaillierte bibliografische Daten sind im Internet über <http://dnb.d-nb.de> abrufbar.

1. Aufl. - Göttingen : Cuvillier, 2014

Zugl.: (TU) Hamburg-Harburg, Univ., Diss., 2014

978-3-95404-621-8

1. Gutachter:	Prof. Dr. Hermann Rohling
2. Gutachter:	Prof. Dr.-Ing. Andreas Czylwik
Tag der mündlichen Prüfung:	09. Januar 2014

© CUVILLIER VERLAG, Göttingen 2014

Nonnenstieg 8, 37075 Göttingen

Telefon: 0551-54724-0

Telefax: 0551-54724-21

www.cuvillier.de

Alle Rechte vorbehalten. Ohne ausdrückliche Genehmigung des Verlages ist es nicht gestattet, das Buch oder Teile daraus auf fotomechanischem Weg (Fotokopie, Mikrokopie) zu vervielfältigen.

1. Auflage, 2014

Gedruckt auf umweltfreundlichem, säurefreiem Papier aus nachhaltiger Forstwirtschaft.

978-3-95404-621-8



Acknowledgements

This thesis was developed during my time as a scientific staff at the Institute of Telecommunications, Hamburg University of Technology, Germany.

Foremost, I would like to express my gratitude to my advisor Prof. Dr. Hermann Rohling for his guidance, support and encouragement throughout the past years. His door was always open for interesting discussions, scientific as well as private. I feel so fortunate to have learned from him and to have worked with him.

Furthermore, I would like to thank Prof. Dr.-Ing. Andreas Czylik from University of Duisburg-Essen for his interest in my work and for review of my thesis, and Prof. Dr. Ernst Brinkmeyer for being the head of the examination committee.

I am also grateful to all my former colleagues at the Institute of Telecommunications. They generated an inspiring and enjoyable environment with many interesting scientific discussions and non-scientific activities inside and outside the campus. In particular, I thank PD Dr.-Ing. habil. Rainer Grünheid sincerely for all fruitful discussions and comments to this thesis, and for all kinds of support to me in the past years. Special thanks also go to Monique Düngen for her collaborative work and for her friendship.

Ultimately, I would like to dedicate this thesis to my husband for his love, support and encouragement during all these years, and to our daughter Mia Yuwen Zhu. Moreover, I am deeply grateful to my parents for their everlasting care and support.

Munich, January 2014

Yajie Ruan





Contents

1	Introduction	1
2	DSL Channel	4
2.1	Physical characteristics of copper lines	4
2.2	Electrical characteristics of a single twisted cable pair	5
2.2.1	Classic direct channel model and measured channels	6
2.3	Crosstalk interference in a twisted pair cable binder	8
2.3.1	Classic crosstalk model and measured crosstalk	9
2.4	Deterministic MIMO model for cable binders	10
2.5	Stochastic MIMO model for cable binders	11
3	Discrete Multi-Tone (DMT)	14
3.1	DMT technique	15
3.2	System structure	17
3.3	Channel capacity for a single cable line	18
4	Multiple-Line DMT	20
4.1	Transceiver structure	21
4.2	Signal model	22
5	Crosstalk Cancellation	25
5.1	Upstream crosstalk cancellation	26
5.1.1	QR-based decision feedback cancellation	27
5.1.2	Zero-forcing based cancellation	29
5.2	Downstream crosstalk cancellation	31
5.3	System performance with perfect CSI	34
5.3.1	Simulation results in US transmission	36
5.3.2	Simulation results in DS transmission	41
6	Channel Estimation	47
6.1	Introduction	47
6.2	Pilot based channel measurement	49
6.3	Step-by-step technique with a single pilot symbol	51
6.4	Techniques to improve the estimation accuracy	52



6.5	System performance with estimated CSI	54
6.5.1	Simulation results in US transmission	54
6.5.2	Simulation results in DS transmission	56
7	Crosstalk Cancellation with Complexity Reduction	58
7.1	Partial crosstalk cancellation	59
7.1.1	Upstream partial crosstalk cancellation	59
7.1.2	Downstream partial crosstalk cancellation	62
7.1.3	Crosstalk interference selection in the partial crosstalk cancellation schemes	64
7.2	System performance with partial crosstalk cancellation	66
7.2.1	Simulation results in the cable binders with equal length cables	66
7.2.2	Simulation results in in the cable binders with different length cables	68
8	QoS-aware Crosstalk Cancellation	75
8.1	QoS-based partial crosstalk cancellation	76
8.2	System performance with QoS-based partial crosstalk cancellation	79
8.3	Crosstalk Cancellation Facing Dynamic Situations	83
8.3.1	Successive cancellation for the dynamic scenario	84
8.3.2	System performance in the dynamic scenario	89
9	Power Allocation for Crosstalk Cancellation	93
9.1	State of the art	93
9.1.1	Water-filling (WF) and iterative water-filling (IWF)	93
9.1.2	Optimal spectrum balancing (OSB)	96
9.2	Sequential power allocation (SPA)	98
9.3	System performance with sequential power allocation	101
10	Summary	108
	Bibliography	110



1 Introduction

Ever since the invention of the first telephone by Phillip Reis in 1861, the twisted-pair copper wiring exists worldwide as part of gradually constructed infrastructure to support speech communications with an extremely large coverage. Developed over a century, the expanding network contains several hundred million copper telephone loop plants.

Indeed, such huge resource can be used not only for voice communications but also for today's digital communications and transmission technique with extremely high data rates. Therefore, the technology which can enable broadband digital communications over the existing telephone infrastructure is urged. Digital subscriber line (DSL) technology was developed to provide digital data transmission as well as telephony since the late 1980s [SCS99] [SSCS03]. In the past three decades consumer-oriented Asymmetric DSL (ADSL) as well as High speed DSL such as high bit rate DSL (HDSL), Symmetric DSL (SDSL) and Very high speed DSL (VDSL) were designed and operated in the market.

Nowadays, driven by the new applications such as the triple play of voice, data and video, consumers start to require fiber-fast broadband capacity and additionally high reliable transmission. Unfortunately, extending fiber to every home is still economically infeasible. Modern DSL systems such as VDSL2 systems are expected to be the last mile between the customer premise equipments (CPE) and the fiber-network core, and to enable the transmission with higher data rate and better quality of service (QoS).

Accordingly, modern DSL systems require those transmission techniques using larger frequency bands. Unfortunately, using larger frequency bands naturally leads to the problem of high crosstalk interference among copper lines which are originally designed for the purpose of speech communications. As the dominant impairment of DSL systems, crosstalk interference is typically 10 - 15 dB larger than background noise [GDJ06]. Therefore, crosstalk interference is the major issue need to be considered in modern DSL systems. Furthermore, the preferred transmission techniques should also have higher bandwidth efficiency and more flexibility and adaptivity to deal with various users and transmission scenarios.

In reply to those challenges, some technical solutions have been provided by researches.

CHAPTER 1. INTRODUCTION

In particular, Multiple-Input-Multiple-Output (MIMO) technology has been studied for years. Normally, MIMO systems refer to multiple antenna systems in wireless communication systems where similar challenges exist. Due to the high capacities and the potential to dramatically improve the data transmission reliability, MIMO technology is highly recommended in wireless communication systems [TV05]. Generally, a MIMO system can be regarded as a system having multiple transmitters and receivers. In this respect, we can also apply the MIMO technology of multiple antenna systems into multiple copier line systems to deal with crosstalk interference. In other words, MIMO technology can be adopted for crosstalk cancellation in DSL systems where a plurality of copier lines are bundled together.

Typically, there is a central office (CO) of a DSL system being connected to the core of the fiber network via fiber. As shown in Figure 1.1, copper lines provide the further connection between the CO and the CPEs. From the user's perspective, the upstream (US) transmission is defined as the transmission from CPEs towards the CO. Conversely, the downstream (DS) transmission is from the CO to CPEs. A plurality of transceivers can be co-located in the CO while different CPEs are distributively located according to the users. Such deployments ensure that MIMO applications are feasible.

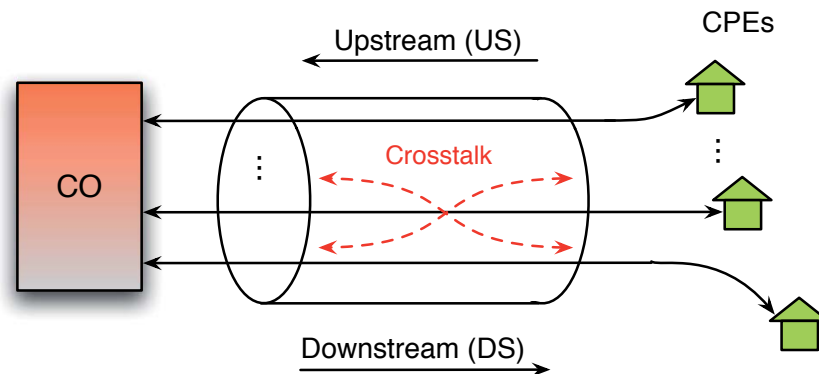


Figure 1.1: Transmission with co-located transceiver in CO

For many years, Discrete Multi-Tone (DMT) technique has been applied in DSL systems. In a single copper line, the DSL channel has very long transmission taps and is highly frequency selective. DMT technique, also known as Orthogonal Frequency Division Multiplexing (OFDM) technique [Roh11] in wireless communications can effectively partition a frequency selective channel into a large number of independent narrowband subchannels. By this means, high frequency selectivity over the complete channel band is converted into individual complex fading factors for each subchannel. With a sufficient long cyclic prefix inserted in each symbol, intersymbol interference (ISI) due to long transmission taps can be avoided. Meanwhile, adaptive modulation technique can be applied as

each subchannel can be modulated individually according to the quality of the subchannel or possibly also to the transmission scenarios.

Furthermore, DMT/OFDM technique can be efficiently combined with MIMO techniques. The combination is natural and beneficial since DMT/OFDM technique dramatically simplifies the equalization procedures in MIMO systems, thereby supporting more transmitters and wider bandwidths in the combined systems.

Within the above-described context, this thesis is to analyze the crosstalk interference in modern DSL systems and focuses on the topic of crosstalk interference cancellation techniques. MIMO-OFDM transmission techniques are applied for crosstalk interference cancellation. The computation complexity of interference cancellation techniques is investigated for providing a reasonable trade-off in the systems. Moreover, QoS requirements of different users or lines are considered in the systems. Besides the interference cancellation techniques, power allocation for crosstalk cancellation is further studied.

Chapter 2 describes the physical as well as electrical characteristics of copper lines and the modeling for system simulations are introduced. In Chapter 3, the fundamentals of DMT transmission technique are discussed. In view of MIMO technology, the concrete system structures and models are given in Chapter 4.

After that, crosstalk interference cancellation techniques for both upstream transmission and downstream transmission are presented in Chapter 5 and the channel estimation (CE) aspects are considered in Chapter 6. The performance of the crosstalk interference cancellation techniques with and without perfect channel state information (CSI) is given in chapters 5 and 6, respectively. In Chapter 7, partial crosstalk cancellation with computation complexity reduction is proposed and the corresponding system performance is analyzed.

Faced with high QoS demands driven by those new applications, crosstalk cancellation techniques being aware of QoS requirements of different users are presented in Chapter 8. In particular, the crosstalk cancellation technique facing dynamic situations occurring in the systems is proposed.

In Chapter 9, power allocation for crosstalk interference cancellation is introduced. A heuristic method of distributing the transmit power of individual lines and its combination with partial crosstalk cancellation techniques are given, and the corresponding performance is provided.

In the end, summary is made in Chapter 10.

2 DSL Channel

Backing to the original invention of telephone in 1879, copper lines have served for more than one century as transmission lines between transmitters and receivers. The DSL channel itself is very old and not much changed; however, a system design is confined by the property of the channel. The designer shall be aware of the channel characteristics. In this chapter, physical as well as electrical characteristics of telephone loops are described, then the crosstalk interference issue is addressed and the channel model considering crosstalk interference is given.

2.1 Physical characteristics of copper lines

The quality of the early approach of telephony was very poor since only a single conducting wire with the ground acting as the return path was used as the transmission line. The situation was dramatically improved by using a second conductor for differential mode signaling instead of the common mode. Meanwhile, within a cable the two wires of each pair are twisted around each other to form an unshielded twisted pair (UTP). Each pair is insulated by plastic material in distinctive color. To isolate the cable pairs from outside sources of electronic interference they are surrounded with a metallic shield.

In a cable with 25 twisted pairs or less, the pairs are usually enclosed in bindings of a certain color and forming a cylindrical shape. For larger cables, units of 25 pairs or super-units of 50 or 100 pairs are assembled to form a substantially cylindrical shape [GDJ06]. Each unit binder or super-unit binder are color coded such that each 25 pair group can be identified from the others. In this thesis, we focus our research on the cable scare within one or two units. A cable with a certain number of twisted pairs is referred to as a *cable binder*.

In the following, we first consider a single cable situation and describe the general electrical characteristics of twisted cable pairs in Section 2.2. Then, a cable binder situation is considered in sections 2.3 - 2.5 where crosstalk interference among the cable binder dominates the system performance degradation.

2.2 Electrical characteristics of a single twisted cable pair

As transmission lines, the twisted cable pairs have the electrical characteristics which can be derived from the classic transmission line theory [Dwo79]. One can consider an infinitely small portion of uniform line dx as depicted in Figure 2.1. The circuit is made of the concatenation of a series impedance and a shunt impedance. Without the loss of generality, the series impedance is made of a resistance Rdx and an inductance Ldx ; the shunt impedance is made of a conductance Gdx and a capacitance Cdx . The parameters R , L , G , and C are the so-called *primary parameters* and cited per unit length. So they are usually frequency dependent but assumed to be independent of length. The RLGC-parameters characterize the behavior of the transmission line. The *propagation constant* γ and *characteristic impedance* Z_0 of the transmission line are defined as

$$\gamma = \sqrt{(R + j2\pi fL)(G + j2\pi fC)}, \quad (2.1)$$

$$Z_0 = \sqrt{\frac{R + j2\pi fL}{G + j2\pi fC}}. \quad (2.2)$$

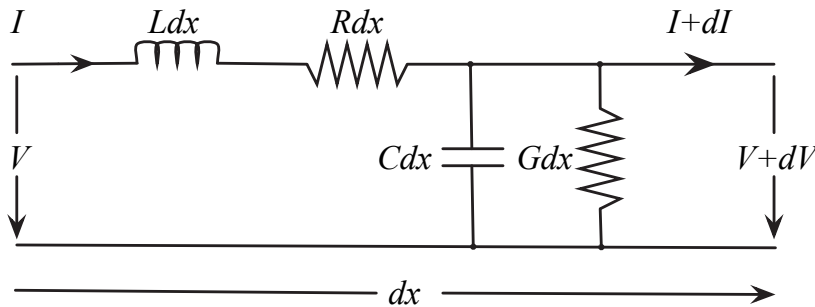


Figure 2.1: Line section of length dx with primary parameters

Now considering a line of length l connected with a voltage source V_S with the impedance Z_S and terminated with a load impedance Z_L as described in Figure 2.2, the cable line can be modeled as a two-port network with $ABCD$ parameters. If the load impedance Z_L matches the characteristic impedance Z_0 , *i.e.*, $Z_L = Z_0$, the *transfer function* between V_L and V_S at frequency f becomes

$$H(f, l) = \frac{V_L}{V_S} = \frac{1}{2} e^{-l\gamma(f)}. \quad (2.3)$$

For practical reasons, it is often more relevant to use the concept of insertion loss instead of the transfer function. From a measurement perspective, it's very difficult to access V_S

due to internal loading of the source. So telecommunication engineers use the ratio between the voltage over the load V_L , with the wireline inserted between the source and load, and the voltage over the load when it is connected directly to the source without the wireline in between. In many cases it is actually the insertion loss that is referred to as the transfer function.

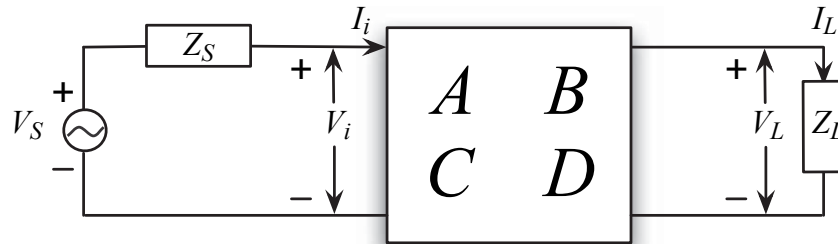


Figure 2.2: Uniform line of length l modeled as a two-port network

2.2.1 Classic direct channel model and measured channels

As described above, for a single transmission line the direct transmission channel can be considered as a Linear Time-Invariant (LTI) system characterized by its impulse response $h(t)$ and the corresponding channel transfer function $H(f)$. From equation (2.3) it can be seen that the channel transfer function $H(f)$ of a twisted pair depends on the length l of the wire and the propagation constant γ . Indeed, the frequency dependent propagation constant $\gamma(f)$ is a very accurate (± 0.2 dB) predictor of the attenuation at frequencies above about 20 kHz [Bin00].

The propagation constant is also called the complex propagation constant and can be written as

$$\gamma = \alpha + j\beta, \quad (2.4)$$

where the real part α is the so-called attenuation constant and the imaginary part β is the phase constant. The attenuation constant is often measured in nepers per meter and a neper is approximately 8.7 dB. It can be obtained by RLGC-parameters, as shown in equation (2.1).

2.2. ELECTRICAL CHARACTERISTICS OF A SINGLE TWISTED CABLE PAIR

Massive measurements have been done to accurately model the RLGC-parameters of copper cables. One of the empirical models is defined as

$$\begin{aligned}
 R(f) &= (r_{0c}^4 + a_c f^2)^{1/4} \\
 L(f) &= (l_0 + l_\infty (f/f_m)^b) / (1 + (f/f_m)^b) \\
 C(f) &= c_\infty + c_0 f^{-c_e} \\
 G(f) &= g_0 f^{g_e},
 \end{aligned}$$

where r_{0c} , a_c , l_0 , l_∞ , f_m , b , c_∞ , g_0 , and g_e are line constants and depend on the cable diameter, materials and construction. For the cables employed in different countries or regions, the values are different and some parameter sets are provided in the standard specification [vdB98]. Table 2.1 lists the line constants for three widely used cable types specified by American National Standards Institute (ANSI) and European Telecommunications Standards Institute (ETSI). For the performance evaluation in this thesis, line constants for British DWUG (drop wire for underground distribution) cables are chosen.

Table 2.1: Line constants for ANSI and ETSI standard cables

Standard cable type	ANSI		ETSI
	TP1	TP2	BT _{DWUG}
diameter (mm)	0.4	0.5	0.5
r_{0c} (Ω / km)	286.17578	174.55888	179
a_c	0.1476962	0.053073481	0.03589
l_0 (μ H/km)	675.36888	617.29539	695
l_∞ (μ H/km)	488.95186	478.97099	585
b	0.92930728	1.1529766	1.2
f_m (kHz)	806.33863	553.760	1000
c_∞ (nF/km)	49	50	55
c_0 (nF/km)	0.0	0.0	1.0
c_e	0.0	0.0	0.1
g_0 (nS/km)	43	0.00023487476	0.5
g_e	0.70	1.38	1.033

In Figure 2.3, the measured direct channel transfer function for a 1 km cable line is shown and the direct channel transfer function obtained by the corresponding empirical model is also plotted. The measurement data are provided by Forschungszentrum Telekommunikation Wien (FTW) [Nor03] and the cable diameter is 0.4 mm (type F-02YHJA2Y). It can be seen that the empirical model fits quite well with the real measurement for a single twisted cable pair.

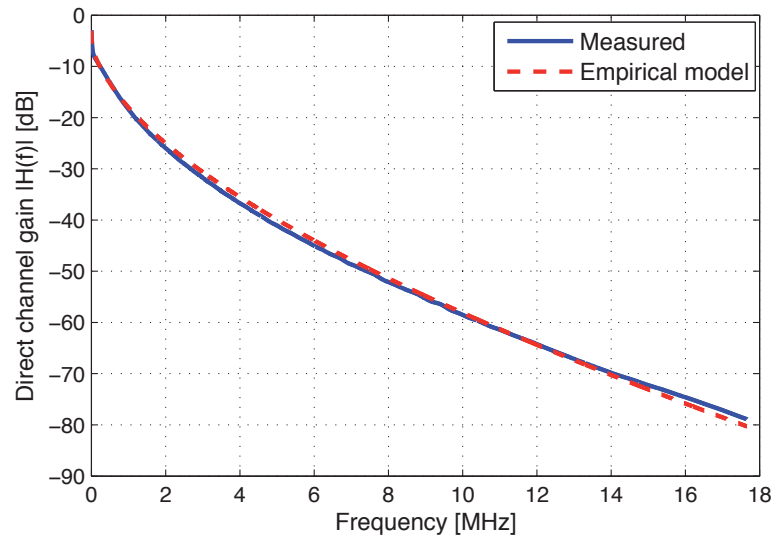


Figure 2.3: Direct channel transfer functions for a 1 km cable line with diameter 0.4 mm

2.3 Crosstalk interference in a twisted pair cable binder

From this section, a telephone loop transmission system which contains multiple cables in a cable binder is considered, for example, shown in Figure 1.1. Indeed, such system faces a variety of impairments. In general, they can be classified as extrinsic or intrinsic to the cable environment [CKB⁺99]. The extrinsic impairments are rather unpredictable and geographically variable, for example, the impulse noise originating from rapid voltage changes and radio frequency interference (RFI) from broadcasting and radio transmitters. The intrinsic impairments are typically the thermal noise, echoes and reflections, crosstalk interference and so on. By far, crosstalk interference contributes the most significant performance degradation in DSL systems. Therefore, in the scope of this thesis, we mainly consider this dominant impairment.

Crosstalk is the leakage into one channel of signal power from another channel. In the subscriber-line systems, crosstalk is caused by capacitive and inductive coupling between the twisted cable pairs within a cable binder. Therefore, crosstalk is strongly related to the construction of a cable binder. In most cases, it is worst among adjacent pairs. For any two twisted cable pairs inside a binder, the crosstalk coupling does not usually change appreciably over time, and it is symmetrical in that the same coupling function can be observed between two ends when measured in either direction. In this thesis, we focus only on the so-called far-end crosstalk (FEXT) which is the crosstalk coupling between transmitters and receivers at the opposite ends of a binder, as shown in Figure 1.1.

2.3.1 Classic crosstalk model and measured crosstalk

The characteristics of FEXT can be derived from transmission line theory [Bin00] and the crosstalk models in common use are empirically based. The early research based on cable measurements has found out that FEXT has an f^2 power law in frequency and is proportional to cable length; it also suffers the same attenuation as signals in the cable.

It is very common to use “99% worst case crosstalk models”, which are constructed such that in 99% of cases the crosstalk is less severe than that predicted by the models. Specifically, the worst-case FEXT coupling in a equal-length cable binder is given by

$$\left| H_{FEXT}(f, L, N) \right|^2 = N^{0.6} K_{FEXT} f^2 L \left| H(f, L) \right|^2, \quad (2.5)$$

where L here denotes the cable length, N is the number of the disturbing lines in the cable binder, f is the frequency, $K_{FEXT} = 10^{-19.5}$ is a constant for European cables and $H(f, L)$ is the transfer function of the disturbed lines [GDJ06].

It can be seen in equation (2.5) that the crosstalk interference increases with the number of disturbing lines N . The mean power coupling must also increase and be proportional to N . However, the model does not represent the mean value but rather a near worst case bound. When the number of disturbers increases, some disturbers are located far from the victim loop so that they generate less crosstalk. Therefore, the model provides a less than linear increment of the bound as the number of disturber increases. The exponent term of the disturber number N reflects this fact.

Equation (2.5) provides the 99% worst case crosstalk models for equal-length cable binders. In reality, the transmitters and/or the receivers of individual cable lines are often not co-located as shown in Figure 2.4. The empirical crosstalk model between a transmitter TX_j and receiver RX_i is specified by the standard [ETS03]:

$$H_{ij}(f) = \delta_{ij} \left(f, L_{ij}^{\text{coupling}} \right) \left| H(f, L_{ij}) \right|, \quad (2.6)$$

where the crosstalk coupling coefficient is

$$\delta_{ij} \left(f, L_{ij}^{\text{coupling}} \right) = K_{xf} f \sqrt{L_{ij}^{\text{coupling}}}$$

and $K_{xf} = 0.0056$ is a constant, f is the frequency in MHz. Shown in Figure 2.4, L_{ij} in km denotes the distance between the disturbing transmitter TX_j and victim receiver RX_i , and $H(f, L_{ij})$ is the line transfer function for a channel of length L_{ij} given by equation (2.3). L_{ij}^{coupling} is the so-called coupling length between cable lines indicating within which distance range the crosstalk coupling between line i and line j physically occurs.

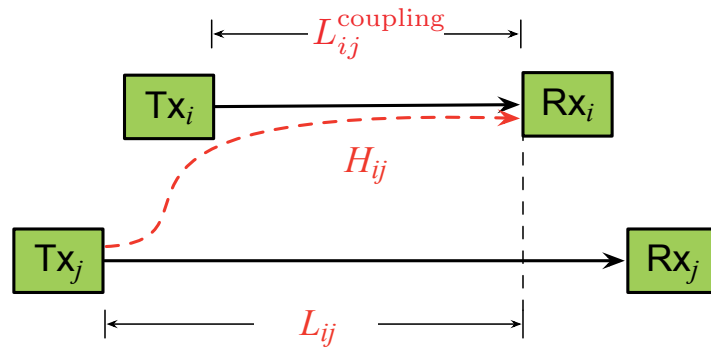


Figure 2.4: crosstalk coupling between two cable pairs

2.4 Deterministic MIMO model for cable binders

In the view of MIMO technology, the physical channel between the multiple transmitters and receivers in DSL systems can be described as the direct channels characterized in different cable lengths and the crosstalk channels characterized by the crosstalk coupling lengths and the lengths between disturbing transmitters and victim receivers.

Considering a cable binder composing M twisted cable pairs and each cable with specific length L_i , the channel transfer function of all direction channels $H(f, L_i)$ is given by equation (2.3), and the crosstalk channel transfer function $H_{ij}(f, L_{ij}^{\text{coupling}}, L_{ij})$ between a transmitter TX_j and a receiver RX_i is defined by equation (2.6).

In the scope of this thesis, we merely consider the scenario where the transceivers are co-located in the central office (CO) as generally illustrated in Figure 1.1.

In the upstream (US) transmission where the signal is transmitted from the customer premise equipment (CPE) to the CO, the receivers are co-located in the CO, shown in Figure 2.5. In this case, the distance L_{ij} between the disturbing transmitter TX_j and victim receiver RX_i is equal to the length of the disturbing line L_j and the corresponding line transfer function for the channel of length L_{ij} is equal the channel transfer function of the disturbing line:

$$H(f, L_{ij}) = H(f, L_j). \quad (2.7)$$

Thus, the crosstalk channel transfer function between a transmitter TX_j and a receiver RX_i can be expressed as the multiplication of the crosstalk coupling coefficient and direct channel transfer function of the disturbing line:

$$H_{ij}(f, L_{ij}^{\text{coupling}}, L_{ij}) = \delta_{ij}(f, L_{ij}^{\text{coupling}}) \left| H(f, L_j) \right|. \quad (2.8)$$

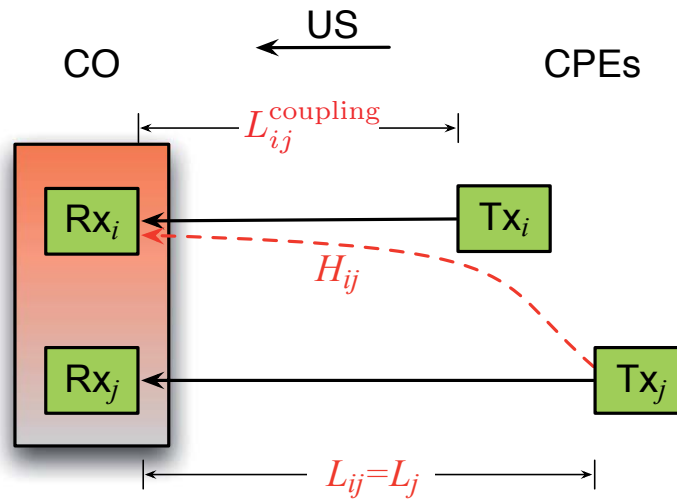


Figure 2.5: US crosstalk coupling

However, in the downstream transmission (DS) the channel transfer function looks different. As shown in Figure 2.6 the transmitters are co-located in the CO. So the distance L_{ij} between the disturbing transmitter TX_j and victim receiver RX_i is equal to the length of the victim line L_i and the corresponding line transfer function for the channel of length L_{ij} is equal to the channel transfer function of the victim line:

$$H(f, L_{ij}) = H(f, L_i). \quad (2.9)$$

Therefore, on the contrary to that of the US transmission, the DS crosstalk channel transfer function between a transmitter TX_j and a receiver RX_i shall be expressed as the multiplication of the crosstalk coupling coefficient and direct channel transfer function of the victim line:

$$H_{ij}(f, L_{ij}^{\text{coupling}}, L_{ij}) = \delta_{ij}(f, L_{ij}^{\text{coupling}}) \big| H(f, L_i) \big|. \quad (2.10)$$

2.5 Stochastic MIMO model for cable binders

In the above section, MIMO modelling for a cable binder is described. However, it is based on the so-called 99% worst case modelling of the crosstalk for the lines in a binder which only depends on different transmission ranges, crosstalk coupling lengths and frequencies. For the purpose of the simulation and evaluation of the signal processing techniques dealing with FEXT in the systems, a more accurate modelling of the MIMO crosstalk channel is needed.

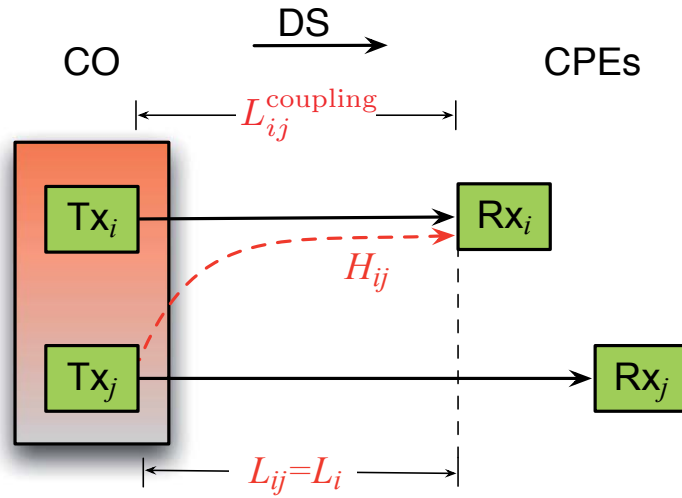


Figure 2.6: DS crosstalk coupling

In this thesis, we adopt the stochastic MIMO model as proposed in [Ver08] which is based upon measurements on real cables and is much more realistic in describing the coupling coefficients among transmitting lines and receiving lines.

The stochastic MIMO model still uses the 99% worst case modelling, but further introduces an amplitude offset of the crosstalk transfer function:

$$H_{ij} = |H_{ij,WC}| \exp \{ j\varphi(f) \} 10^{\frac{X_{dB}}{20}}, \quad (2.11)$$

where $H_{ij,WC}$ is the crosstalk channel transfer function based on the 99% worst case model and obtained from equation 2.8 for the upstream transmission and from equation 2.10 for the downstream transmission, $\varphi(f)$ is the phase of the crosstalk transfer function and X_{dB} is the amplitude offset of the crosstalk transfer function, relative to the amplitude of the 99% worst case model and expressed in dB.

The phase $\varphi(f)$ is linearly dependent on frequency, with a slope that is identical to the slope of the phase of the direct path. The probability density function (pdf) of the phase, at any frequency, is uniformly distributed over the range $[0, 2\pi]$ as crosstalk measurements show a nearly linear phase behavior over frequency.

The amplitude offset X_{dB} is independent of frequency, and its pdf has a BETA distribution:

$$p(X_{dB}) = \frac{(X_{dB} - a)^{\alpha-1} (b - X_{dB})^{\beta-1}}{B(\alpha, \beta) (b - a)^{\alpha+\beta-1}} \quad (2.12)$$



2.5. STOCHASTIC MIMO MODEL FOR CABLE BINDERS

where $B(\alpha, \beta)$ is the beta function.

The parameters used for the BETA distribution are found empirically as follows:

$$\begin{aligned}a &= -60\text{dB} \\b &= 10\text{dB} \\ \alpha &= 11 \\ \beta &= 6.6.\end{aligned}$$

As the amplitude offset X_{dB} is independent of frequency, this stochastic model results in a shifted replica of the worst case crosstalk curve, shifted by a value drawn from the random amplitude offset variable X_{dB} . In other words, for a number of FEXT coupling the model generates several curves, each with a random amplitude offset which is constant over frequencies.

Real cables on the other hand do have frequency variation of their relative amplitude compared to the worst case model. However, such simplification in the model can be done based on the fact that measurements have revealed that this frequency variation of the amplitude is usually rather small for the stronger crosstalkers. That's to say: if the crosstalk coupling between two pairs is strong on one frequency, it will probably also be strong on other frequencies. Therefore, for the performance simulation the frequency variation of the amplitudes in real cables is neglected in this thesis and such simple stochastic MIMO model is used.

3 Discrete Multi-Tone (DMT)

In broadband transmission systems such as VDSL, the transmission channel behaviour is strongly frequency selective. As an example shown in Figure 2.3, there exists tens of dB channel gain difference within the overall transmission band. Considering a single cable line, inter symbol interference (ISI) is a main issue in the systems due to such channel condition. Conventionally, ISI is removed by the use of a decision feedback equalizer (DFE) in the receiver and/or a Tomlinson-Harashima precoder at the transmitter. Thus, the systems might have high run-time complexity and also experience error propagations [GDJ06].

To combat this problem, it is preferred to use the Discrete Multi-Tone (DMT) technique, which is robust against ISI and also known as the Orthogonal Frequency Division Multiplexing (OFDM) technology in wireless communications.

The principle of DMT technique is to effectively partition the frequency selective channel into a large number of orthogonal narrowband subchannels. A single subchannel is also called a tone in DSL systems. Due to the orthogonality, each subchannel can be used independently. Thus, the signals can be modulated individually and transmitted in a superimposed form. As the sinusoidal transmit waveforms are actually the eigenfunctions of an LTI channel in a DMT system, the orthogonality is maintained at the receiver. If the bandwidth of an individual subchannel is sufficiently narrow and the resulting symbol duration is long enough, any ISI contribution can be avoided in the received signal. Consequently, very simple equalization can be applied at the receiver.

Furthermore, DMT systems with multiple subcarriers have the possibility of transmitting different numbers of bits across the bandwidth according to the signal-to-noise ratio (SNR) of the subcarriers and the desired symbol error probability. Therefore, as a key benefit of the DMT technique, transmission in noisy or highly attenuated regions of the channel can be avoided.

The following sections describe the DMT technique in detail.

3.1 DMT technique

The essential idea of the DMT technique is to represent a high rate input bit stream by a superposition of several subcarrier-modulated waveforms of low rate substreams. The transmit signal is the sum of K independent subcarrier signals with equal subchannel bandwidth Δf . The subchannel bandwidth is also called subcarrier spacing. When the subchannel bandwidth Δf is so narrow that the channel frequency response is effectively flat across it, the Nyquist criterion is satisfied and ISI from one symbol to the next can be eliminated [Pro00].

Although the partitioning of a channel into subchannels can be accomplished using any set of orthonormal basis function, the DMT technique employs the Fourier transform as the OFDM technique does, in particular, the inverse discrete Fourier transform (IDFT). IDFT has the advantage in implementation due to the development of digital signal processor and the introduction of the fast Fourier transform (FFT).

To keep the orthogonality among the subchannels, the transmit symbol duration T_s is chosen in relation to the subcarrier spacing Δf as

$$T_s = \frac{1}{\Delta f}. \quad (3.1)$$

The transmit samples $\{x_n\}$, $n \in [0, N-1]$ are calculated by taking the IDFT of the N -dimension sequence $\{X_k\}$:

$$x_n = \frac{1}{\sqrt{N}} \sum_{k=0}^{N-1} X_k e^{j2\pi kn/N}, \quad \forall n \in [0, N-1], \quad (3.2)$$

where N is twice the number of subchannels K :

$$N = 2K. \quad (3.3)$$

DSL systems are baseband transmission systems. The signals transmitted over copper lines are naturally one dimensional (real-valued). In other words, the time domain signal, the output of IDFT in the DMT modulation shall be real and able to be transmitted directly to the channel after digital-to-analog conversion. For this reason, the signal spectrum must be prepared in a Hermitian way. The input N -dimension sequence $\{X_k\}$, $k \in [0, N-1]$ of IDFT shows the property of Hermitian symmetry:

$$X_k = \begin{cases} \Re\{X_K\} & k = 0 \\ X_k & k = 1, \dots, K-1 \\ \Im\{X_K\} & k = K \\ X_{N-k}^* & k = K+1, \dots, N-1. \end{cases} \quad (3.4)$$

CHAPTER 3. DISCRETE MULTI-TONE (DMT)

The sequence $\{X_k\}$, $k \in [0, K - 1]$ is the frequency domain signal sequence for K subcarriers. In fact, DMT modulation performs N -point complex-to-real IDFT for the transmission of signals on K subcarriers.

Ideally, when the number of subcarriers K is sufficiently large, the subchannels are free of ISI. However, in practice, the frequency response of individual subchannel might not be always flat and its channel impulse response length is greater than one. To completely eliminate the effect of ISI, a *cyclic prefix* is added at the beginning of each DMT symbol as shown in Figure 3.1. The cyclic prefix is also called *guard interval* in the OFDM technique. The number of time domain samples of the cyclic prefix N_{CP} is chosen to be larger than the channel impulse response length. In this case, the DMT symbol rate f_s can be calculated as:

$$f_s = \frac{f_{\text{sample}}}{N + N_{CP}}, \quad (3.5)$$

where f_{sample} is the sampling rate which is twice of the system bandwidth.

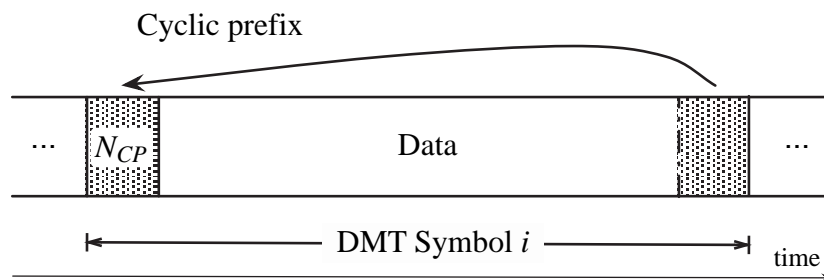


Figure 3.1: Illustration of the cyclic prefix

As introduced above, the DMT technique uses Fourier transform to partition the overall channel into independent subchannels. Shown in equation 3.2, a transmit sample is in fact a superposition of orthogonal exponentials weighted by the frequency domain symbols $\{X_k\}$. As complex exponentials are always eigenfunctions of an LTI system, the orthogonality among the subcarriers remains even at the receiver despite of the propagation delay. Thus, if cyclic prefix is applied to completely remove ISI, the received symbol in frequency domain Y_k can be simply expressed as

$$Y_k = H_k X_k + Z_k, \quad \forall k \in [0, K - 1] \quad (3.6)$$

where H_k denotes the channel transfer factor on subcarrier k and Z_k is the corresponding noise component.

3.2 System structure

Figure 3.2 shows the general schematic diagram of a coded DMT transceiver structure. The info bit stream is encoded by a forward error correction (FEC) code with a certain constraint length and then scrambled by a bit-level interleaver for the purpose of correcting burst errors. In DSL systems, trellis coding is applied. After interleaving, the coded bits are mapped onto complex modulation symbols $\{X_k\}$ using an appropriate QAM-constellation diagram.

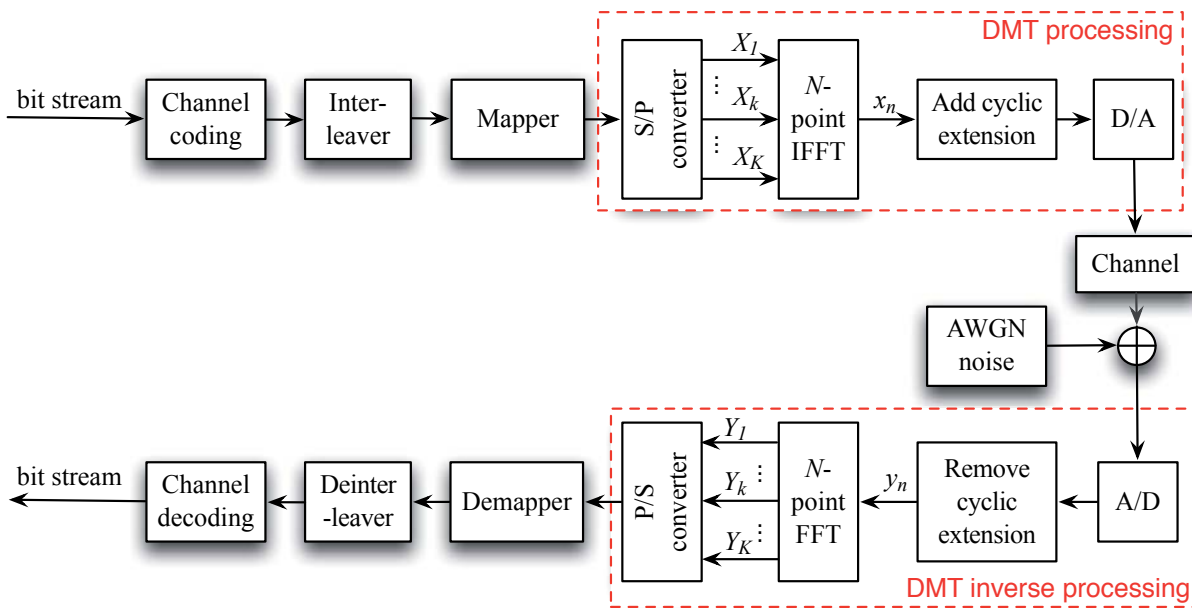


Figure 3.2: Schematic diagram of a coded DMT transceiver structure

Thereafter, the DMT processing is performed: a serial-to-parallel converter segments every K modulated symbols, and then the N -point complex-to-real IDFT/IFFT is performed to each segment yielding a discrete-time sequence $\{x_n\}$, $n \in [0, N - 1]$. To completely remove the ISI, a cyclic prefix is added at the front of the sequence $\{x_n\}$. Following the digital-to-analog (D/A) conversion, the corresponding continuous-time signal is generated and further transmitted over a twisted cable pair.

At the receiver the inverse procedure in accordance with the signal processing at the transmitter is performed. After the analog-to-digital (A/D) conversion, the cyclic extension which might be corrupted is discarded. An N -point real-to-complex DFT/FFT converts the received time domain signals $\{y_n\}$, $n \in [0, N - 1]$ back to the frequency domain. Then, the parallel-to-serial conversion is performed. After the DMT inverse processing, the proce-

ture may follow sequentially with the frequency domain equalization, de-mapping, de-interleaving and channel decoding.

3.3 Channel capacity for a single cable line

In 1948, Claud Shannon introduced the remarkable mathematical theory to compute the performance of communication systems [Sha48]. He referred the maximum transmission rate over a given channel as the *channel capacity* of the communication system which can be defined as

$$C = \max_{P(\mathbf{X})} \{I(\mathbf{X}, \mathbf{Y})\}, \quad (3.7)$$

where $I(\mathbf{X}, \mathbf{Y})$ is the *mutual information* between the transmit signal \mathbf{X} and received signal \mathbf{Y} , and $P(\mathbf{X})$ is the probability distribution of the transmit signal \mathbf{X} .

Considering a single cable line, this channel capacity in presence of additive white Gaussian noise (AWGN) is determined by system bandwidth W and the quality of the transmission in terms of the post-estimated SNR:

$$\begin{aligned} C &= W \log_2(1 + \text{SNR}) \\ &= W \log_2 \left(1 + \frac{|H|^2 \sigma_s^2}{\sigma_z^2} \right), \end{aligned} \quad (3.8)$$

$$\text{with } \text{SNR} = \frac{|H|^2 \sigma_s^2}{\sigma_z^2}, \quad (3.9)$$

where H is the channel transfer factor, σ_s^2 and σ_z^2 are the transmission power and the noise power.

In a DMT system, the overall channel has been partitioned into a large number of independent parallel narrowband subchannels. According to equation (3.8), each of those subchannels with a bandwidth of Δf has a channel capacity C_k

$$C_k = \Delta f \log_2(1 + \text{SNR}_k), \quad (3.10)$$

$$\text{with } \text{SNR}_k = \frac{|H_k|^2 \sigma_{s,k}^2}{\sigma_z^2}, \quad \forall k \in \{0, 1, \dots, K-1\} \quad (3.11)$$

where H_k , $\sigma_{s,k}^2$ and σ_z^2 are the channel transfer factor, transmit power and noise power on subcarrier k , respectively. It is assumed that the noise power on each subcarrier is

3.3. CHANNEL CAPACITY FOR A SINGLE CABLE LINE

identical. Thus, the capacity of the overall channel in the DMT system can be calculated as the sum of all K subchannel capacities:

$$C = \Delta f \sum_{k=0}^{K-1} \log_2 \left(1 + \frac{|H_k|^2 \sigma_{s,k}^2}{\sigma_z^2} \right). \quad (3.12)$$

For each amplitude modulation, in particular QAM performed in DMT modulation, the bit error rate is a function of the signal-to-noise ratio and the number of bits per symbol. So the number of bit b_k being able to be loaded on a subcarrier k can be derived by so-called gap approximation given a desired bit error rate P_e and the signal-to-noise ratio SNR_k on the subcarrier k [Cio91]:

$$b_k = \log_2 \left(1 + \frac{\text{SNR}_k}{\Gamma} \right), \quad (3.13)$$

$$\text{with } \Gamma = \frac{\Gamma(P_e) \gamma_m}{\gamma_c} \quad (3.14)$$

where γ_c is the coding gain for a FEC code, γ_m is the noise margin for proper operation of the system and $\Gamma(P_e)$ is the Shannon gap at the desired bit error rate. For QAM with $P_e = 10^{-7}$, the Shannon gap is 9.75 dB.

Thus, the achievable data rate R in a DSL system for a single cable line can be calculated by summing up the data rates R_k on individual subcarriers:

$$\begin{aligned} R &= \sum_{k=0}^{K-1} R_k \\ &= f_s \sum_{k=0}^{K-1} b_k \\ &= f_s \sum_{k=0}^{K-1} \log_2 \left(1 + \frac{1}{\Gamma} \cdot \frac{|H_k|^2 \sigma_{s,k}^2}{\sigma_z^2} \right). \end{aligned} \quad (3.15)$$

Hereinafter, such practical data rate instead of the theoretical channel capacity will be used for system performance evaluation.

4 Multiple-Line DMT

In the last two decades, MIMO techniques have been developed rapidly in the wireless communication area. Multiple antennas are used in radio systems to take the advantage of the fact that different antennas are spatially separated in a dense multipath scattering environment. Depending on the objective, MIMO techniques can be categorized into two groups: diversity techniques and spatial multiplexing techniques.

MIMO diversity techniques are aiming at increasing transmission reliability and improving the receive signal-to-noise ratio. Examples of these diversity techniques include the space-time block codes (STBC) [Ala98], [TJC99], space-time trellis codes (STTC) [TSC98], maximum-ratio combining (MRC) and so on.

MIMO spatial multiplexing techniques linearly increase the channel capacity without requiring additional spectral resources [Tel99]. Examples of multiplexing techniques can be beamforming techniques, V-BLAST detection techniques [WFGV98] and so on. In MIMO spatial multiplexing, independent data symbols are sent via sufficiently-separated antennas which use the same frequency resource. In this aspect, an overall DSL system comprising multiple transmission cable lines can be regarded as a MIMO system and the MIMO spatial multiplexing techniques developed in wireless communications can be also applied among multiple cable lines.

Furthermore, in a broadband radio environment combining MIMO techniques together with the OFDM technique is an effective method to combat fading and to achieve high data rate communications. By combining the OFDM technique, the transmission in broadband is converted to the transmission in a large number of narrow bands and the MIMO signal processing in the broadband transmission can be implemented in a much easier way on each subcarrier. Thus, the transceiver structure and the signal processing procedure can be simplified in wireless communications. Similarly, such technique combination and advantages can be also adopted in the wireline transmission for the same purpose.

In the following the transceiver structure and the signal model of multiple-line DMT transmission systems is introduced.

4.1 Transceiver structure

In a modern DSL system, transceivers can be co-located in the CO where joint signal processing is feasible. However, the transceivers on the user side are located in a distributed way. For this reason, the MIMO techniques requiring both transmitter and receiver coordination can not be directly applied. Nevertheless, we can obtain the capacity gain by only exploiting the MIMO signal processing in the CO.

Figures 4.1 and 4.2 illustrate the block diagrams of multiple-line DMT systems in the upstream and downstream transmission respectively. M represents the number of twisted cable pairs in the cable binder and it is assumed that the system only comprises one cable binder.

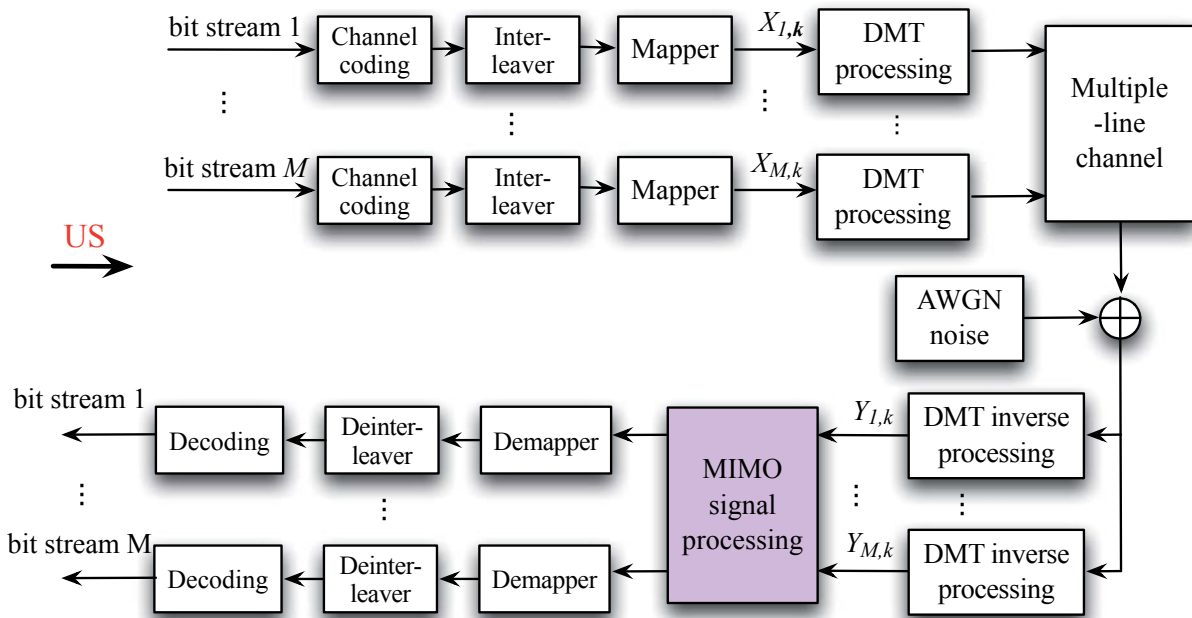


Figure 4.1: Block diagram of the US transceiver structure

In the upstream transmission, the signal processing at each transmitter of M individual lines is an independent procedure from one to another. Thus, it can be performed on each customer side without the aid from other transmitters. Under the circumstances, the transmitter structure for each line is the ordinary DMT system transmitter structure as depicted in Figure 3.2 of Section 3.2, namely channel coding followed by interleaving, mapping and DMT processing.

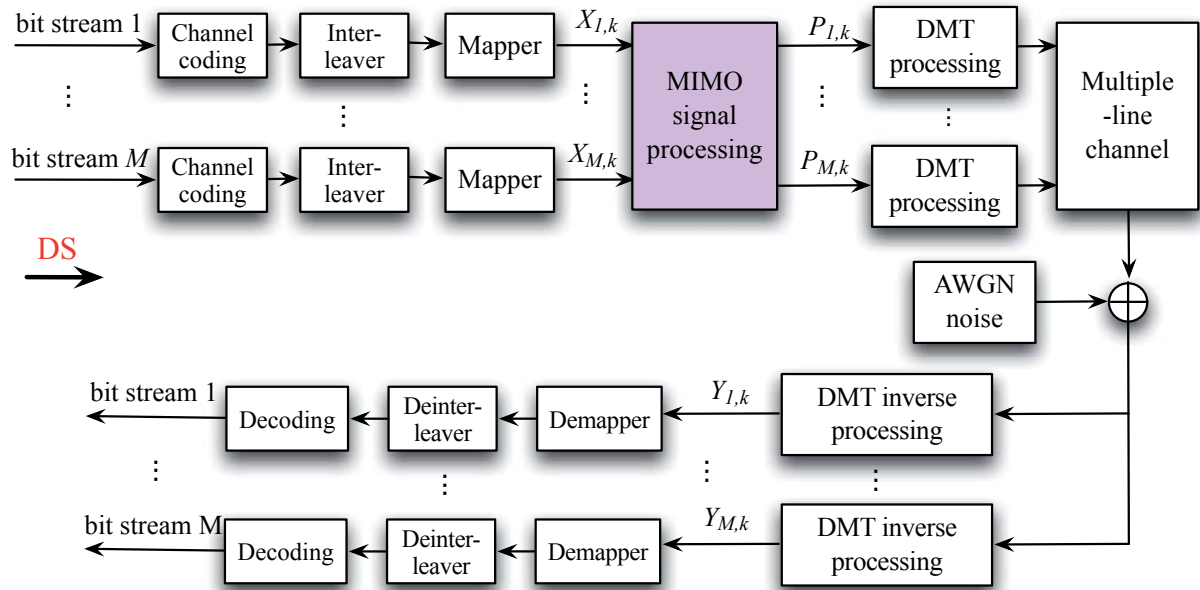


Figure 4.2: Block diagram of the DS transceiver structure

As the signals transmitted through the multiple-line channel having AWGN noise, DMT inverse processing is performed for each individual line on the CO side. Afterwards, MIMO signal processing is applied simultaneously to all M received signals. The obtained signals are then de-mapped, de-interleaved and decoded independently.

For the downstream transmission, as shown in Figure 4.2, each bit stream corresponding to the source data for the individual lines or users is encoded, interleaved and mapped independently in the CO. Then, MIMO signal processing is performed simultaneously on M input signals. Thereafter, the obtained signals are individually processed by DMT modulation and further transmitted over the multiple-line channel as described in Section 3.2.

On the receiver side, as the modems are distributively located, the receiver structure of the individual line can be exactly the same as the receiver structure described in Section 3.2.

4.2 Signal model

It has been introduced that with DMT modulation, the overall bandwidth of a broadband transmission can be divided into a large number of narrow bands and the transmission

channel is partitioned into corresponding parallel subchannels. If the number of subchannels is large enough, the subchannels are free of ISI and a one tap frequency domain equalizer (FEQ) is sufficient on each subcarrier. In other words, the frequency-selective broadband channel is turned into a large number of parallel flat subchannels. Therefore, the narrowband MIMO signal processing is feasible and can be performed on each subcarrier.

As shown in Figure 4.1, for the upstream transmission the input signal is referenced after the mapper at the transmitter and the output signal is referred to the signals obtained by DMT inverse processing at the receiver. Let $X_{i,k}$ represent the transmit signal for line i on subcarrier k , where $i \in [1, M]$, $k \in [0, K - 1]$ and K is the number of subcarriers. The received signal $Y_{i,k}$ for the line i on the k -th subcarrier having been transmitted through the multiple-line channel can be expressed as

$$Y_{i,k} = H_{ii,k}X_{i,k} + \sum_{j=1, j \neq i}^M H_{ij,k}X_{j,k} + Z_{i,k}, \quad (4.1)$$

where index j denotes any line other than the i -th line, $H_{ij,k}$ is the flat subchannel transfer coefficient from line j to line i on subcarrier k and $Z_{i,k}$ is the corresponding noise component.

Let \mathbf{H}_k denote the multiple-line channel transfer function on subcarrier k . The matrix \mathbf{H}_k holds all $M \times M$ channel coefficients on subcarrier k as

$$\mathbf{H}_k = \begin{pmatrix} H_{11,k} & \dots & H_{1M,k} \\ \vdots & \ddots & \vdots \\ H_{M1,k} & \dots & H_{MM,k} \end{pmatrix}. \quad (4.2)$$

The transmit symbols for all considered M cable lines and for a single subcarrier k can be described as a transmit signal vector

$$\mathbf{X}_k = (X_{1,k}, X_{2,k}, \dots, X_{M,k})^T, \quad (4.3)$$

where $(*)^T$ denotes the transpose of the matrix/vector $(*)$. The received signals for all M adjacent cable lines and for subcarrier k are thus described by a received signal vector

$$\mathbf{Y}_k = (Y_{1,k}, Y_{2,k}, \dots, Y_{M,k})^T, \quad (4.4)$$

which can be calculated by the following linear equation:

$$\mathbf{Y}_k = \mathbf{H}_k \mathbf{X}_k + \mathbf{Z}_k, \quad (4.5)$$

where \mathbf{Z}_k is the noise vector comprising the AWGN noise samples for each line on the subcarrier k and given as

$$\mathbf{Z}_k = (Z_{1,k}, Z_{2,k}, \dots, Z_{M,k})^T. \quad (4.6)$$

CHAPTER 4. MULTIPLE-LINE DMT

In the downstream transmission, referring to the corresponding Figure 4.2, the input signal is again referenced after the mapper at the transmitter and the output signal is regarded as the signals obtained by DMT inverse processing at the receiver. Let $X_{i,k}$ represent the QAM modulated symbol for line i on subcarrier k . The sequence $\mathbf{X}_i = \{X_{i,k}\}, k = 0, 1, \dots, K-1$ corresponds to a DMT symbol for line i and the sequence $\mathbf{X}_k = \{X_{i,k}\}, i = 1, 2, \dots, M$ corresponds to the symbols for all M lines on the subcarrier k .

Denoting \mathbf{W}_k as the precoding matrix of the MIMO signal processing on subcarrier k , the signal vector $\mathbf{P}_k = (P_{1,k}, P_{2,k}, \dots, P_{M,k})^T$ obtained after the MIMO processing can be expressed as

$$\mathbf{P}_k = \mathbf{W}_k \mathbf{X}_k. \quad (4.7)$$

Like in the upstream transmission, the received signal $Y_{i,k}$ for line i on the k -th subcarrier can also be calculated as

$$Y_{i,k} = H_{ii,k}P_{i,k} + \sum_{j=1, j \neq i}^M H_{ij,k}P_{j,k} + Z_{i,k}. \quad (4.8)$$

Using a matrix expression, all received signals for M adjacent cable lines on subcarrier k can be simply presented as

$$\begin{aligned} \mathbf{Y}_k &= \mathbf{H}_k \mathbf{P}_k + \mathbf{Z}_k \\ &= \mathbf{H}_k \mathbf{W}_k \mathbf{X}_k + \mathbf{Z}_k. \end{aligned} \quad (4.9)$$

5 Crosstalk Cancellation

Starting with the classical digital subscriber line technology, which uses a bandwidth of several Kilohertz for voice signal transmission, modern very-high-speed digital subscriber line systems, e.g., VDSL systems and VDSL2 systems extend the system bandwidth to more than ten megahertz for high-speed internet access and other applications. In this case the crosstalk interference due to electromagnetic coupling between adjacent twisted pairs inside a cable binder is one of the major system limitations. Typically, the crosstalk interference level is 10 – 15 dB larger than the background noise power.

Conventionally, such kind of crosstalk interference is regarded as unknown and uncontrollable random noise and is accepted as a performance limitation. Correspondingly, the DSL deployments are always engineered to function in a statistically worst case scenario. Such simple but conservative treatment of crosstalk interference often leads to unnecessarily low bit rates.

Figure 5.1 shows the data rate performance achieved by a small cable binder having 10 twisted cable pairs. The adjacent cable pairs are mutually interfering one another. As crosstalk interference is tolerated in the system, the achieved data rate averaged over all lines in the cable binder are significantly lower than the achievable data rate without the existence of crosstalk interference. Especially, when the cable lengths are relatively short, there exists a huge data rate performance gap in between.

Therefore, it will be advantageous for future systems to consider the crosstalk not as just noise contributions but as deterministic interference. In this case the crosstalk signal parameters can be measured adaptively, the crosstalk interference can be cancelled out by signal processing procedures. Consequently, the system performance can be improved significantly.

In the following crosstalk cancellation techniques based on the MIMO signal processing techniques and DMT modulation for the upstream transmission as well as for the downstream transmission are discussed.

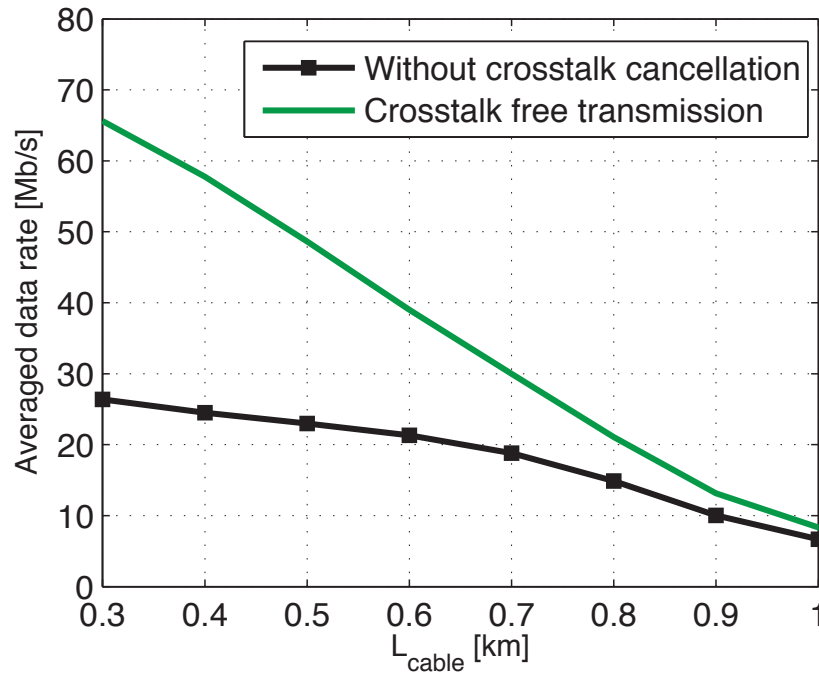


Figure 5.1: Data rate performance gap due to the crosstalk interference

5.1 Upstream crosstalk cancellation

As it is introduced in Chapter 3, the ISI of a transmit signal due to the frequency selective channel is combated by DMT modulation in DSL systems, and the resulting narrowband transmission over a twisted-pair copper line is only impaired by the direct channel attenuation and background noise. The achieved data rate is given by equation (3.15).

Now an upstream transmission system as illustrated in Figure 4.1 is considered. It is also assumed that the cable binder comprises M twisted cable pairs and the transmit signals $\{X_{i,k}\}, \forall i \in [1, M]$ on subcarrier k experience the multiple-line channel \mathbf{H}_k as shown in equation (4.2), and the received signal for line i and on subcarrier k is given by equation (4.1).

As addressed above, crosstalk interference is conventionally considered as additive random noise and as an accepted performance limitation in the system. Accordingly, the received signal $Y_{i,k}, \forall i \in [1, M]$ is simply equalized by the so-called one-tap equalizer with the corresponding direct channel coefficient $H_{ii,k}$ for each individual line. The estimated transmit signal $\tilde{X}_{i,k}$ for line i and on subcarrier k is

5.1. UPSTREAM CROSSTALK CANCELLATION

$$\tilde{X}_{i,k} = \frac{Y_{i,k}}{H_{ii,k}} = X_{i,k} + \frac{1}{H_{ii,k}} \cdot \left(\sum_{j=1, j \neq i}^M H_{ij,k} X_{j,k} + Z_{i,k} \right). \quad (5.1)$$

In this case, crosstalk interference is contained in the equalized signal. Actually, it is the signal to interference-plus-noise ratio (SINR) that shall be considered for line i and on subcarrier k at the receiver. Assuming that the same transmit power is provided on each subcarrier for all lines, the SINR can be expressed as

$$\text{SINR}_{i,k} = \frac{|H_{ii,k}|^2 \sigma_s^2}{\sum_{j=1, j \neq i}^M |H_{ij,k}|^2 \sigma_s^2 + \sigma_z^2}, \quad (5.2)$$

As shown in Figure 5.1, the resulting data rate thus is significantly decreased.

To eliminate crosstalk interference, several crosstalk cancellation techniques have been considered. For example, a so-called multichannel linear equalizer is suggested in [HCS92] to remove crosstalk interference based on minimum mean square error (MMSE) criterion; in [DP02] maximum likelihood (ML) multiuser detection is addressed; an equalization based on singular value decompositions of the system channel matrices is suggested in [TH00]. In particular, QR-based decision feedback equalization (DFE) [GC02] is of interest, that is known as providing high performance gain.

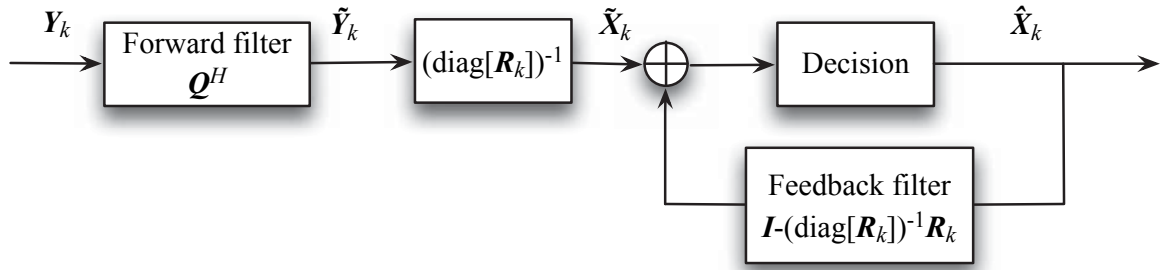
5.1.1 QR-based decision feedback cancellation

DFE has been studied for decades and it is the most commonly known non-linear equalizer applied in DSL systems. Conventionally, it is used to deal with the ISI imposed by frequency selective channels. By using DMT technique, DFE can be replaced by one-tap FDE. However, its principle of combating against ISI can be applied to eliminate the co-channel-interference (CCI), otherwise known as crosstalk interference in DSL systems.

In the upstream transmission, the co-location of receivers at the CO provides the opportunity for processing the received signals jointly. The channel transfer matrix \mathbf{H}_k on each subcarrier k can be decomposed into a unitary matrix and an upper triangular matrix:

$$\mathbf{H}_k = \mathbf{Q}_k \mathbf{R}_k, \quad (5.3)$$

where matrix \mathbf{Q}_k is the unitary matrix and \mathbf{R}_k is the upper triangular matrix.


Figure 5.2: US block diagram with DFE

As shown in Figure 5.2, the received signals \mathbf{Y}_k are first filtered by the transpose of matrix \mathbf{Q}_k and yield to

$$\tilde{\mathbf{Y}}_k = \mathbf{Q}_k^H \mathbf{Y}_k \quad (5.4)$$

$$= \mathbf{R}_k \mathbf{X}_k + \tilde{\mathbf{Z}}_k, \quad (5.5)$$

where the noise $\tilde{\mathbf{Z}}_k = \mathbf{Q}_k^H \mathbf{Z}_k$ has the same covariance matrix as the noise \mathbf{Z}_k due to the property of the unitary matrix \mathbf{Q}_k . As matrix \mathbf{R}_k is an upper triangular matrix and the noise is uncorrelated to signals, the signals contained in vector \mathbf{X}_k can be calculated by back-substitution combined with symbol-by-symbol detection.

Thus, the decision feedback structure is derived with the feedback matrix $\mathbf{I} - \mathbf{R}_k$ and the estimated transmit signal $\tilde{X}_{i,k}$ for line i and on subcarrier k is expressed as

$$\tilde{X}_{i,k} = \frac{1}{R_{ii,k}} \left(\tilde{Y}_{i,k} - \sum_{j=i+1}^M R_{ij,k} \hat{X}_{j,k} \right), \quad (5.6)$$

$$j = M, M-1, \dots, 1$$

where $R_{ij,k}$ is the (i, j) element of matrix \mathbf{R}_k and $\hat{X}_{j,k} = \text{dec} \left[\tilde{X}_{j,k} \right]$ is the detected symbol for line j on subcarrier k after the decision operation based on the corresponding estimated symbol $\tilde{X}_{j,k}$.

If it is assumed that the previous decisions are always correct, the crosstalk interference for each line i can be cancelled out and the resulting estimated transmit signal $\tilde{X}_{i,k}$ contains only the transmit signal $X_{i,k}$ and the scaled noise:

$$\tilde{X}_{i,k} = X_{i,k} + \frac{\tilde{Z}_{i,k}}{R_{ii,k}}. \quad (5.7)$$

5.1. UPSTREAM CROSSTALK CANCELLATION

The corresponding SNR for line i and on the subcarrier k can be calculated as

$$\text{SNR}_{i,k} = \frac{|R_{ii,k}|^2 \sigma_s^2}{\sigma_z^2}. \quad (5.8)$$

However, in reality all decision directed equalization schemes suffer from two aspects: the phenomenon of error propagation and the latency. The former results from the further decision error caused by the erroneous past decisions fed to the decision operation unit. The latter is the direct consequence of the feedback structure and the impact to the system grows with the number of lines contained in cable binder. Nowadays, real-time applications require reliable transmission with low complexity and low latency.

5.1.2 Zero-forcing based cancellation

In this subsection, a simple linear crosstalk cancellation technique [RDR08] based on the zero-forcing criterion is introduced.

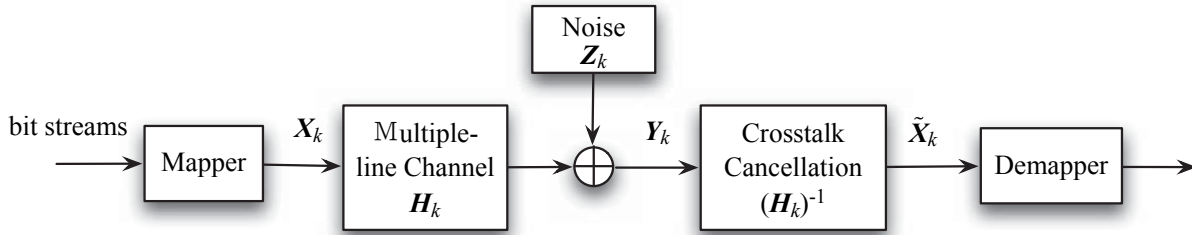


Figure 5.3: The upstream transmission block diagram with crosstalk cancellation

As shown in Figure 5.3, the joint multiple-line signal processing is performed by a matrix multiplication of the received vector with the inverse of the multiple-line channel transfer matrix \mathbf{H}_k^{-1} . The estimation of all transmitted signals on subcarrier k will be:

$$\begin{aligned} \tilde{\mathbf{X}}_k &= \mathbf{H}_k^{-1} \mathbf{Y}_k \\ &= \mathbf{X}_k + \mathbf{H}_k^{-1} \mathbf{Z}_k, \end{aligned} \quad (5.9)$$

with the error vector $\mathbf{e} = \tilde{\mathbf{X}}_k - \mathbf{X}_k = \mathbf{H}_k^{-1} \mathbf{Z}_k$ and its corresponding covariance matrix

$$\begin{aligned} E\{\mathbf{e}\mathbf{e}^H\} &= E\{\mathbf{H}_k^{-1} \mathbf{Z}_k \mathbf{Z}_k^H (\mathbf{H}_k^{-1})^H\} \\ &= \mathbf{H}_k^{-1} \sigma_z^2 \mathbf{I} (\mathbf{H}_k^{-1})^H \\ &= \sigma_z^2 \mathbf{H}_k^{-1} (\mathbf{H}_k^{-1})^H. \end{aligned} \quad (5.10)$$

CHAPTER 5. CROSSTALK CANCELLATION

For each individual line i , the power of the estimation error $\sigma_{e,i}^2$ is described by the auto-correlation term on the i th diagonal of the covariance matrix:

$$\begin{aligned}\sigma_{e,i}^2 &= \sigma_z^2 \left(\text{diag} \left[\mathbf{H}_k^{-1} \left(\mathbf{H}_k^{-1} \right)^H \right] \right)_i \\ &= \left\| \left(\mathbf{H}_k^{-1} \right)_{\text{row } i} \right\|^2 \sigma_z^2\end{aligned}\quad (5.11)$$

where $\text{diag}[*]$, $(*)_i$ and $(*)_{\text{row } i}$ denote the diagonal elements, the i th element and the i th row of the matrix $(*)$, respectively. Moreover, $\|*\|$ is the Frobenius norm of the matrix $(*)$. Thus, the obtained post-estimated SNR for line i on subcarrier k is given by

$$\text{SNR}_{i,k} = \frac{\sigma_s^2}{\left\| \left(\mathbf{H}_k^{-1} \right)_{\text{row } i} \right\|^2 \sigma_z^2}.\quad (5.12)$$

Since a zero-forcing canceller always removes the channel influence, the estimated transmission signals are free of the interference.

In the wireless transmission area, the zero-forcing based cancellation technique has been well studied and is used in favor of its low complexity. However, its drawback is also quite well-known, namely the effect of the noise enhancement. As the zero-forcing based canceller only concentrates on the ISI, the noise might be boosted with the inverse of the transmission matrix. In particular, in high frequency transmit region, the attenuation of the direct channel transfer factor is so large that the resulting post-estimated SNR is too small for the useful signal being transmitted over the corresponding subcarriers with the given BER requirement. In this case, such subcarriers will be not used for the transmission taking the advantage of the DMT technique.

One could try to alleviate noise enhancement in such situation by alternatively using the canceller applying the minimum mean square error (MMSE) criterion which aims for low interference plus noise. In other words, try to reduce noise enhancement at the expense of leaving some residual interference. Nevertheless, the performance of the canceller can not be much improved simply because on those subcarriers the dominating crosstalk interference components are much larger than background noise.

Another prompt of using zero-forcing cancellation in modern VDSL systems is that the channel transfer matrix H is normally invertible. This is due to the channel properties of the wireline transmission. In contrast to wireless transmission, where the channel transfer matrix might be singular or ill-conditioned, in wireline transmission the channel transfer matrix is normally diagonal dominated. Thus, rank deficiency will not occur and the matrix is always invertible for performing zero-forcing based cancellation.

5.2. DOWNSTREAM CROSSTALK CANCELLATION

As described in Chapter 2, the crosstalk interference is the major impairment of DSL systems and conventionally, it is tolerated as one of the noise components in the systems. There is a so-called “near-far problem”, which is quite critical in the systems. This problem occurs in the absence of power control - if all modems were to transmit at the same power level, the one closest to the CO could overpower all others as the signal power drops exponentially with the distance. So the transmit power for each user must be reduced in accordance with the individual distance so as to limit interference and maintain an acceptable signal-to-interference ratio (SIR) for all other users. In this case, the system capacity can be maximized.

However, in VDSL2 systems with crosstalk cancellation, the crosstalk is treated as interference signals rather than just unknown noise, and the zero-forcing based signal processing is used for mitigating them. It can be seen in equation (5.9) that for each individual line in the cable binder, the estimated signal contains only the transmit signal and scaled noise signal. As addressed above, the interference signals are perfect eliminated if the channel state information (CSI) is known and the time/frequency is perfect synchronized. So, in most cases power control due to the near-far situation is not necessary in the system with zero-forcing based cancellation.

5.2 Downstream crosstalk cancellation

For the downstream transmission, individual receivers are located separately and receiver co-ordination as performed in the upstream transmission is no longer available. However, in the CO transmitter co-ordination can be instead performed by crosstalk cancellation techniques such as precoding. The transmission block diagram in downstream is shown in Figure 5.4.

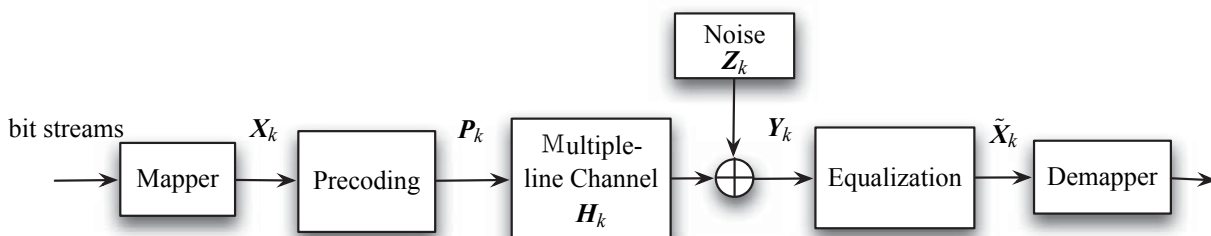


Figure 5.4: The downstream transmission block diagram with crosstalk cancellation

There are various ways to do precoding such as the direct zero-forcing precoding or QR decomposition based precoding [GC02]. But direct zero-forcing precoding will cause significant power increment at the transmitters. Even with power control, the performance is poor since all modems see the channel of the worst line within the binder [CMV⁺04]. In the QR decomposition based precoding, the operation may also cause undesired energy increase. Using the concept of Tomlinson-Harashima precoding can ensure that the transmission power is not increased [FYL07], but the method requires a modulo-operation at the receiver which leads the hardware modification in the modems.

Therefore, channel decomposition based precoding is proposed [RDR08]. It is observed that the channel transfer matrix for subcarrier k can be written as:

$$\mathbf{H}_k = \begin{pmatrix} H_{11,k} & H_{12,k} & \dots & H_{1M,k} \\ H_{21,k} & H_{22,k} & \dots & H_{2M,k} \\ \vdots & \vdots & \ddots & \vdots \\ H_{M1,k} & H_{M2,k} & \dots & H_{MM,k} \end{pmatrix} = \begin{pmatrix} H_{11,k} & \delta_{12}H_{11,k} & \dots & \delta_{1M}H_{11,k} \\ \delta_{21}H_{22,k} & H_{22,k} & \dots & \delta_{2M}H_{22,k} \\ \vdots & \vdots & \ddots & \vdots \\ \delta_{M1}H_{MM,k} & \delta_{M2}H_{MM,k} & \dots & H_{MM,k} \end{pmatrix}. \quad (5.13)$$

Apparently, we could distinguish the direct channel attenuation effect and the crosstalk interference effect by decomposing the channel transfer matrix for each subcarrier k into

$$\mathbf{H}_k = \mathbf{H}_{\text{diag}}\mathbf{H}_{\text{norm}}, \quad (5.14)$$

where

$$\mathbf{H}_{\text{diag}} = \begin{pmatrix} H_{11,k} & 0 & \dots & 0 \\ 0 & H_{22,k} & \ddots & \vdots \\ \vdots & \ddots & \ddots & 0 \\ 0 & \dots & 0 & H_{MM,k} \end{pmatrix} \quad (5.15)$$

is a diagonal matrix containing the direct channel transfer factors for all M lines on subcarrier k , and

$$\mathbf{H}_{\text{norm}} = \begin{pmatrix} 1 & \delta_{12,k} & \dots & \delta_{1M,k} \\ \delta_{21,k} & 1 & \ddots & \vdots \\ \vdots & \ddots & \ddots & \delta_{(M-1)M,k} \\ \delta_{M1,k} & \dots & \delta_{M(M-1),k} & 1 \end{pmatrix} \quad (5.16)$$

is an M -by- M matrix which contains the elements corresponding to the crosstalk coupling effect and matrix \mathbf{H}_{norm} can be obtained by normalizing the channel transfer matrix \mathbf{H}_k on subcarrier k with the corresponding direct channel transfer factors as expressed in equation (5.17):

$$\mathbf{H}_{\text{norm}} = \mathbf{H}_{\text{diag}}^{-1}\mathbf{H}_k. \quad (5.17)$$

5.2. DOWNSTREAM CROSSTALK CANCELLATION

The modulated symbols \mathbf{X}_k therefore can be linearly precoded by the inverse of the normalized channel transfer matrix \mathbf{H}_{norm} and the resulting transmit symbols \mathbf{P}_k are

$$\mathbf{P}_k = \mathbf{H}_{\text{norm}}^{-1} \mathbf{X}_k. \quad (5.18)$$

As shown in Figure 5.4, the received signal vector will be

$$\begin{aligned} \mathbf{Y}_k &= \mathbf{H}_k \mathbf{P}_k + \mathbf{Z}_k \\ &= \mathbf{H}_{\text{diag}} \mathbf{X}_k + \mathbf{Z}_k. \end{aligned} \quad (5.19)$$

Obviously, as the symbols \mathbf{X}_k are pre-distorted by the inverse of the normalized channel transfer matrix \mathbf{H}_{norm} prior to being transmitted and further passed through the multiple-line channel with transfer matrix \mathbf{H} , the resulting signals \mathbf{Y}_k in the individual receivers are completely independent of each other. More specifically, as shown in equation (5.19) each received signal for a certain line i is only influenced by its direct channel transfer factor $H_{ii,k}$ contained in the diagonal matrix \mathbf{H}_{diag} and the corresponding noise component.

It is thus possible to only perform the equalization for the received signal on the individual line independently on the downstream receiver side where the individual modems are distributedly located. Moreover, a very simple one-tap equalizer is sufficient for each line. The estimated signals for all M lines on subcarrier k will be:

$$\tilde{\mathbf{X}}_k = \mathbf{H}_{\text{diag}}^{-1} \mathbf{Y}_k \quad (5.20)$$

$$= \mathbf{X}_k + \mathbf{H}_{\text{diag}}^{-1} \mathbf{Z}_k. \quad (5.21)$$

Similar to the upstream zero-forcing based crosstalk cancellation, channel decomposition based precoding in the downstream transmission also results in crosstalk-free reception and the background noise is only enhanced by the inverse of the corresponding direct channel transfer factor $H_{ii,k}$. The obtained post-estimated SNR for line i on subcarrier k is

$$\text{SNR}_{i,k} = \frac{|H_{ii,k}|^2 \sigma_s^2}{\sigma_z^2}. \quad (5.22)$$

As introduced in the beginning of this section, directly applying zero-forcing based precoding may cause transmission power increment. However, when the channel decomposition based precoding is applied, such transmission power increment can be avoided due to the normalization of the channel transfer matrix.

The normalized channel transfer matrix \mathbf{H}_{norm} comprises the diagonal elements which are all equal to 1 and off-diagonal elements which are corresponding to the crosstalk coupling coefficients. Due to the channel property, on each subcarrier k , the crosstalk transfer factor $H_{ij,k}$ from an interfering line j to a victim line i is normally much smaller than

the direct channel transfer factor $H_{ii,k}$ on line i : $H_{ij,k} \ll H_{ii,k}$. Correspondingly, after the normalization, the off-diagonal elements of precoding matrix \mathbf{H}_{norm} are far smaller than 1, i.e., the diagonal element: $\delta_{ij} \ll 1$, with $i \neq j$. Hence, the transmission power enhancement on the individual line i is

$$\left\| \left(\mathbf{H}_{\text{norm}}^{-1} \right)_{\text{row } i} \right\|^2 \approx 1, \quad (5.23)$$

meaning that there will be no significant transmission power increment.

Therefore, in the downstream transmission power control is also not necessary when precoding is applied to pre-equalize the crosstalk interference so that crosstalk-free transmission can be obtained.

5.3 System performance with perfect CSI

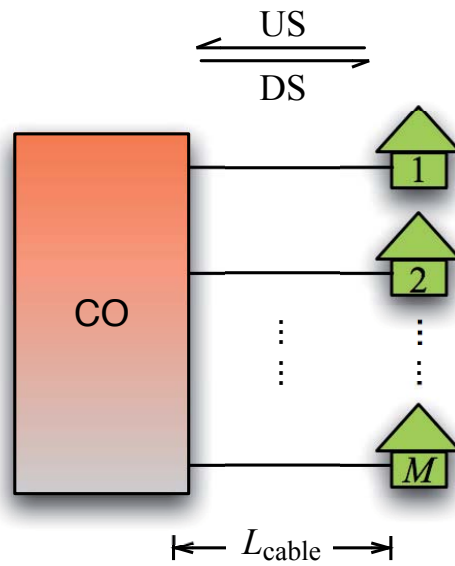
In this section, the data rate performance of the systems is evaluated in various scenarios. Referring to Figure 5.5 we consider the cable binders of equal length cables and different length cables, respectively, with the parameter of the line number in the cable binder M , in both upstream and downstream transmission. In the following, the simulation results are categorized by the transmission links: US transmission and DS transmission.

At this stage perfect CSI is assumed for the performance evaluation. The VDSL2 transmission systems with the bandwidth $W = 17.667\text{MHz}$ and the overall number of subcarriers $K = 4096$ are considered. The band plan 998ADE17 [ITU] defined by International Telecommunication Union (ITU) and approved by ETSI is shown in Table 5.1.

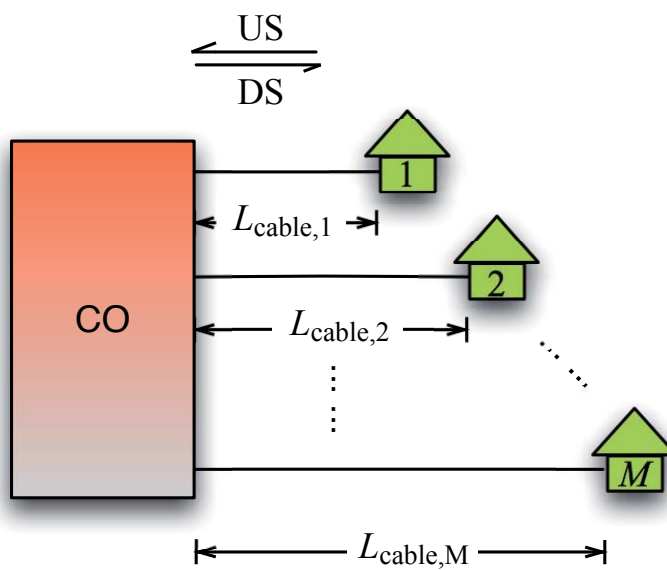
Table 5.1: Band plan

Band	Band-edge frequencies (kHz)
US0	120 - 276
DS1	276 - 3750
US1	3750 - 5200
DS2	5200 - 8500
US2	8500 - 12000
DS3	12000 - 17664

5.3. SYSTEM PERFORMANCE WITH PERFECT CSI



(a) Equal lengths scenario



(b) Different lengths scenario

Figure 5.5: Various scenarios

CHAPTER 5. CROSSTALK CANCELLATION

The achievable data rates are calculated by the SNR-gap capacity approximation introduced in Section 3.3, equation (3.15). The required symbol error rate for the transmission is 10^{-7} . No channel coding is applied. Hence, the coding gain is 0 dB. The noise margin is considered to be 6 dB. The other important system parameters used in the simulation are summarized in Table 5.2.

Table 5.2: System parameters

Parameter	Value
Bandwidth W	17.664 MHz
Number of subcarriers K	4096
Subcarrier spacing Δf	4.3125 kHz
Transmit symbol duration T_s	0.232 ms
DMT symbol rate f_s	4 kHz
Transmit PSD	-60 dBm/Hz
Background noise PSD	-140 dBm/Hz

Current VDSL system standards require that modems transmit under a special mask of -60dBm/Hz. It is assumed here that all modems are operating at this mask in the simulations.

5.3.1 Simulation results in US transmission

a) Cable binder with equal length cables

In the upstream transmission, we first consider the scenario as shown in Figure 5.5a . In this scenario all individual twisted cable pairs in the cable binder have the same length L_{cable} , which also represents the length of the cable binder. The simulation runs from the cable binder length of 0.3 km to the length of 1.2 km with 0.1 km increase.

Figure 5.6 depicts the data rate performance in case that the zero-forcing based crosstalk cancellation procedure is applied or not. The performance for crosstalk free transmission is also shown as a reference. The number of cable lines in the binder M is considered to be 10. In this case, the data rate performance is averaged over 10 cable lines.

It can be observed that for the relatively short length of cable binders, e.g. less than 0.8 km, the data rate performance degradation due to the crosstalk among adjacent cables

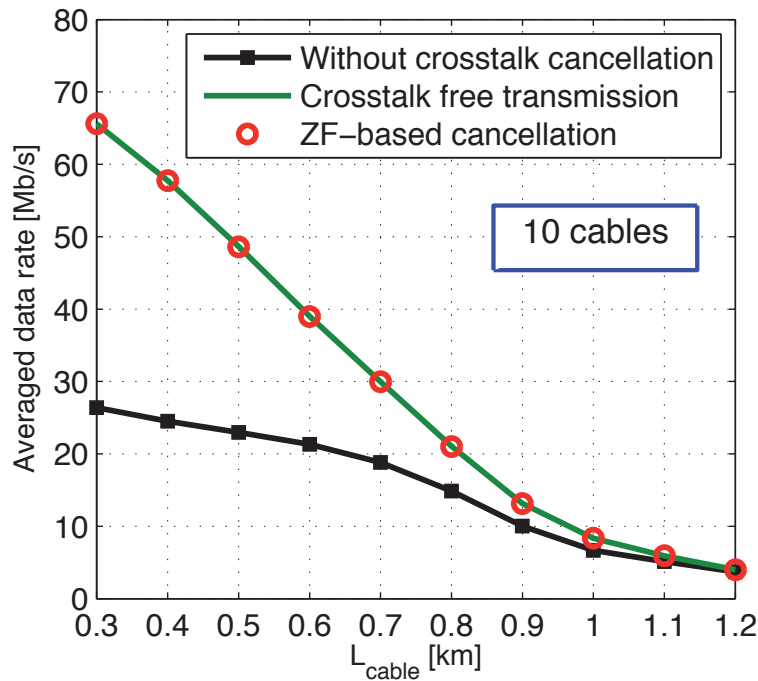


Figure 5.6: US averaged data rates performance in an equal length cable binder

are very high compared with the performance of the cable lines without the existence of crosstalk interference. However, when a zero-forcing based canceller is applied, crosstalk interference is fully eliminated as shown in the figure and a huge performance gain is achieved.

Figure 5.7 shows a similar performance figure as shown in Figure 5.6. But the number of cable lines in the binder M is consider to be 25 and the data rate performance is averaged over 25 lines.

As the solid line without any symbol shows the performance of the achievable data rate in an ideal case, namely the crosstalk free case, the performance curve is exactly the same as in Figure 5.6. However, since more cable lines are considered in this case, the crosstalk interference level for the individual lines in the binder increases. Therefore, as shown in Figure 5.7, without crosstalk cancellation, the averaged data rates among 25 lines is decreased. In another view, the gap between the crosstalk free performance and the performance without applying any cancellation scheme becomes larger. Thankfully, the gap can be filled out by the zero-forcing based canceller.

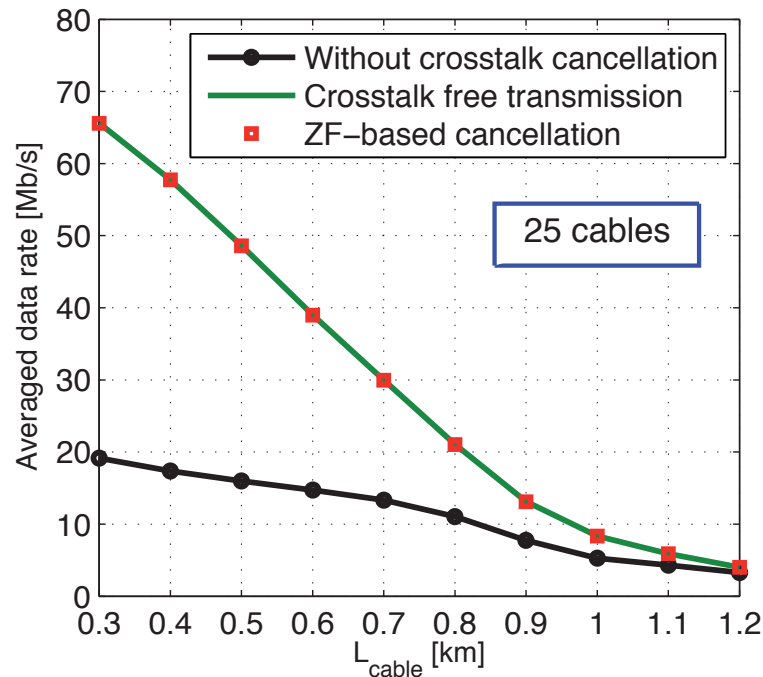


Figure 5.7: US averaged data rates performance in another equal length cable binder

It should be noticed that although the performance curves of zero-forcing based cancellation in both Figures 5.6 and 5.7 look similar, they are indeed corresponding to two different systems. As the zero-forcing based cancellation scheme can eliminate all crosstalk interference components in the systems, it provides great advantages in those cable binders with large number of cable lines, e.g., the cable binder corresponding to the performance in Figures 5.7. More specifically, in such cable binders, crosstalk interference level is very high, and without cancellation the data rate performance is poor even for the short transmission distance. In this case, when zero-forcing based cancellation is applied, crosstalk free performance can be achieved by spending the computation complexity to fully eliminate all crosstalk components in the binder.

It can also be noticed that in both Figures 5.6 and 5.7, the three data rate performance curves tend to be the same when the cable binder length gets very long, e.g. more than 1 km. This phenomenon is due to the reason that with very long cable length, the direct channel transfer factors of cable lines attenuate so much and correspondingly the crosstalk interference also gets smaller. In this case, background noise in the system becomes the dominant factor of performance degradation. Therefore, crosstalk cancellation does not play an important role in these systems any more.

b) Cable binder with different length cables

In this subsection the scenario shown in Figure 5.5b is considered, wherein the individual cable lines in the binder have completely different lengths denoted by $L_{\text{cable},i}$.

Similar as in the cable binder with equal length cables, performance evaluation is firstly done for a cable binder with $M = 10$ lines. The lengths range from 0.3 km to 1.2 km with 0.1 km increase.

Figure 5.8 shows the data rate performance of the individual lines with and without zero-forcing based cancellation compared with that of crosstalk free transmission. Reference performance figure of crosstalk free transmission is used.

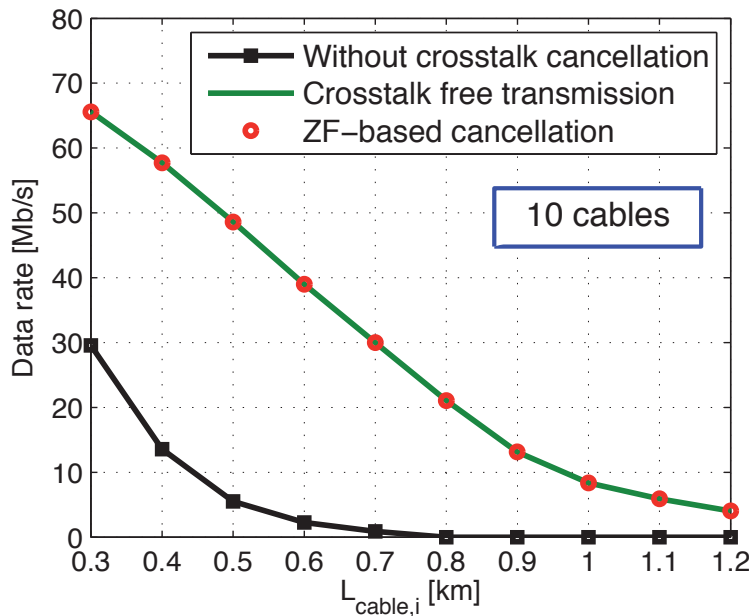


Figure 5.8: US data rate performance in a different length cable binder

Similar to the performance figures in case of equal length cable binder, a large gap between the data rates obtained without crosstalk cancellation and crosstalk free transmission can be observed and zero-forcing based cancellation successfully achieves the crosstalk free performance.

When comparing with the performance curve in Figure 5.6, it can be further observed in Figure 5.8 that on the one hand, for the very short line, i.e., the one with 0.3 km long, the



CHAPTER 5. CROSSTALK CANCELLATION

data rate obtained without crosstalk cancellation is a bit higher; on the other hand, the performance of cable lines with longer lengths is dramatically decreased.

This phenomenon is due to the reason that in the upstream transmission without crosstalk cancellation, the data rate of one cable line is strongly influenced by the cable lines having transmitters closer to the co-located receivers. Therefore, the short length cables in a cable binder with different lengths do have the distance advantage in comparing with the longer ones and the longer cable lines suffer from the stronger interference coming from the shorter lines. Consequently, the obtained data rate of a short length cable in the cable binder with different length cables is a bit higher than the averaged data rate assuming all cable lines have the same lengths in the binder. And in contrast, for the longer length cables in the non-equal-length binder, the data rate tends to be very low as the interference from shorter length cables getting higher. As shown in Figure 5.8, the cable lines with lengths longer than 0.7 km can barely transmit anything and even the data rate of the middle range cable lines is much lower than they were in the binders with equal lengths.

Despite the fact that without crosstalk cancellation the data rate performance of the major cable lines gets much worse than that in the equal length cable binders, the achieved data rate performance with zero-forcing based cancellation is not much influenced by the lengths of the other lines in the cable binder. Thus, we can conclude that zero-forcing based cancellation also provides advantages in the cable binders with different cable lengths.

Furthermore, we consider more cable lines in a cable binder, for example, arranging the cable lines from 0.3 km to 1.2 km with 0.05 km increase. In this case, there are $M = 19$ cable lines in the binder. Similarly, the system performance in terms of the data rates achieved with and without zero-forcing based cancellation as well as crosstalk free transmission is shown in Figure 5.9.

Not surprising, the data rates obtained by some of these 19 cable lines in the case without crosstalk cancellation become lower than the corresponding cable lines' performance shown in Figure 5.8 since the number of lines in the binder increases and the interference level for individual lines also increases. In this scenario, without cancellation, the individual cable lines suffer from crosstalk interference so much that the data rates of major lines tend to be zero. In other words, data transmission on the major cable lines in the binder is not possible any more.

However, by applying the zero-forcing based cancellation technique, crosstalk free performance can be achieved for the individual lines in the binder and the data transmission over longer length cables is enabled.

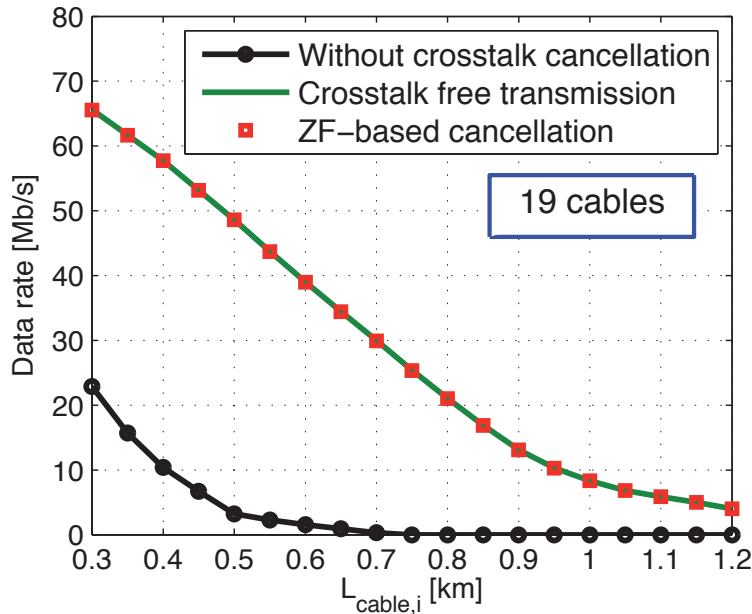


Figure 5.9: US data rate performance in another different length cable binder

In summary, zero-forcing based cancellation provides significant performance enhancement in the upstream transmission, especially in the cable binder with a large number of lines and/or with different cable lengths where some of cable lines suffer so much from the crosstalk interference coming from the adjacent lines that data transmission is barely possible. Optimal performance in terms of the data rates for crosstalk free transmission can be nearly achieved by zero-forcing based cancellation.

5.3.2 Simulation results in DS transmission

In this subsection, system performance in the downstream transmission is investigated. Similar to the case in the upstream transmission, performance evaluation is done also in two scenarios as shown in Figures 5.5a and 5.5b. Furthermore, our discussions are mainly focused on the similarities and the differences of the observations in comparing with the upstream transmission.

a) Cable binder with equal length cables

Figures 5.10 and 5.11 depict the data rate performance of the system according to the first scenario shown in Figure 5.5a. Both simulations run from the cable binder length of

CHAPTER 5. CROSSTALK CANCELLATION

0.3 km to the length of 1.2 km with 0.1 km increase. However, the former figure shows the performance for the cable binder comprising $M = 10$ lines and the latter corresponds to the binder with $M = 25$ lines.

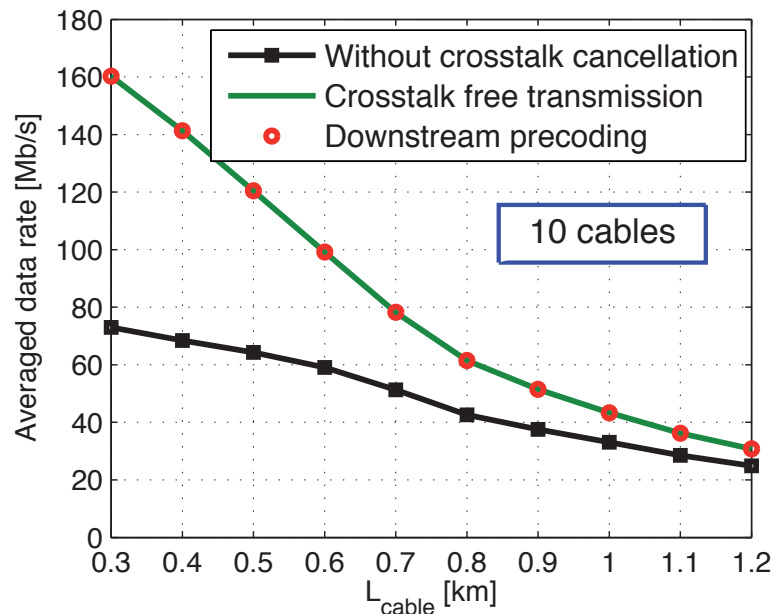


Figure 5.10: DS averaged data rates performance in an equal length cable binder

In both performance figures, the averaged data rates are shown for the case that channel decomposition based precoding is applied or not. The optimal performance in terms of crosstalk free transmission is also shown as a reference.

Similar to the performance obtained in upstream transmission, in the equal length cable binder, the averaged data rates achieved in downstream transmission without performing precoding are influenced by the cable binder lengths and by the number of the adjacent crosstalk interference components. In general, although the crosstalk interference level for each cable line decreases as the cable length increases, the achieved averaged data rate decreases along with the cable binder length as shown in both figures since the direct channel attenuation increases faster than the rate of crosstalk decreasing.

It can also be observed that a significant data rate gap exists between the performance of crosstalk free transmission and that of the transmission without crosstalk cancellation, namely without downstream precoding. In particular, when the cable binder contains more cable lines, the performance gap becomes larger.

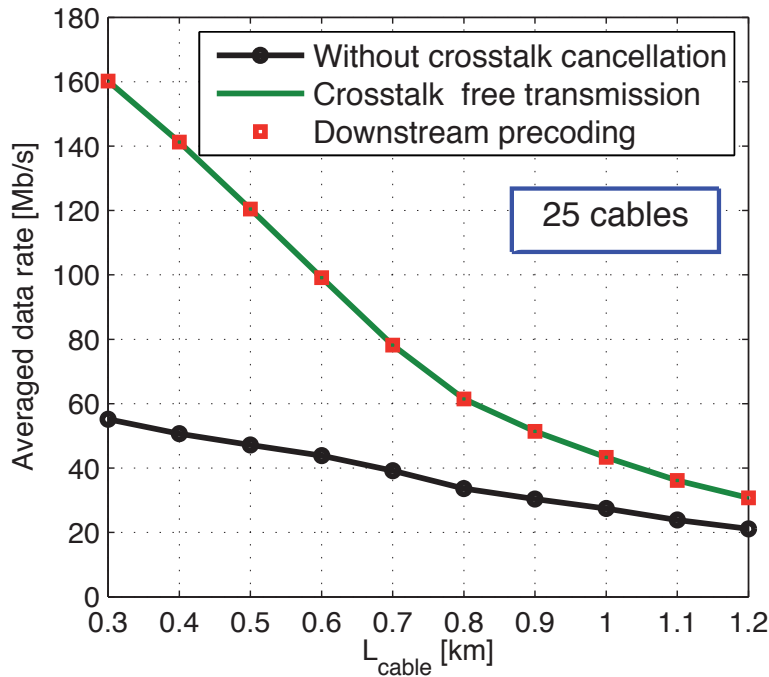


Figure 5.11: DS averaged data rates performance in another equal length cable binder

Fortunately, such gap is filled up by performing channel decomposition based precoding as the proposed precoding technique fully eliminates the crosstalk interference for each individual cable line.

b) Cable binder with different length cables

Next, we consider the downstream transmission in the scenario shown in Figure 5.5b, where individual twisted cable pairs in the binder have different lengths $L_{\text{cable},i}$.

The cable length parameters chosen for the binder with different length cables in the upstream transmission are also used here in the downstream. The cable lengths range from 0.3 km to 1.2 km and even increasements of 0.1 km and of 0.05 km are considered, respectively. In other words, data rate performance in a cable binder of $M = 10$ cables and in another $M = 19$ cable binder has been evaluated and the corresponding quantitative results are shown in Figure 5.12 and Figure 5.13 .

In contrast to the other scenarios previously considered, it can be observed in both performance figures that without precoding, the data rate performance of all cable lines tend to be similar as that of the cable line with 1.2 km, i.e. the worst performance. The gaps when compared with the performance of crosstalk free transmission are extremely large

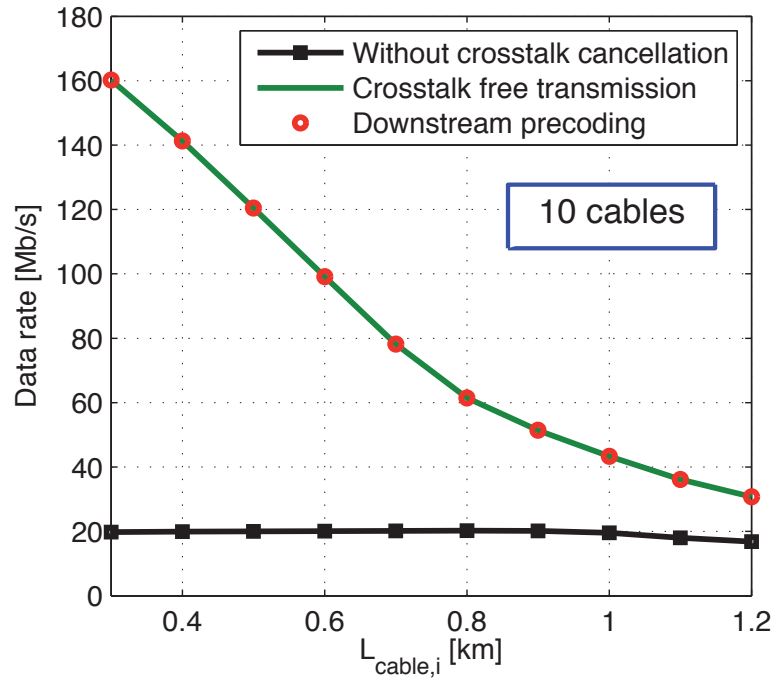


Figure 5.12: DS data rate performance in a different length cable binder

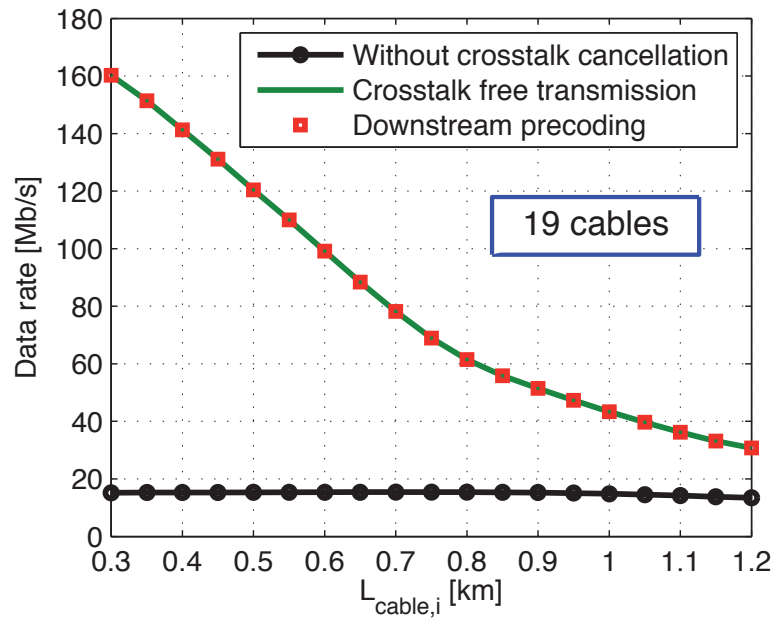


Figure 5.13: DS data rate performance in another different length cable binder

5.3. SYSTEM PERFORMANCE WITH PERFECT CSI

in both figures. In general, the achieved data rate for a cable line is only about 10% to 50% of the data rate without crosstalk interference.

However, such phenomenon is not difficult to be understood: although the short cable lines experience smaller direct channel attenuation when compared with those longer cable lines, they do suffer from much higher level crosstalk interference. As shown in equation (2.10), the transfer factors H_{ij} of the crosstalk interference to the victim line i is proportional to the direct channel attenuation H_i . Although the crosstalk coupling coefficient δ_{ij} increases for longer lines, the direct channel transfer function H_i is the dominant factor and causes higher interference level to short lines and lower interference level to long lines in a cable binder.

Therefore, for the downstream transmission in the binder with different length cables, high data rate transmission is barely possible without precoding. Even for the short lines in the cable binder, the performance is very poor. Channel decomposition based precoding provides a possibility to enable high data rate transmission which achieves the performance as crosstalk free.

In this chapter, subcarrier-based crosstalk cancellation techniques are introduced for VDSL2 systems. In particular, zero-forcing based upstream crosstalk cancellation and downstream channel decomposition based precoding are proposed. System performance in terms of achievable data rates is evaluated in both upstream and downstream transmission. Cable binders with different numbers of lines M have also been considered. Perfect CSI is assumed on the receiver side in the upstream and on the transmitter side in the downstream.

It is shown that the proposed upstream zero-forcing based crosstalk cancellation technique and downstream channel decomposition based precoding technique provide crosstalk free performance and significantly burst the data rates when compared with the performance achieved without applying any crosstalk cancellation technique.

More specifically, in the upstream transmission the data rate performance without cancellation is severely affected by the number of lines in the cable binder, i.e., the number of adjacent crosstalk components. It also strongly depends on the length of the individual cable line. In particular, within the cable binder having cables with different lengths, the middle range and long range lines can barely transmit anything. Thus, zero-forcing based cancellation in the upstream provides great advantages in performance enhancement, especially in the cable binder having a large number of cable lines and/or with different cable lengths.



CHAPTER 5. CROSSTALK CANCELLATION

In the downstream transmission, the data rate performance without precoding/cancellation is also affected by the number of lines in the binder, especially for the binders having equal length cables. Moreover, in the binders with cables having different lengths, the performance of all cables are very poor and tends to be same as the worst performance corresponding to the longest cable line. High data rate transmission is not possible without precoding. However, when the proposed channel decomposition based precoding is applied, it is possible to boost the data rates of the existing cables lines and achieve very high system performance.

6 Channel Estimation

In the previous chapter it is shown that nearly optimal performance can be achieved in the upstream transmission with zero-forcing based crosstalk cancellation or in the downstream transmission with channel decomposition based precoding, given the perfect CSI. However, in reality perfect CSI could never be known a priori. So, one of the key issues in the transmission applying crosstalk cancellation schemes is channel estimation (CE). The performance of the cancellation techniques highly relies on the estimation of the crosstalk channel among cable pairs as well as the direct channels of each individual cable pair.

In general, the channels of DSL copper lines are regarded as time-invariant channels. However, they might change very slowly with temperature, humidity, pressure and so on [DRR10]. More severe cases will occur when newly activated users generate new channels. So, channel estimation algorithms in the considered VDSL2 systems should be able to deal with different scenarios and provide fast, reliable and accurate estimation of CSI for upstream crosstalk cancellation and downstream precoding.

6.1 Introduction

For coherent demodulation, channel estimation techniques have long been investigated in wireline transmission systems as well as in wireless transmission systems. The main task of the channel estimation is to provide the receiver and/or transmitter the channel information as accurate as possible so that the channel influence can be compensated. Typically, channel estimation techniques could be considered to estimate the channel impulse response (CIR) with the time domain signal processing based on its deterministic or stochastic parameters [ZJOP03], [VdBES⁺95],[MB00], or to estimate the channel transfer functions with the frequency domain signal processing [HW98], [CEPB02a], or to estimate the channel based on both time and frequency characteristics of the channel [LCJS98].

As introduced in the previous chapters, in multiple-line DMT based transmission systems a frequency selective channel can be converted into a large number of parallel flat

CHAPTER 6. CHANNEL ESTIMATION

channels and ISI is eliminated by extending the symbol duration. Under such condition, crosstalk interface among adjacent cable lines can be handled much more easily per sub-carrier in frequency domain than in the time domain. Therefore, it is straightforward in this thesis to consider the channel estimation techniques in frequency domain for each individual subcarrier.

In general, the classical channel estimation techniques for conventional Single-Input-Single-Output (SISO) system fall in three main categories: channel estimation with pilot symbols, blind channel estimation and semi-blind channel estimation.

Channel estimation using pilot symbols which are known by both transmitter and receiver is a prominent technique. On the transmitter side, the pilot symbols are inserted into data symbols and are transmitted over the physical channel. With each pilot symbol, channel measurement can be made. Pilot symbols are transmitted periodically in time and spread over the whole frequency band so that channel estimation can be performed [BFH⁺98].

Typically, depending on how the pilot symbols are allocated in the two-dimensional time-frequency grid for OFDM systems, there are three major types of pilot patterns [TL07]: the *comb-type* in which pilot symbols are always allocated at a fraction of the subcarriers in the considered frequency band, the *block-type* in which pilot symbols are allocated on all subcarriers but such pilot OFDM symbols are interleaved with data OFDM symbols, and the *mixed-type* including e.g., the rectangular-type, diamond-type, linearly increasing-type etc. [CL04], in which pilot symbols are allocated in a fraction of the subcarriers and different pilot OFDM symbols are interleaved with data OFDM symbols.

On the receiver side, the pilot symbols are first analyzed to obtain the CSI at the pilot position, and then the CSI at the other data position is interpolated by employing the coherence between channel samples in time and frequency directions [CEPB02b] [CEPB02a]. Finally, the data symbols can be estimated at the receiver.

The second category is the so-called blind channel estimation/identification techniques. In these techniques, pilot symbols are not used and the techniques are mainly based on second or higher order statistics, for example, applying correlation methods at the receiver [ZDS00] [CA00]. The blind channel identification techniques have the benefit of reducing the overhead compared with the pilot based techniques, however might suffer from the slow convergence rate.

The third category is the semi-blind channel estimation/identification techniques. Limited pilot symbols are used in conjunction with blind algorithms so as to improve the convergence rate and reduce the computation complexities. For example, a decision-directed channel estimation method is introduced in [RGR⁺03].

In this chapter we mainly focus on the channel estimation techniques based on pilot symbols and extend the conventional methods used in SISO systems so as to be applied in the multiple-line transmission systems.

6.2 Pilot based channel measurement

Pilot symbol based channel measurement is a well established technique to measure the channel transfer factors. In multiple-line DMT systems, the channel measurement can be performed subcarrier-wise. Figure 6.1 and Figure 6.2 show the block diagrams of pilot based channel measurement for subcarrier k in a multiple-line DMT system with upstream crosstalk cancellation and downstream precoding, respectively.

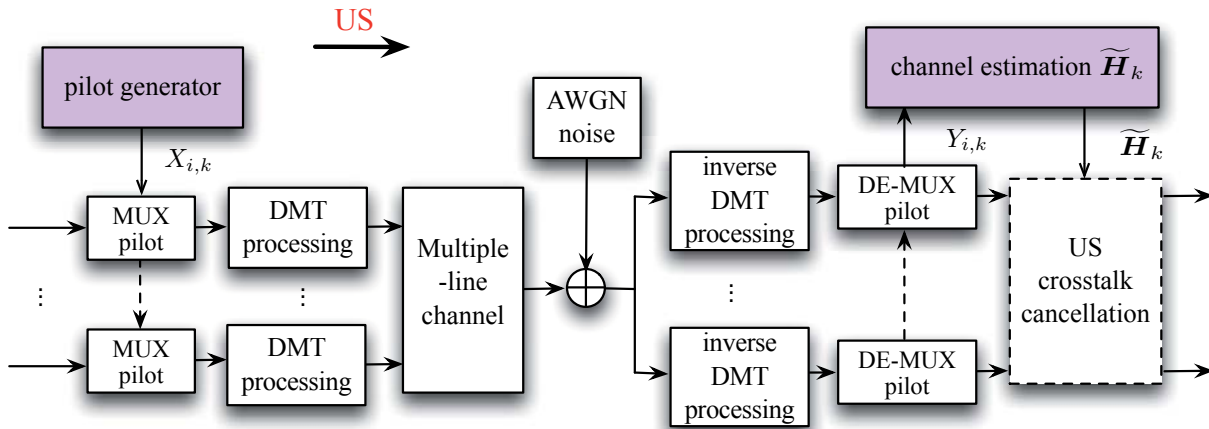


Figure 6.1: Block diagram of the US pilot based channel measurement

Referring to the two figures, the procedure of the pilot based channel measurement in the system can be described as follows. On the transmitter side, pilot symbol $X_{i,k}$ is generated for each line $i, \forall i \in [1, M]$ on the k -th subcarrier and integrated before performing DMT modulation on each line according to a pilot distribution pattern. The modulated symbols are transmitted over the multiple-line channel with transfer function \mathbf{H}_k . On the receiver side, after inverse DMT modulation the received pilot symbol $Y_{i,k}$ for each line i is extracted for measuring the channel transfer matrix \mathbf{H}_k on subcarrier k of the multiple-line channel:

Given the known modulated symbol, pilot symbol $X_{j,k}, \forall j \in [1, M]$, a single complex division at the receiver i yields the measurement of the channel transfer factor

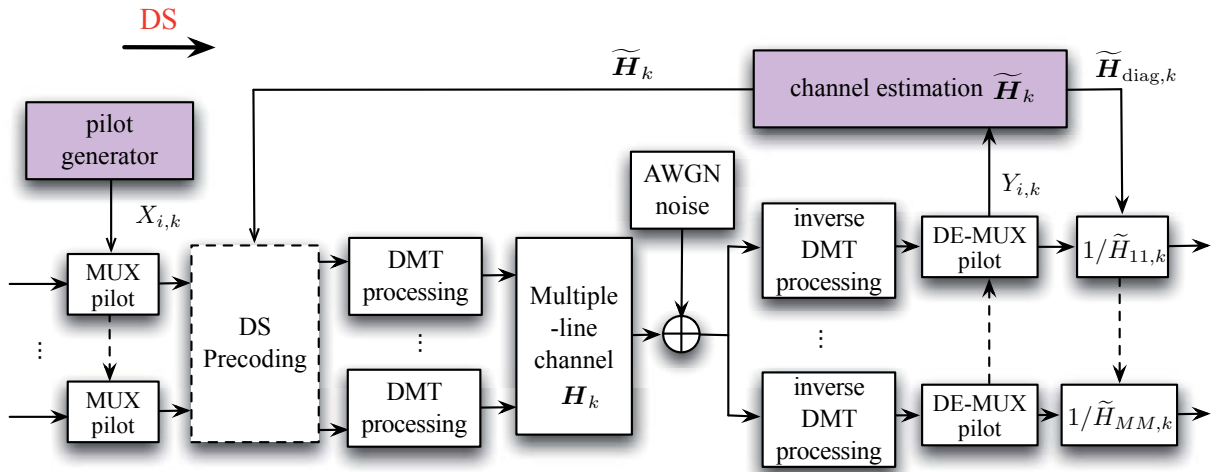


Figure 6.2: Block diagram of the DS pilot based channel measurement

$$\tilde{H}_{ij,k} = \frac{Y_{i,k}}{X_{j,k}}. \quad (6.1)$$

According to the expression of a received signal shown in equation (4.1), the measurement error $\varepsilon_{ij,k}$ of the channel transfer factor $H_{ij,k}$ on subcarrier k can be calculated as:

$$\begin{aligned} \varepsilon_{ij,k} &= \tilde{H}_{ij,k} - H_{ij,k} \\ &= \underbrace{\sum_{m=1, m \neq j}^M \frac{H_{im,k} X_{m,k}}{X_{j,k}}}_{\text{Interference}} + \underbrace{\frac{Z_{i,k}}{X_{j,k}}}_{\text{Noise}} \end{aligned} \quad (6.2)$$

comprising the noise portion and the interference portion.

As shown in Figure 6.1, in the upstream transmission the estimated results \tilde{H}_k can be directly applied for the upstream crosstalk cancellation. However, in the downstream transmission CSI has to be fed back to the transmitter side as the receivers are located distributedly and precoding is performed in the centralized transmitters. According to the proposed channel decomposition based precoding in Section 5.2, it is only needed to feed back the off-diagonal coefficients of matrix $\tilde{H}_{norm,k}$, which is obtained by normalizing the estimated channel transfer matrix \tilde{H}_k with the corresponding estimated direct channel transfer factor $\tilde{H}_{ii,k}$ of each line i . Then, the normalized matrix $\tilde{H}_{norm,k}$ is applied on the transmitter side for the downstream precoding as shown in Figure 6.2 and the direct channel transfer factor $\tilde{H}_{ii,k}$ is used at the receiver side for the equalization for each individual line i .

Several techniques for channel estimation with pilot symbols have been introduced in [RDR08]. In the following, the techniques for reducing the channel estimation error in view of the interference and/or noise in the multiple-line transmission are described.

6.3 Step-by-step technique with a single pilot symbol

A straightforward way to eliminate crosstalk interference in measuring the crosstalk and direct channel coefficients simultaneously is to transmit pilot symbols exclusively for a single cable line, i.e. to sequentially transmit the pilot symbols cable by cable. The transmission pattern for M copper lines in M time slots is illustrated in Figure 6.3.

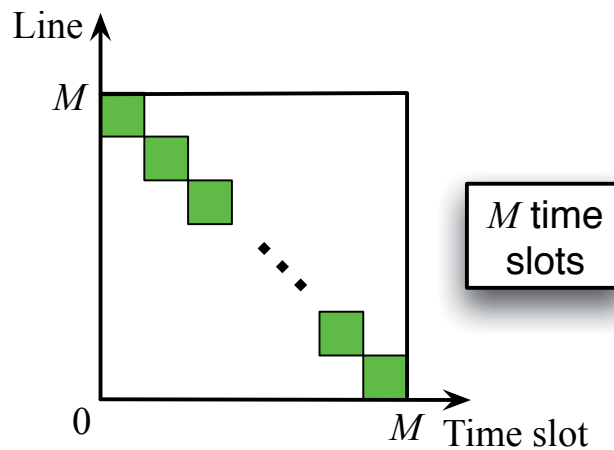


Figure 6.3: Transmission pattern for the step-by-step technique

In each time slot, a single transmitter j transmits a pilot symbol $X_{j,k}$ on subcarrier k and all receivers $i, \forall i \in [1, M]$ detect the signals and further estimate the crosstalk coefficients $\{H_{ij,k}\}, \forall i \neq j$ and the direct channel coefficient $H_{jj,k}$. The procedure continues from one transmitter to another until all channel and crosstalk coefficients $\{H_{ij,k}\}, \forall i, j \in [1, M]$ are estimated.

By this means, the received signal in a certain time slot at a receiver $i, \forall i \in [1, M]$ is

$$Y_{i,k} = H_{ij,k}X_{j,k} + Z_{i,k}, \quad (6.3)$$

which contains only the direct channel component and the measurement noise at the j -th receiver or contains only a crosstalk component and the measurement noise at an

arbitrary receiver i , $i \neq j$. Therefore, the crosstalk coefficient or direct channel coefficient $H_{ij,k}$, $\forall i, j \in [1, M]$ can be easily estimated as

$$\tilde{H}_{ij,k} = H_{ij,k} + \frac{Z_{i,k}}{X_{j,k}}. \quad (6.4)$$

In this case, the interference in the measurements is fully eliminated and the crosstalk and channel measurements are effected only by noise:

$$\varepsilon_{ij,k} = \tilde{H}_{ij,k} - H_{ij,k} = \frac{Z_{i,k}}{X_{j,k}}. \quad (6.5)$$

Based on the average transmit power σ_s^2 and noise power σ_z^2 , the mean squared error (MSE) of the channel estimation procedure for each crosstalk or channel coefficient can be described quantitatively as:

$$\text{MSE} = E\left\{\left|\varepsilon_{ij,k}\right|^2\right\} = \frac{\sigma_z^2}{\sigma_s^2}. \quad (6.6)$$

In this pilot based technique, the estimation of the crosstalk and channel matrix $\tilde{\mathbf{H}}_k$ is performed in a step by step procedure. During each time slot, a single column of the matrix $\tilde{\mathbf{H}}_k$ is estimated in the upstream or downstream transmission. In total, at least M time slots corresponding to the number of cable lines are needed to estimate the complete crosstalk and channel matrix $\tilde{\mathbf{H}}_k$.

6.4 Techniques to improve the estimation accuracy

As shown in equation (6.5) the resulting MSE of the estimation procedure is influenced by the noise power and the transmit power. To improve the estimation quality and resulting accuracy the following three alternatives of pilot signal structures as illustrated in Figure 6.4 could be considered:

(a) A pilot sequence of length L instead of a single pilot symbol is transmitted for each cable line. In this case the total transmit energy is increased, the MSE is reduced and the estimation accuracy is improved by a factor of L . However, the measurement time is also extended by a factor of L .

(b) A set of L orthogonal pilot sequences each of which comprises L pilot symbols is transmitted over the adjacent cable lines. For example, a set of Walsh-Hadamard orthogonal

6.4. TECHNIQUES TO IMPROVE THE ESTIMATION ACCURACY

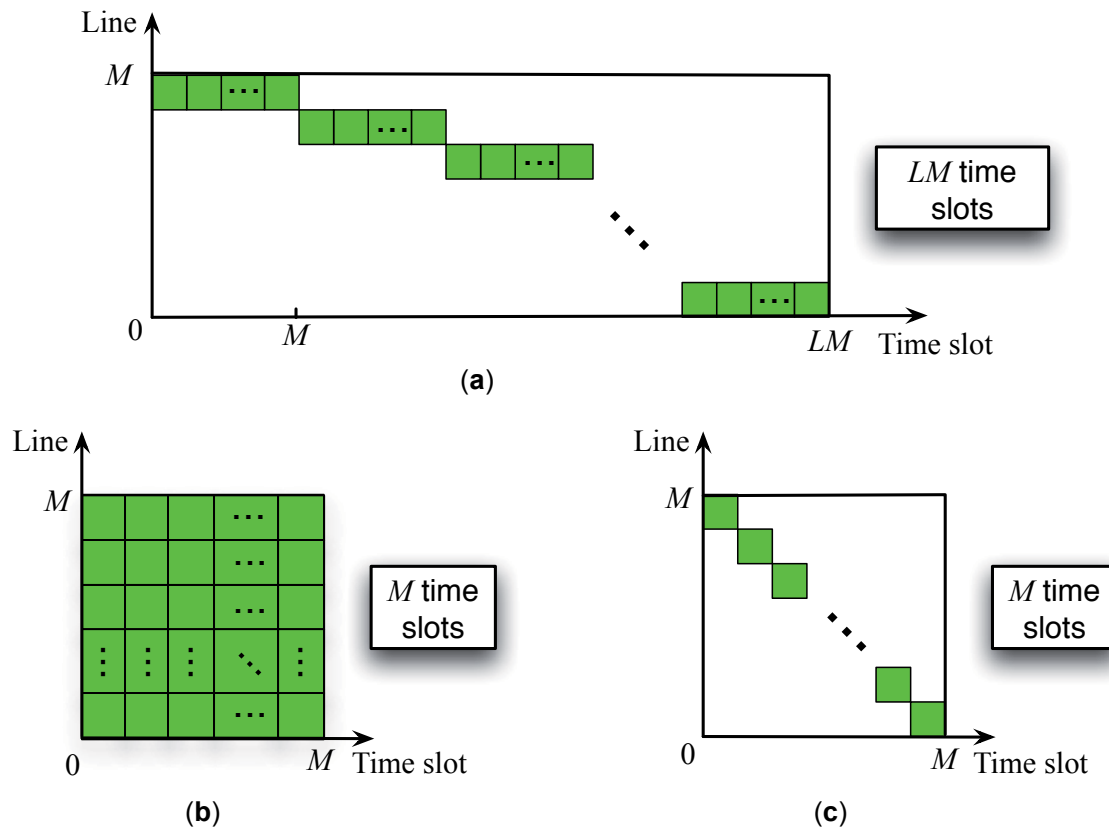


Figure 6.4: Pilot pattern for the improved measurement accuracy

sequences can be applied. In this case again the overall transmit energy is increased, the MSE is reduced and the estimation accuracy is improved by the factor of L . The measurement time is not extended in this case.

(c) Pilot symbols are transmitted with the power boosted by L times. The estimation accuracy is improved in the same way as in case (b).

With all these three pilot signal patterns, the MSE of the estimation procedure and for each crosstalk coefficient is reduced by the factor of L to

$$\text{MSE} = \frac{\sigma_z^2}{L \cdot \sigma_s^2}. \quad (6.7)$$

Although in Figure 6.4a the pilot sequence of each cable is illustrated as a sequence transmitted in a consecutive way, it is also possible to arrange the pilot symbols for a cable line with the spacing of the time slot for transmitting the pilot symbols for other cable

lines. In this case, the transmission of a pilot sequence of one line is interrupted by the transmission of the pilot sequence of other lines, for example, as shown in Figure 6.5.

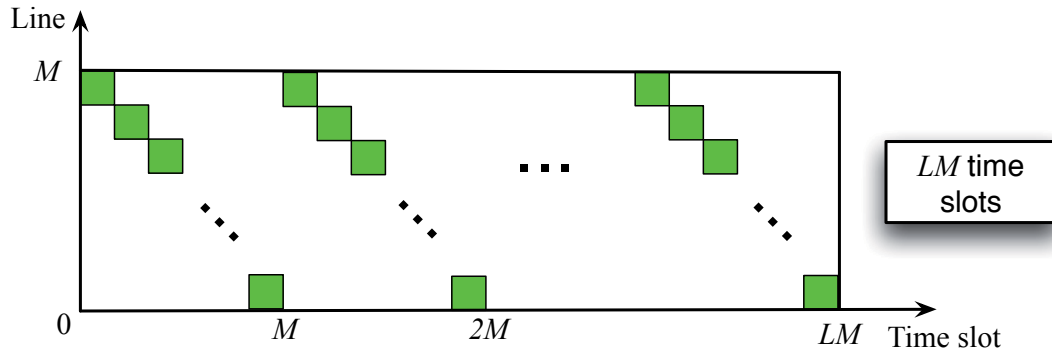


Figure 6.5: Alternative pilot pattern for the improved measurement accuracy

6.5 System performance with estimated CSI

In this section, system performance in terms of the achievable data rates with respect to different channel estimation accuracies is investigated with upstream crosstalk cancellation as well as downstream precoding.

The basic system parameters are set as in Table 5.2 of Section 5.3.

6.5.1 Simulation results in US transmission

In the upstream transmission, we consider the scenario where copper lines with different lengths are comprised in the cable binder. The scenario is shown in Figure 5.5b.

To have a better comparison, the parameters of the number of lines M and the length of each individual line are chosen to be the same as those in Section 5.3.1.b: $M = 10$ and the line lengths range from 0.3 km to 1.2 km with 0.1 km increase.

In Figure 6.6, the data rates achieved by the upstream crosstalk cancellation schemes with estimated channel as well as with perfect channel knowledge are illustrated.

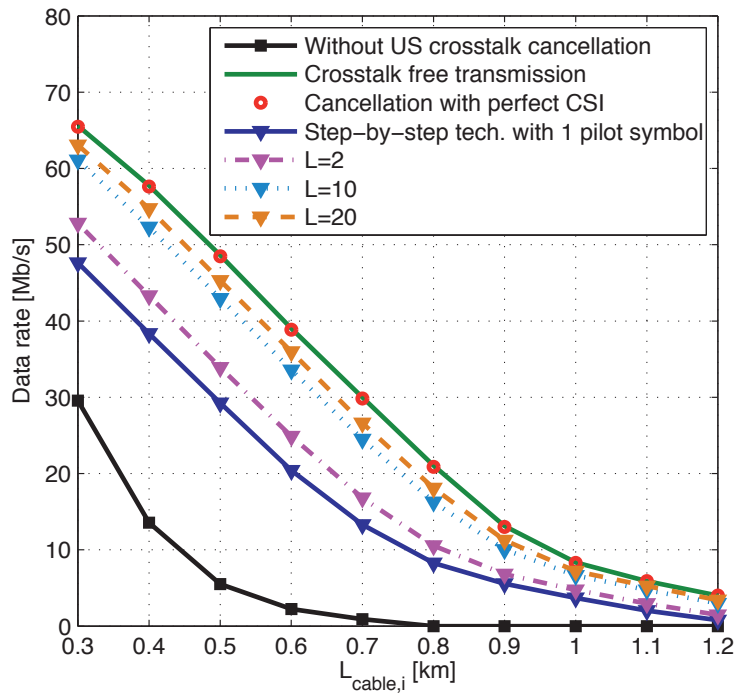


Figure 6.6: US achievable data rates based on pilot sequences

It can be observed that although the data rates achieved by using a cancellation technique with perfect CSI can approach the data rates obtained in the crosstalk free transmission, there is a significant data rate loss in the crosstalk cancellation procedure if the CSI is provided by the step-by-step technique with a single pilot symbol being applied. Therefore, the estimation accuracy has to be improved.

According to Section 6.4, the channel estimation accuracy can be improved by a factor L . Figure 6.6 further shows three performance curves with the factor L equal to 2, 10 and 20, respectively. From the curves, how the estimation accuracy influences the achievable data rates can be observed. In particular, we can find that when the factor L grows to 10, the gap between the performance with perfect CSI and with estimated CSI has been significantly reduced and there is left only a very small performance loss due to the channel estimation.

6.5.2 Simulation results in DS transmission

Similar to the upstream transmission, the scenario as shown in Figure 5.5b is considered in the downstream transmission. The number of lines M is chosen to be 10 and cable lines in the binder are arranged from 0.3 km to 1.2 km with 0.1 km increase.

Figure 6.7 shows the data rate performance which is achieved by the discussed precoding procedure with estimated channel coefficients and perfect CSI as well as the worst case assumption where no precoding is applied. Similar to the case of the upstream transmission, the data rates decrease a lot if the estimated channel information is obtained by the step-by-step technique with just one single pilot symbol for each line.

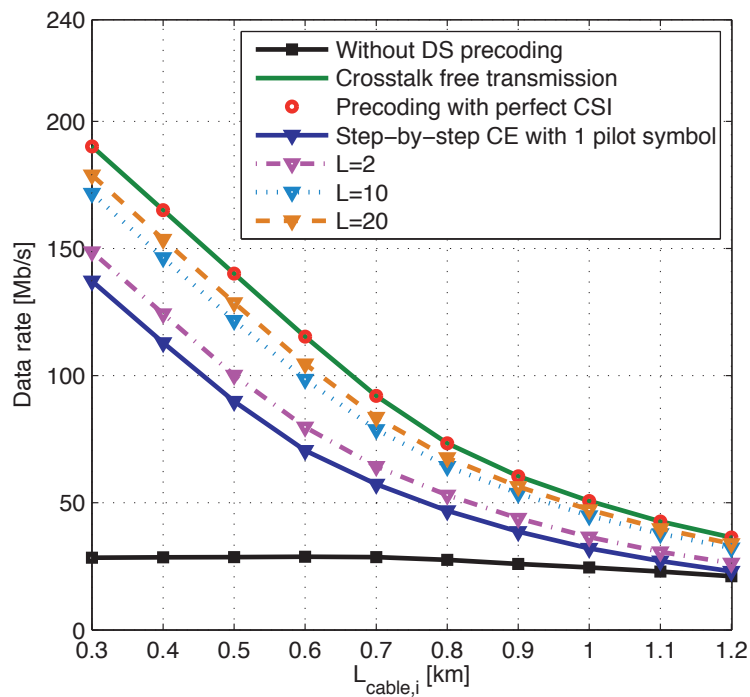


Figure 6.7: DS achievable data rates based on pilot sequences

Figure 6.7 also shows how strongly the system performance is improved if the crosstalk measurement accuracy is increased. The precoding technique shows nearly the same performance enhancement with respect to the improvement of the crosstalk measurement accuracy. With the factor $L = 10$, the resulting data rate with estimated crosstalk coefficients are close to the performance of an ideal case.

6.5. SYSTEM PERFORMANCE WITH ESTIMATED CSI

In this chapter, the upstream crosstalk cancellation schemes as well as downstream precoding schemes are evaluated in case there is provided non-perfect channel knowledge. The step-by-step technique based on pilot signals is proposed for channel and crosstalk estimation. Three alternatives of pilot signal structures are further introduced to improve the quality and resulting accuracy of the estimation by a factor of L .

Performance curves Figures 6.6 and 6.7 illustrate the fact how the achievable data rates are affected by the channel estimation quality and accuracy for the upstream and downstream transmission, respectively. It can be observed that there exists significant performance loss due to the limited channel estimation accuracy. However, the performance curve can be improved by the proposed three techniques in both upstream and downstream transmission. With the factor $L = 10$, the data rates achieved by the crosstalk cancellation techniques with estimated channel knowledge are already close to the performance of the ideal case. Moreover, similar performance improvement of the data rates can be observed in both transmission directions.

7 Crosstalk Cancellation with Complexity Reduction

In Chapter 5, subcarrier-based crosstalk cancellation techniques are introduced for VDSL2 systems. It has been shown that tremendous performance gain in terms of achievable data rates can be obtained by applying the proposed zero-forcing based upstream crosstalk cancellation and downstream channel decomposition based precoding techniques. But unfortunately, such performance gain never comes alone: a high computational complexity has to be paid.

Supposing a cable binder comprises $M + 1$ cable lines, the crosstalk cancellation for such a cable binder requires a computational complexity of $\mathcal{O}(M^2)$ multiplication for each tone/subcarrier. So, for a single DMT symbol, $\mathcal{O}(KM^2)$ multiplications have to be processed, where K is the number of tones. In a realistic system with 30 cable lines inside a single binder, a DMT symbol rate of 4KHz and $K = 4096$ tones, the complete crosstalk cancellation will lead to a computation complexity of 1.5×10^{10} multiplication/sec, which is a huge burden to the hardware implementation. Therefore, it is of interest to find low complexity crosstalk cancellation techniques which provide a reasonable trade-off between the achievable data rates and the computation complexity to be paid.

In this chapter techniques for reducing computation complexity in the subcarrier-based crosstalk cancellation schemes are introduced. The trade-off between computation complexity and resulting system performance is analyzed.

For convenience, the notation M is used to indicate the number of crosstalk interference components instead of the total number of cable lines hereafter. Furthermore, perfect synchronization as well as perfect channel state information is assumed in the systems.

7.1 Partial crosstalk cancellation

It has been found out that the crosstalk coupling between adjacent cables can be very different from lines to lines. In most cases, the major crosstalk interference for a certain line comes from only a few "crosstalkers", for example, the directly adjacent cables in the binder. This is mainly due to the geometry of the cable binder or the near-far situation of the lines. Therefore, it is theoretically possible to neglect the small crosstalk interference components during the crosstalk cancellation procedure so that the computation complexity of crosstalk cancellation can be reduced.

In this section, partial crosstalk cancellation schemes cancelling only the crosstalk interference from the lines that cause the most interference are introduced. The objective is to maximize the data rates given a certain computation complexity in terms of the number of multiplication for the cancellation. The partial crosstalk cancellation schemes in both upstream and downstream transmission are investigated and the trade-off between achievable data rates and the computation complexity is studied.

7.1.1 Upstream partial crosstalk cancellation

In a multiple-line channel transfer matrix \mathbf{H}_k on subcarrier k , the diagonal element $H_{ii,k}$ represents the direct channel transfer factor of receiver i and the non-diagonal elements $\{H_{ij,k}\}, \forall j \neq i$ in the i -th row of matrix \mathbf{H}_k corresponds to the individual crosstalk transfer factors generated from other cable lines to line i . Therefore, partial crosstalk cancellation can be processed for each line i by properly selecting the crosstalk components to be cancelled or to be neglected in the cancellation.

As partial cancellation is to be performed in the same way on each subcarrier, the subcarrier index k is dropped for the variables in the following description to clarify the notations.

Define index set Ω_i as the set of the line indices showing the lines which generate the crosstalk interference components to be cancelled in the partial cancellation scheme for line i . The elements of set Ω_i should exclude index i : $\Omega_i \subseteq \{1, 2, \dots, M, M+1\} \setminus i$. The corresponding complement set $\bar{\Omega}_i$ contains the indices of the crosstalk components which are neglected in the cancellation procedure. For each cable line i , a shrunk crosstalk matrix \mathbf{T}^i can be generated from the channel transfer matrix \mathbf{H} by first crossing out the rows and columns corresponding to the crosstalk components neglected in the partial cancellation procedure and then ordering the shrunk matrix so that its first element describes the direct channel of line i .

The individual shrunk matrix for line i can be mathematically represented as

$$\mathbf{T}^i = \begin{pmatrix} H_{ii} & (\mathbf{H})_{\text{row } i, \text{cols } \Omega_i} \\ (\mathbf{H})_{\text{rows } \Omega_i, \text{col } i} & (\mathbf{H})_{\text{rows } \Omega_i, \text{cols } \Omega_i} \end{pmatrix} \quad (7.1)$$

where $(*)_{\text{rows } \Omega_i, \text{cols } \Omega_i}$ denotes the submatrix formed by the rows Ω_i and columns Ω_i of the original matrix $(*)$.

As an example, Figure 7.1 illustrates this procedure of generating the shrunk crosstalk matrix \mathbf{T}^i for line i . It is assumed that the upstream partial crosstalk cancellation is to be performed on line 3 in a cable binder which comprises 8 cable lines. The dimension of the channel transfer matrix \mathbf{H} is chosen purely for the purpose of convenience in drawing. Each block in the figure represents an element in matrix \mathbf{H} .

Supposing that set $\Omega_{i=3}$ is selected as $\{1, 4, 5\}$ in this example, namely the crosstalk interference components generated by lines 1, 4 and 5 are selected to be cancelled for the victim line 3, the crosstalk channel transfer factors with respect to transmission lines $\bar{\Omega}_{i=3} = \{2, 6, 7, 8\}$ are thus not considered in the partial crosstalk cancellation procedure. Consequently, the corresponding elements in the rows $\bar{\Omega}_{i=3}$ and columns $\bar{\Omega}_{i=3}$ of the channel transfer matrix \mathbf{H} can be crossed out and the shrunk matrix can be obtained. The shrunk matrix is then further rearranged so that the first row of the obtained crosstalk matrix $\mathbf{T}^i, i = 3$ describes the channel information of the considered victim line 3.

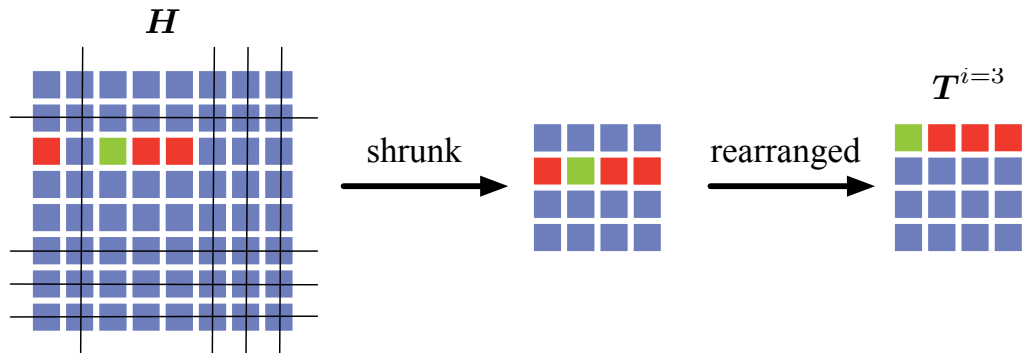


Figure 7.1: Crosstalk matrix regeneration in the US partial crosstalk cancellation scheme

Having obtained the shrunk crosstalk matrix \mathbf{T}^i for line i , a receive signal vector \mathbf{Y}^i containing only those received signals needed in the partial crosstalk cancellation is prepared

7.1. PARTIAL CROSSTALK CANCELLATION

for line i in a received vector selection procedure shown in Figure 7.2. In this line-wise procedure, the elements of the receive signal vector \mathbf{Y}^i are selected and arranged in accordance with the channel and crosstalk element indices in the shrunk crosstalk matrix \mathbf{T}^i :

$$\mathbf{Y}^i = \begin{pmatrix} Y_i \\ (\mathbf{Y})_{\Omega_i} \end{pmatrix}. \quad (7.2)$$

Therefore, the first element of the receive signal vector \mathbf{Y}^i is the received signal on line i and the other elements correspond to the received signals on those lines which generate the crosstalk interference to be cancelled in the partial cancellation scheme.

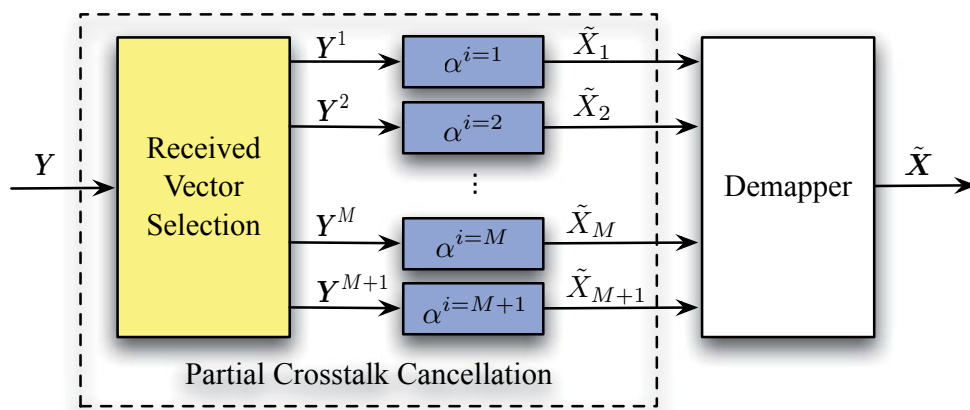


Figure 7.2: The receiver structure in the US partial crosstalk cancellation scheme

Further, zero-forcing based crosstalk cancellation is performed among the victim line i and the selected lines which generate the crosstalk interference considered in the partial cancellation scheme. The rest of the lines in the cable binder are omitted in the interference cancellation procedure. Define the partial cancellation coefficients for line i as a vector

$$\boldsymbol{\alpha}^i = \left((\mathbf{T}^i)^{-1} \right)_{\text{row } 1}, \quad (7.3)$$

which is the first row of the inverse of the shrunk crosstalk matrix inverse \mathbf{T}^i . As illustrated in Figure 7.2, the transmit signal on line i is thus estimated as

$$\tilde{X}_i = \boldsymbol{\alpha}^i \mathbf{Y}^i. \quad (7.4)$$

It has been shown in Section 5.1.2 that the upstream zero-forcing based crosstalk cancellation can fully eliminate the crosstalk interference considered in the cancellation scheme

and the remaining noise is scaled by the cancellation coefficients. Similarly, in the partial crosstalk cancellation scheme, the crosstalk interference components being selected and considered in the cancellation are fully removed, and the rest of the interference components being treated as noise are scaled by the cancellation coefficients.

The receive signal vector \mathbf{Y}^i indeed can be described mathematically as

$$\mathbf{Y}^i = \mathbf{T}^i \mathbf{X}^i + \bar{\mathbf{T}}^i (\mathbf{X})_{\bar{\Omega}_i} + \mathbf{Z}^i, \quad (7.5)$$

with the vectors $\mathbf{X}^i = \left(X_i, (\mathbf{X})_{\Omega_i}^T \right)^T$ and $\mathbf{Z}^i = \left(Z_i, (\mathbf{Z})_{\Omega_i}^T \right)^T$ representing the transmit signal vector and noise vector corresponding to the selected and rearranged receive signal vector \mathbf{Y}^i for the partial crosstalk cancellation on line i and matrix $\bar{\mathbf{T}}^i$ including all the crosstalk transfer factors concerning those interference components not being considered in the partial cancellation procedure for line i :

$$\bar{\mathbf{T}}^i = \begin{pmatrix} (\mathbf{H})_{\text{row } i, \text{cols } \bar{\Omega}_i} \\ (\mathbf{H})_{\text{rows } \Omega_i, \text{cols } \bar{\Omega}_i} \end{pmatrix}. \quad (7.6)$$

Hence, the estimated transmit signal on each line i can be expressed as

$$\tilde{X}_i = X_i + \alpha^i \left(\bar{\mathbf{T}}^i (\mathbf{X})_{\bar{\Omega}_i} + \mathbf{Z}^i \right), \quad (7.7)$$

which comprises only the transmit signal on line i and the scaled summation of the noise and crosstalk interference not considered in the partial cancellation.

The obtained SINR in this case can be calculated for line i as

$$\text{SINR}_i = \frac{\sigma_s^2}{\left\| \alpha^i \bar{\mathbf{T}}^i \right\|^2 \sigma_s^2 + \left\| \alpha^i \right\|^2 \sigma_z^2}. \quad (7.8)$$

7.1.2 Downstream partial crosstalk cancellation

As described in Section 5.2, crosstalk interference cancellation in the downstream transmission can be performed on the transmitter side since in the CO, the transmitters are co-located and downstream precoding can be done with the normalized channel transfer matrix \mathbf{H}_{norm} instead of the crosstalk transfer matrix \mathbf{H} used in the upstream transmission. The partial crosstalk cancellation structure introduced in the upstream transmission can be applied in a similar way in the downstream transmission.

Downstream partial crosstalk cancellation is also a line-wise processing and the precoding matrix is obtained by calculating the precoding coefficients for each line. Figure 7.3 shows the procedure of obtaining the precoding matrix in downstream partial cancellation.

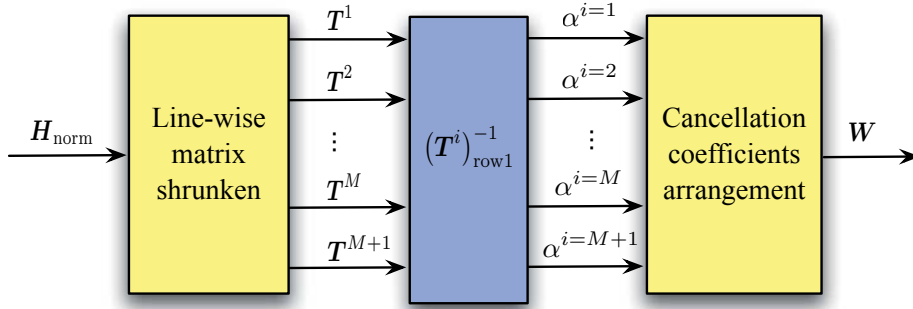


Figure 7.3: Precoding matrix generation in the DS partial crosstalk cancellation scheme

Starting with the normalized channel transfer matrix \mathbf{H}_{norm} , each line i generates its own shrunk crosstalk matrix \mathbf{T}^i with an index set Ω_i . The set Ω_i denotes the properly selected lines considered in the downstream partial cancellation scheme. The procedure of generating a shrunk matrix is illustrated in Figure 7.1 and described in detail in Section 7.1.1.

Again, defining the partial cancellation coefficients α^i for line i as the first row of the inverse of the shrunk crosstalk matrix inverse \mathbf{T}^i , the vector α^i is calculated as in equation (7.3) for each cable line. The precoding matrix \mathbf{W} for all cable lines in the partial crosstalk cancellation scheme is then obtained by first arranging the individual elements of each partial cancellation coefficient vector α^i into its i -th row according to the indices Ω_i and then padding zeros to those entries of matrix \mathbf{W} corresponding to the interference components being neglected in the partial cancellation scheme. In other words, the partial precoding matrix \mathbf{W} is arranged so that the following expression is fulfilled:

$$\alpha^i = \left(W_{ii}, (\mathbf{W})_{\text{row } i, \text{cols } \Omega_i} \right). \quad (7.9)$$

With the obtained precoding matrix \mathbf{W} , crosstalk cancellation can be applied to all cable lines in the binder and the transmit signals after this processing can be expressed as

$$\mathbf{P} = \mathbf{W}\mathbf{X}. \quad (7.10)$$

Since the precoding matrix \mathbf{W} contains only the coefficients for cancelling the crosstalk interference considered in the partial cancellation procedure and zeros are padded in the

entries corresponding to the neglected crosstalk components, the precoding is performed partially among each victim line and the properly selected lines which generate crosstalk interference. Nevertheless, the transmission and reception structures in downstream partial crosstalk cancellation remain unchanged as shown in Figure 5.4 and the received signal vector \mathbf{Y} can be also described by equation (5.19) omitting the subcarrier index k .

Although in downstream partial crosstalk cancellation the precoding matrix \mathbf{W} differs from the precoding matrix $\mathbf{H}_{\text{norm}}^{-1}$ in the ordinary downstream crosstalk cancellation scheme, the equalization on the receiver side can be performed in the same way for each individual line i as described in equation (5.20).

The estimated signals for all $M + 1$ cable lines can further be expressed as:

$$\tilde{\mathbf{X}} = \mathbf{H}_{\text{norm}} \mathbf{W} \mathbf{X} + \mathbf{H}_{\text{diag}}^{-1} \mathbf{Z}, \quad (7.11)$$

and the estimated signal for each individual line i is calculated as:

$$\begin{aligned} \tilde{X}_i &= \left(\mathbf{H}_{\text{norm}} \right)_{\text{row } i} \mathbf{W} \mathbf{X} + \frac{Z_i}{H_{ii}} \\ &= X_i + \left(\mathbf{H}_{\text{norm}} \right)_{\text{row } i, \text{cols } \bar{\Omega}_i} \mathbf{X}_{\bar{\Omega}_i} + \frac{Z_i}{H_{ii}}. \end{aligned} \quad (7.12)$$

As shown in equation (7.12), partial crosstalk cancellation in the downstream transmission pre-processes the transmit signals so that the considered interference components with the indices Ω_i for a line i are fully removed on the receiver side and the rest of the interference components with indices $\bar{\Omega}_i$ are neglected in the partial cancellation procedure and remain in the estimation.

The SINR achieved in the downstream partial crosstalk cancellation scheme can be given as

$$\text{SINR}_i = \frac{|H_{ii}|^2 \sigma_s^2}{\sum_{j \in \bar{\Omega}_i} |H_{ij}|^2 \sigma_s^2 + \sigma_z^2}. \quad (7.13)$$

7.1.3 Crosstalk interference selection in the partial crosstalk cancellation schemes

As described in sections 7.1.1 and 7.1.2, the crosstalk interference components being cancelled for each line i have to be properly selected in the upstream or downstream partial crosstalk cancellation schemes and the indices of those lines which contribute those

7.1. PARTIAL CROSSTALK CANCELLATION

crosstalk components to the victim line i are given in the index set Ω_i . In this section, the algorithms of selecting the crosstalk interference components are introduced.

Equations (7.7) and (7.12) show that the estimated data signal \tilde{X}_i in both upstream and downstream partial cancellation schemes contains only scaled noise and crosstalk interference from the lines which are not considered in partial crosstalk cancellation. Ideally, the optimal selection of the crosstalk interference components for each line i to be cancelled out should guarantee that the remaining interference and noise contributions after partial cancellation are minimized.

However, as it also can be concluded from equations (7.7) and (7.12), the SINR increase of cancelling one particular crosstalker depends not only on the amount of the interference being cancelled but also on the existence of other crosstalk interference components. Apparently, enumerating all the possibilities and comparing the achievable data rates or SINRs are not practical due to the resource limitation in hardware. Thus, for the purpose of achieving the maximum data rate in the partial cancellation, we try to maximize the interference power being cancelled out. Two possible selection algorithms can be considered:

Algorithm 1: choose the index set Ω_i for each line i to contain those lines which can generate the most significant crosstalk interference contribution in the received signal Y_i .

This can easily be performed by sorting each row of the channel transfer matrix \mathbf{H} or the normalized channel transfer matrix \mathbf{H}_{norm} for the upstream or downstream transmission and looking for the largest elements for each line i .

Algorithm 2: choose the index set Ω_i for each line i to contain the lines $j, j \in \{1, 2, \dots, M, M+1\} \setminus i$ which provide the highest potential gain G_{ij} for line i :

$$G_{ij} = ld \left(1 + \frac{1}{\Gamma} \cdot \frac{|H_{ii}|^2 \sigma_s^2}{\sigma_z^2} \right) - ld \left(1 + \frac{1}{\Gamma} \cdot \frac{|H_{ii}|^2 \sigma_s^2}{|H_{ij}|^2 \sigma_s^2 + \sigma_z^2} \right). \quad (7.14)$$

The potential gain here is defined as the data rate loss due to one particular crosstalker j assuming no other crosstalkers existing. The higher the gain, the more crosstalk interference the crosstalker j might contribute to the estimated signal. Hence, the effect of the crosstalker j has to be considered in the signal processing procedure.

The second algorithm has also been proposed in [CGM⁺03]. With the assumptions $\frac{1}{\Gamma} \cdot \frac{|H_{ii}|^2 \sigma_s^2}{\sigma_z^2} \gg 1$ and $\frac{1}{\Gamma} \cdot \frac{|H_{ij}|^2 \sigma_s^2}{|H_{ij}|^2 \sigma_s^2 + \sigma_z^2} \gg 1$, the second selection algorithm is actually equivalent to the first one. The partial crosstalk cancellation schemes have been investigated with both of the selection algorithms in [Rua08] and it is shown that the performance difference due to two different algorithms are negligible. In this thesis, the first algorithm is used for the performance evaluation of the partial cancellation schemes.

Let q denote the number of crosstalk interference components to be removed in the crosstalk cancellation schemes. It may be selected from 0 to M , where $q = 0$ represents no cancellation and $q = M$ represents full cancellation. The computation complexity spent in the partial cancellation can be evaluated as the ratio of the number q to the total number of crosstalk components M .

7.2 System performance with partial crosstalk cancellation

In this section the system performance in terms of the data rates achieved in the partial crosstalk cancellation schemes is investigated in the upstream and downstream transmission. Different computation complexity requirements are given in the partial cancellation schemes. The data rates achieved with different complexities are compared.

Perfect channel knowledge is assumed and the system parameters used in the simulations are the same as those defined in Section 5.3. Furthermore, the system performance is categorized by different cable binders: the cable binder with equal length cables and the cable binder with different length cables.

7.2.1 Simulation results in the cable binders with equal length cables

First, the system performance with partial crosstalk cancellation in the cable binder with equal length cables is presented. The considered scenario is illustrated as in Figure 5.5a.

In this scenario all cable lines have the same cable length L_{cable} and in total there are 21 lines considered in the cable binder. In other words, there exist $M = 20$ crosstalk interference components for each line i . The performance simulation runs from the cable length L_{cable} equal to 0.3 km to 1 km with 0.1m increase.

Figures 7.4 and 7.5 show the performance results for the upstream and downstream transmission, respectively.

7.2. SYSTEM PERFORMANCE WITH PARTIAL CROSSTALK CANCELLATION

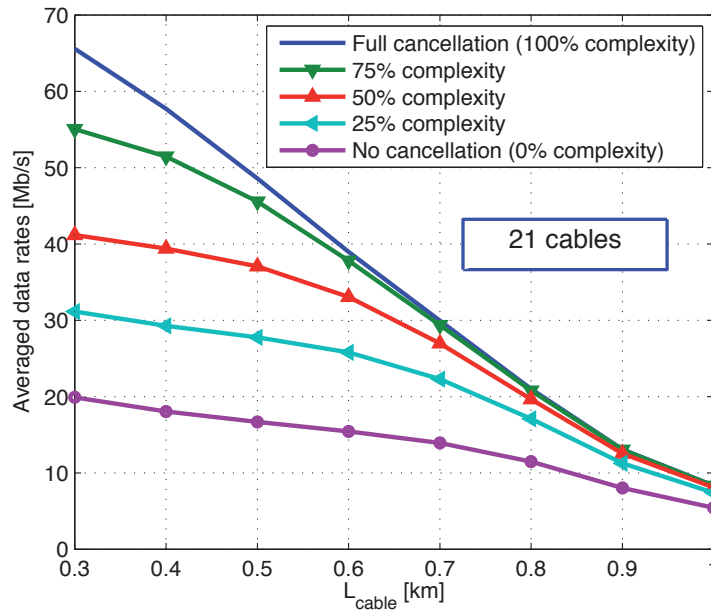


Figure 7.4: US partial crosstalk cancellation performance

In each transmission direction, the data rate curves obtained by partial cancellation schemes with different computation complexity are depicted with different markers. The effort spent on full crosstalk cancellation, i.e., $q = 20$ are referred to 100% complexity and the case where no crosstalk cancellation is performed corresponds to 0% complexity. The data rate curves for these two cases are plotted as reference.

Comparing to the case without crosstalk cancellation, a significant performance improvement can be observed in both figures even with 25% complexity spent. It can be further observed that for a cable binder with short length, for example, 0.3 km to 0.6 km, increasing the computation complexity up to 75% of the full cancellation complexity will improve the data rate performance in a relatively linear way. In such cable line binders, crosstalk interference is much higher than the background noise and acts as the major performance limitation. Furthermore, as the cable lengths in the binder are the same, the major crosstalk interference levels being strongly influenced by cable lengths are also very similar. Therefore, the data rate increase due to cancelling one interference component is relatively the same as that of cancelling another interference component.

However, for a binder with longer cable length, e.g., 0.7 km to 1 km, the major crosstalk interference components are higher than noise while the rest of the interference components may be not. Therefore, on the one hand, spending low computation complexity in partial cancellation can provide an obvious improvement of the data rate performance

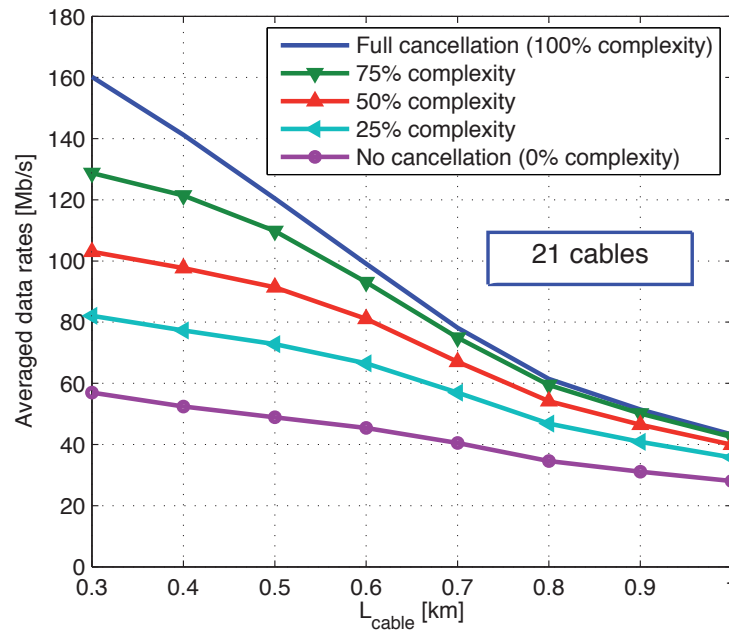


Figure 7.5: DS partial crosstalk cancellation performance

for the lines in those cable binders. On the other hand, after cancelling the most significant crosstalk components, the noise becomes more dominant in the system and near maximum SINR is achieved. In this stage, spending additional computation complexity, namely cancelling more interference components can not further improve the system performance.

Therefore, in such long length cable binders only a small number of interference components need to be considered in the partial crosstalk cancellation schemes. As shown in both Figure 7.4 and Figure 7.5, spending 50% of the full complexity can already achieve the performance close to that in the full crosstalk cancellation schemes. However, spending further computation effort, e.g., 75% complexity will not significantly improve the performance. In these cases, computation complexity can be saved without dramatically reducing the data rate performance.

7.2.2 Simulation results in in the cable binders with different length cables

After the discussion of the date rate performance in the binders which have the equal length cable lines, the performance in the cable binders with different length cables is

7.2. SYSTEM PERFORMANCE WITH PARTIAL CROSSTALK CANCELLATION

evaluated in this section for the upstream transmission as well as for the downstream transmission. The considered scenario is illustrated in Figure 5.5b.

Similar as in the previous section, the considered cable binder comprises in total 21 cable lines and for each cable line there are 20 crosstalk interference components. Whereas in the former scenario cable lines have the same length, in this scenario individual cable lines have different lengths $L_{\text{cable},i}, \forall i \in \{1, 2, \dots, 21\}$ which range from 0.3 km to 1 km with 35m increase.

a) Performance in the upstream transmission

Figure 7.6 illustrates the data rate performance achieved by the partial crosstalk cancellation with 50% computation complexity for the upstream transmission as an example. The achieved data rates of each line is plotted in bars. Line indices 1 to 21 are corresponding to the cable lines with the length $L_{\text{cable},i}$ equal to 0.3 km to 1 km. The performance results obtained with the full crosstalk cancellation and without crosstalk cancellation are also plotted in Figure 7.6. Therefore, for each line index i the data rates obtained in full cancellation, partial cancellation with 50% complexity and without cancellation are shown, respectively, by the bars with different colours.

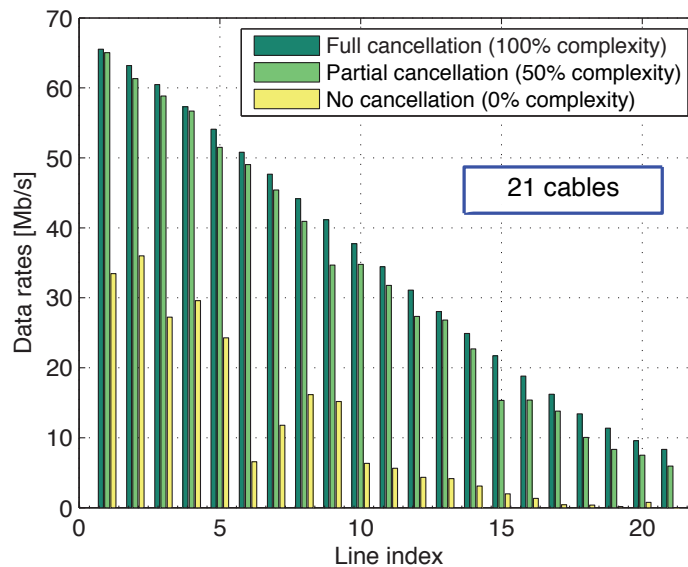


Figure 7.6: US partial crosstalk cancellation performance in terms of data rates

As illustrated in Figure 7.6, when full crosstalk interference is applied, the data rates of each individual line depends only on its cable length due to the complete elimination of crosstalk interference and decrease monotonically with respect to the increase of the

CHAPTER 7. CROSSTALK CANCELLATION WITH COMPLEXITY REDUCTION

lengths; if no cancellation procedure is performed, the achieved data rates of the cable lines do not monotonically decrease with the cable length due to the different crosstalk coupling among the lines in the binder. Shown in the figure, such non-monotonical decreasing also appears in the partial cancellation procedures since there is still crosstalk interference existing after partial cancellation.

Furthermore, it is very obvious that the partial crosstalk cancellation scheme spending only 50% complexity can already achieve magnificent performance. In particular, for those relatively shorter lines, the achieved data rates are nearly the same as the data rate obtained in the full crosstalk cancellation scheme. Even for the long lines, the performance is significantly improved and the obtained data rates are very close to those of the full crosstalk cancellation.

Figure 7.7 shows the performance of the partial crosstalk cancellation schemes in a different view. In the figure, the ratios between achievable data rate of partial cancellation and that of full cancellation versus computation complexity are plotted. Three performance curves for cable lines with 0.3 km, 0.65 km and 1 km representing there categories (the short-, middle- and long-range lines) are depicted.

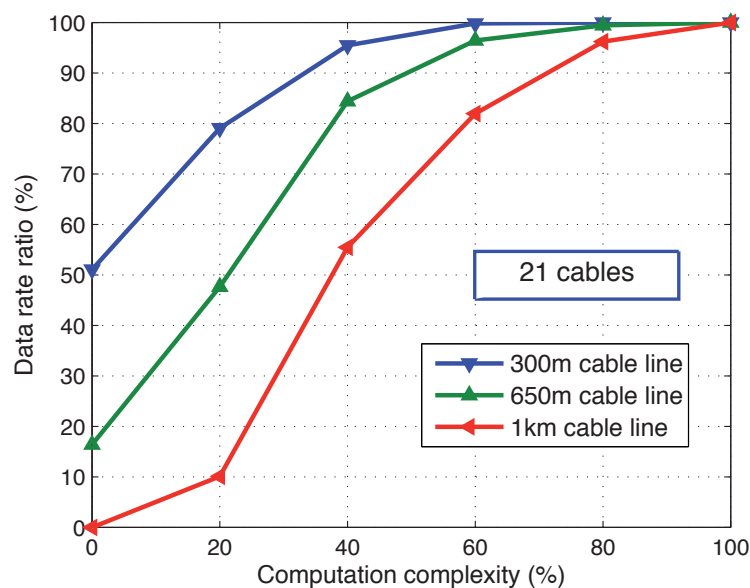


Figure 7.7: US partial crosstalk cancellation performance in terms of data rate ratios

It is observed that each curve starts with different data rate ratios and end up with the 100% data rate ratio corresponding to the full cancellation performance with 100% com-

7.2. SYSTEM PERFORMANCE WITH PARTIAL CROSSTALK CANCELLATION

putation complexity. Shorter cable lines start with higher data rate ratio obtained without crosstalk cancellation since they take advantage of less path loss in the upstream transmission. As the computation complexity spent on partial crosstalk cancellation increases, the data rate ratios of the short- and middle-range lines increase steadily until the computation complexity is increased to about 50% - 60% and the corresponding data rate ratio approaches to 100%. For the long cable lines, e.g. 1 km cable line, the data rate obtained without crosstalk cancellation is very low. As shown in Figure 7.6 barely nothing could be transmitted there. Hence, the starting point of the performance curve of 1 km cable line is close to 0. However, the long cable line does have a highest growing rate when the computation complexity increases.

From Figure 7.7 it can also be observed that when spending the same amount of the computation complexity on each line in the upstream transmission, a shorter line achieves higher performance, as a percentage relative to the ideal full cancellation performance, than the longer ones. In another view, if the same data rate ratios are required for all lines, more computation complexity had to be spent on the long cables.

b) Performance in the downstream transmission

With respect to the downstream transmission, the partial crosstalk cancellation performance in terms of achievable data rate is also evaluated and illustrated in Figure 7.8.

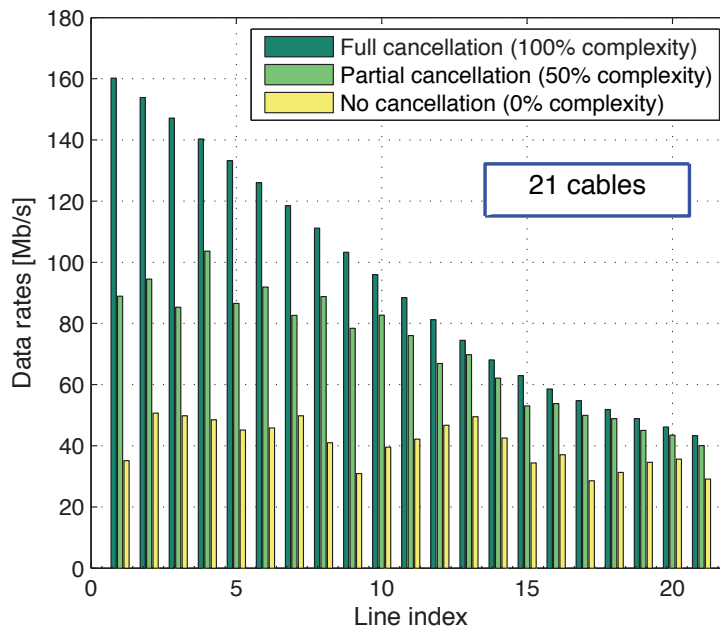


Figure 7.8: DS partial crosstalk cancellation performance in terms of data rates



CHAPTER 7. CROSSTALK CANCELLATION WITH COMPLEXITY REDUCTION

Similar to Figure 7.6, the data rate performance achieved by the partial crosstalk cancellation with 50% computation complexity as well as the performance obtained in full cancellation and without cancellation are plotted in Figure 7.8 with bars for the downstream transmission. The similarities to the upstream transmission will not be addressed and we focus on the different observations or aspects in the downstream transmission with respect to the upstream one.

In the downstream transmission, as shown in Figure 7.8, the achieved data rates for all cable lines without performing crosstalk cancellation are actually at the similar level although the data rate obtained in full cancellation are dramatically different. In other words, the potential gains of applying partial crosstalk cancellation on shorter lines are much higher than longer ones. This is due to the fact that although longer cable lines experience higher attenuation in their direct channel, the crosstalk interference in longer lines also reduced dramatically due to the long transmission distance. For the shorter lines, although the direct channel attenuation is not large, the crosstalk interference is also quite high. So the SINR values obtained in the receivers of short and long cable lines are not much different from each other.

When apply 50% computation complexity in the partial cancellation scheme, the data rate performance of each line is improved. However, shorter cable lines and longer ones improve their performance in a different manner. Clearly, the shorter lines gain much larger amount of the data rate increases than the longer ones. For example, line 1, the 0.3 km cable line has about 50 Mbit/s gain whereas line 16, the 0.825 km cable line gains only about 20 Mbit/s. Therefore, considering a system trying to obtain high overall data rate, spending more computation complexity for crosstalk cancellation on shorter lines would be a wise choice.

With respect to the full data rates achieved by the full crosstalk cancellation scheme, the partial crosstalk cancellation with only 50% computation complexity in longer lines can already provide the data rate performance close to that achieved by full cancellation. However, in the shorter lines, although the data rates are significantly increased, still more crosstalk interference components have to be considered in the cancellation if the full capacity of the cable lines is to be explored. In this aspect, longer lines achieve the near full cancellation performance more easily than the shorter cables. This can be more clearly observed in Figure 7.9.

As the data rate performance without crosstalk cancellation of short lines and longer ones are quite similar whereas the performance with full cancellation on short lines is much higher than that of the longer cables, the data rate ratio of short lines are much lower than those of longer ones when crosstalk cancellation is not applied. As illustrated in

7.2. SYSTEM PERFORMANCE WITH PARTIAL CROSSTALK CANCELLATION

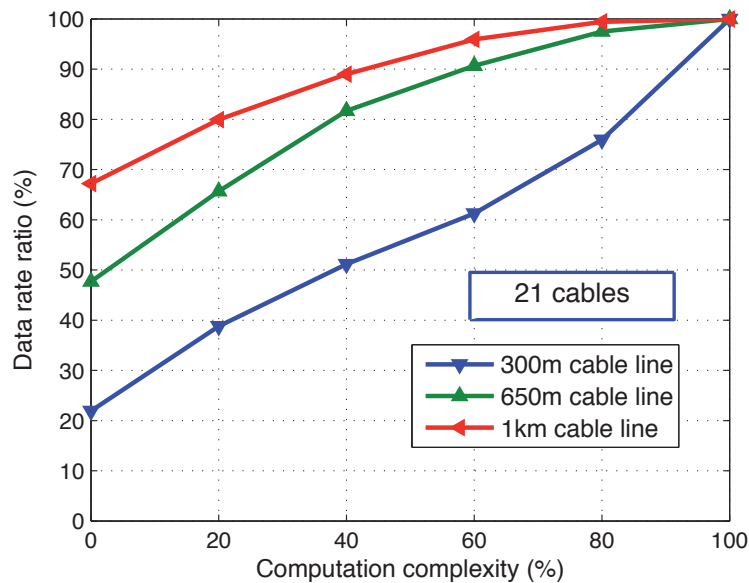


Figure 7.9: DS partial crosstalk cancellation performance in terms of data rate ratios

Figure 7.9, the starting points of each performance curves rank from high to low as the long cable, middle-range cable and then the short cable.

It can also be observed that in the downstream transmission, the long cable obtains a high percentage of data rate ratio with relatively low computation complexity in partial cancellation: spending 40% partial cancellation complexity, 90% of the full data rate on the 1 km cable line can be achieved. In contrast, more computation complexity needs to be spent on the middle-range line, and for the very short line, e.g., 0.3 km cable line plenty of computation effort is indeed needed to reach a certain performance close to the data rate obtained in the full crosstalk cancellation scheme.

In this chapter, the line-wise partial crosstalk cancellation schemes reducing the computation complexity in crosstalk cancellation techniques are introduced and the performance of the cancellation scheme in terms of the achievable data rates as well as the data rate ratios is investigated in both upstream and downstream transmission. The performance evaluation is made for the cable binders with the same cable length and those with different cable lengths, respectively.

For the cable binders with the same cable length, the partial crosstalk cancellation schemes in the up- and downstream transmission perform similarly for improving the achievable data rates. It is shown that with no more than half of the computation complexity spent in full crosstalk cancellation, most cable lines in the binder can achieve the data rate performance close to that of full cancellation.



CHAPTER 7. CROSSTALK CANCELLATION WITH COMPLEXITY REDUCTION

For the cable binder with different cable lengths, the partial crosstalk cancellation schemes perform a bit differently in the upstream and downstream transmission. In the upstream transmission with relatively low complexity spent in partial crosstalk cancellation all cable lines can already obtain quite good performance gain. Furthermore, if the same data rate ratio between the achieved rate on each line and its corresponding full rate are required, more computation complexity has to be spent on the long cables than the shorter ones. In the downstream transmission, the potential performance gain in terms of the achievable data rates on short cable lines is magnificently larger than that of long cable lines. The partial crosstalk cancellation schemes with relatively low computation complexity, e.g. 40% to 50% of the full cancellation can provide very good performance for long cable lines. However, the short cable lines starting with very low data rates comparing with their full data rates improve their achievable data rate substantially by every increase of the computation complexity spent in partial cancellation.

In summary, the proposed line-wise partial crosstalk cancellation schemes can be very flexibly applied in the upstream and downstream transmission with different given computation complexity requirements. Hence, a good trade-off can be provided by the partial cancellation schemes between the data rate performance and the computation complexity needed to be spent for crosstalk cancellation.

8 QoS-aware Crosstalk Cancellation

In Chapter 5, zero-forcing based upstream crosstalk cancellation and channel decomposition based downstream precoding are introduced in VDSL2 systems which are able to provide significant performance gain by means of eliminating all the crosstalk interference components in the systems. Considering the limitation of computation complexity in practical systems, the partial crosstalk cancellation schemes dealing with the most significant crosstalk components are proposed in Chapter 7 for both upstream and downstream transmission. It is further presented that the data rate performance can be improved with a small amount of computation complexity spent in the partial cancellation schemes. However, there exists another technical challenge and performance limitation to be considered in modern systems.

The envisaged new applications for the modern systems, e.g., VDSL2 systems are characterized by completely different multimedia services. The wide range of such applications and associated Quality-of-Services (QoS) criteria are expected to grow substantially in the future. Driven by these applications, consumers have to be served according to different QoS demands. Therefore, it will be a further advantage for future systems to perform crosstalk interference cancellation supporting QoS requirements.

For this purpose, QoS-aware crosstalk cancellation schemes which provide joint signal processing among adjacent cable lines and meanwhile take QoS requirements of different lines into account are developed and described in this chapter.

The main idea in the QoS-aware crosstalk cancellation schemes is to scale the effort of QoS-aware signal processing in an intelligent way for capacity enhancement and for the improvement of supporting future multimedia services in the modern DSL systems. In this thesis, data rates of individual lines, as the only QoS requirement is considered.

8.1 QoS-based partial crosstalk cancellation

In all VDSL2 systems the zero-forcing based upstream crosstalk cancellation procedure or the downstream precoding technique can provide significant performance gain by means of eliminating all the crosstalk interference components. Figure 8.1, as an example, shows the performance gain for each cable in the upstream transmission. The considered cable binder has 21 individual cables and the cable length varies from 0.3 km to 0.8 km with the step of 0.025 km increment. Therefore, the data rate performance varies from cable to cable mainly depending on the length. In the ideal situation where all crosstalk interference components are perfectly cancelled by the zero-forcing based cancellation technique, the data rate performance varies between 65 Mbit/s and 20 Mbit/s. But in a realistic crosstalk situation these performance figures drop down to 35 or even less than 1 Mbit/s.

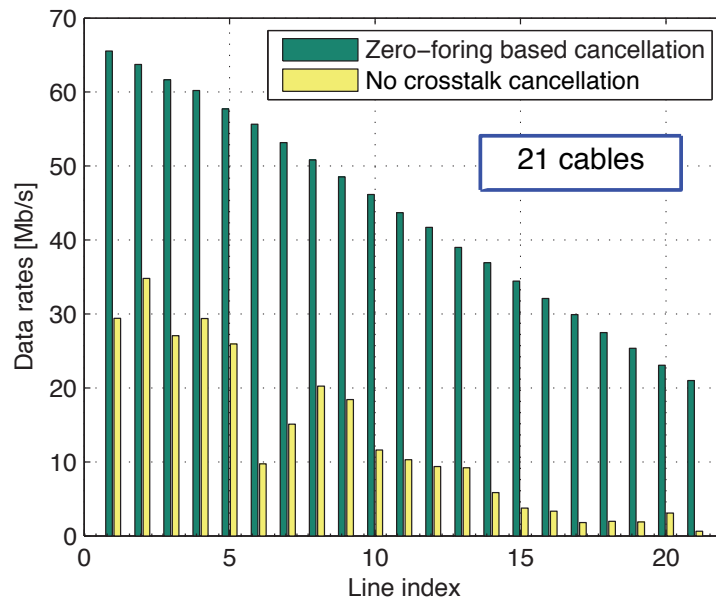


Figure 8.1: Achievable data rate performance with/without crosstalk cancellation

The crosstalk cancellation procedure and the necessary signal processing scheme among all transmission lines and on all subcarriers require an extremely high computation complexity. In the considered example of a cable binder, in total $M = 20$ crosstalk interference contributions should be cancelled out for each individual line. Therefore, the trade-off between the increased performance figures (increasing data rate) and the necessary computation complexity has been considered in Chapter 7 and a line-wise partial crosstalk cancellation procedure with a shrunken matrix per cable is proposed. This technique is referred here as ordinary partial crosstalk cancellation.

8.1. QOS-BASED PARTIAL CROSSTALK CANCELLATION

In practice, once an overall resource is assigned for the signal processing in a system, the effort that could be spent to each cable line or each user in the system is limited. According to the ordinary partial cancellation schemes, the computation complexity resource is given only to eliminate the significant crosstalk interference contributions on each line or for each user. In this case, the individual lines in the cable binder or the individual users are treated equally, namely a fixed number of crosstalk components to be cancelled is considered for each cable line. As an example, Figure 8.2 shows the data rate performance for each cable inside the binder if in total the strongest 8 crosstalk components are considered for each cable. In total, 168 out of 420 crosstalk components are cancelled for all lines and the partial cancellation scheme results in 40% computation complexity effort of the zero-forcing based crosstalk cancellation scheme.

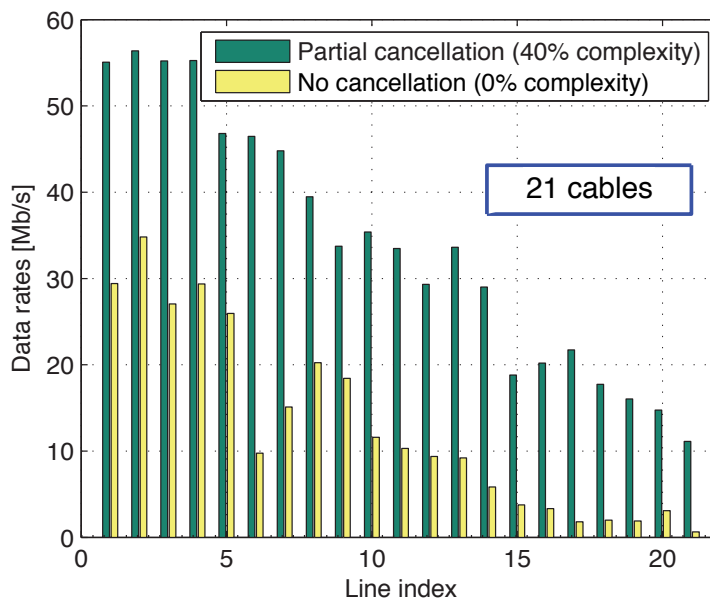


Figure 8.2: Achieved data rate performance by the ordinary PCC

From a computation complexity point of view this leads obviously to the best-effort performance of each user. The obtained data rates dramatically differ from one line to the others, which can be seen in Figure 8.2. However, the effort could in fact be distributed more wisely. That is to say, the computation complexity can be distributed to the lines or users in an intelligent way, so that the user requirements are satisfied. To give an example, it is preferable to spend more computation complexity for those users requesting high data rates and experiencing relatively high interference levels than those with relaxed requirements and a more favorable interference situation.

There is provided in this chapter a QoS-based partial crosstalk cancellation technique which takes QoS requirements of different lines/users as the most important concern in

the crosstalk selection algorithms of the partial crosstalk cancellation procedure [RDR09]. The upstream transmission is considered hereafter as an example but the extension of the proposed QoS-based partial crosstalk cancellation technique in the downstream transmission is straight forward.

In any practical application, a certain data rate needs to be negotiated and guaranteed for each user. Hence, the computation effort of crosstalk cancellation will be spent only as long as the guaranteed data rate is not achieved. For good cable line conditions only a very few crosstalk components need to be cancelled while for bad cable line conditions much more computational effort must be spent for crosstalk cancellation. Apparently, line adaptive crosstalk cancellation procedures are needed. In other words, the effort for signal processing should be spent adaptively for each line and only to the extent which is required.

To organize the crosstalk cancellation procedure in an adaptive way, a successive crosstalk cancellation scheme is proposed here based on QoS figures. The complete successive algorithm is summarized in the following steps.

1. Sort and rank the crosstalk interference components for each individual line i and tone k .
2. Calculate the gaps between the current data rates and defined target data rates: $G_i = R_i^{\text{required}} - R_i^{\text{current}}$ for all lines $i, i \in \{1, 2, \dots, M + 1\}$.
3. For each line i , if the gap $G_i > 0$, cancel the largest *remaining* crosstalk signal on all subcarriers.
4. Calculate the current data rate R_i^{current} of each line i so that the data rate gap G_i is updated for all lines.
5. Repeat steps 2 to 4 until $G_i \leq 0$ for $i = 1, 2, \dots, M + 1$, i.e., all lines achieve their required target data rate.

According to **Algorithm 1** defined in Section 7.1.3, the ranking the crosstalk interference components for a line i can be made based on the amplitude of the crosstalk transfer factors $H_{ij,k}, j \in \{1, 2, \dots, M, M + 1\} \setminus i\}$.

In each iteration step, the ordinary partial crosstalk cancellation scheme as described in Chapter 7 is applied for each line i . With the achieved SINR given in equation (7.8) the current data rate is calculated with the gap approximation

8.2. SYSTEM PERFORMANCE WITH QoS-BASED PARTIAL CROSSTALK CANCELLATION

$$R_i^{\text{current}} = f_s \sum_{k=0}^{K-1} \log_2 \left(1 + \frac{\text{SINR}_i^k}{\Gamma} \right), \quad (8.1)$$

where f_s describes the DMT symbol rate and Γ is SNR gap at certain bit error rate. Γ shows the SNR loss of the actual system with respect to the corresponding capacity.

Letting $q_i = |\Omega_i|$ denote the cardinality of the index set Ω_i , q_i represents the number of crosstalk interference components being considered in the QoS-based partial cancellation scheme for each cable line i . Therefore, the overall computation complexity effort spent in the QoS-based partial cancellation procedure is defined as the ratio between the sum of the number of crosstalk components cancelled on each line and the total crosstalk components existing in the cable binder.

8.2 System performance with QoS-based partial crosstalk cancellation

In this section, the QoS-based partial crosstalk cancellation schemes are investigated in different cable binders. In particular, the data rate performance achieved in the QoS-based partial cancellation is compared with that in the ordinary partial crosstalk cancellation with similar computation complexity.

Considering the cable binder mentioned in Section 8.1, Figures 8.1 and 8.2 illustrate the obtained data rate performance in case where no crosstalk cancellation, full crosstalk cancellation and ordinary partial crosstalk cancellation with 40% complexity are applied. We suppose that the individual lines/users have negotiated their data rates and each line has a certain required data rate which is to be guaranteed by the QoS-based partial crosstalk cancellation. More specifically, the 21 lines in the cable binder are categorized into three groups and the required data rates are defined as 50 Mbit/s, 30 Mbit/s and 15 Mbit/s.

Figure 8.3 shows the required data rates of all cable lines with a solid line and the data rates achieved by the ordinary partial crosstalk cancellation with 40% complexity are plotted in green bars. As also mentioned before, in the ordinary partial cancellation with 40% computation complexity, the number of crosstalk components considered for each line is $q = 8$ and in total 168 crosstalk interference components are cancelled out in the partial cancellation procedure. It can be observed that when considering the required data rates of each individual lines, some cables can be satisfied while the others can not: the data rate performance of lines 5 - 7, 12, 13 and 21 is below the requirements. In this case, nearly 30% users are not satisfied.

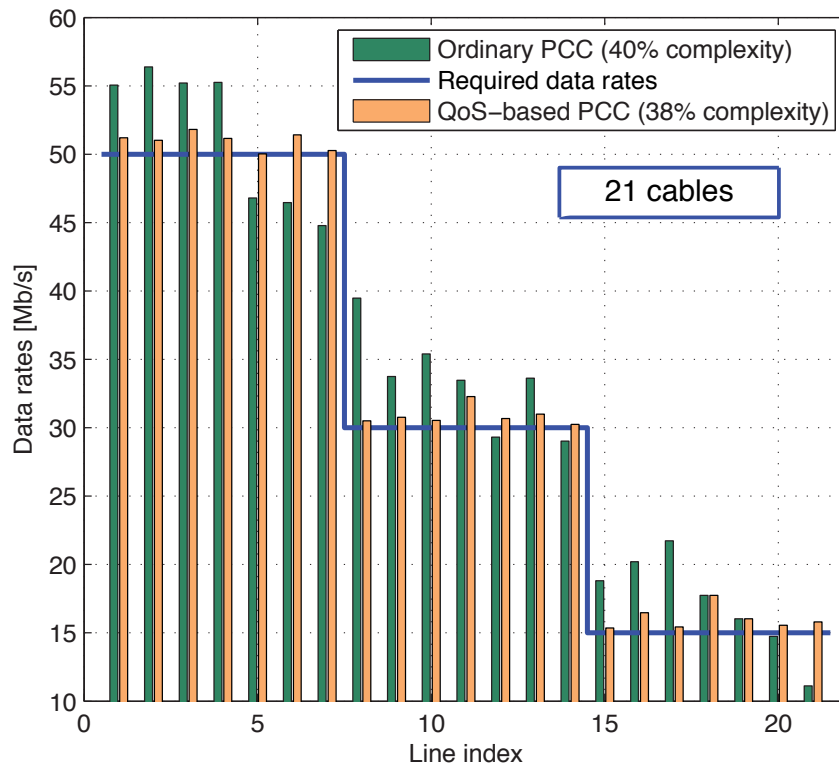


Figure 8.3: Data rate comparison between the ordinary PCC and QoS-based PCC

However, the proposed QoS-based partial cancellation schemes can provide the required data rate performance for each line in the cable binder. In Figure 8.3 the data rate performance of QoS-based partial cancellation is plotted in bars to the right of the performance of the ordinary one.

With QoS-based partial cancellation, the total complexity is distributed according to the crosstalk situation in each individual line. The number q_i of crosstalk components to be cancelled for each line i is listed in Table 8.1. It varies from line to line, from the minimum value of 4 to the maximum value of 11. In total 160 crosstalk signals need to be cancelled. This results in a computation complexity about 38% of full crosstalk cancellation. In this case, the computation effort spent in the QoS-based partial cancellation is even less than what is spent in the ordinary one.

It can be also observed in Figure 8.3 that the data rate overshoot appearing in the ordinary partial cancellation for some lines is reduced in the QoS-based partial cancellation. Thus,

8.2. SYSTEM PERFORMANCE WITH QoS-BASED PARTIAL CROSSTALK CANCELLATION

Table 8.1: Crosstalk component number eliminated by the QoS-based partial cancellation with 40% complexity in the binder with the cable length ranging from 0.3 km to 0.8 km

Line i	1	2	3	4	5	6	7	8	9	10	11
q_i	6	5	7	7	10	10	13	4	7	5	8
Line i	12	13	14	15	16	17	18	19	20	21	Σq_i
q_i	9	6	9	6	6	6	8	8	9	11	160

a portion of the computation resource can be saved and more complexity is spent on the worse lines so that they can also reach their required data rates. By this means, the proposed QoS-based successive cancellation technique shapes the data rate figure to fulfil the practical requirements for all lines.

We further consider a cable binder which contains cable lines with not many variations in length: the cable length $L_{\text{cable},i}$ ranges from 0.3 km to 0.5 km with 0.01 km increment. The number of crosstalk interference components for each cable line is still $M = 20$. The data rate performance comparisons between the ordinary partial crosstalk cancellation and the QoS-based one are made with two different computation complexity parameters and the results are illustrated in the following figures.

Figure 8.4 shows the comparison with 40% computation complexity. Unlike the wide data rate difference (about 45 Mbit/s) obtained in the cable binder with lengths ranging from 0.3 km to 0.8 km (see Figure 8.3), maximum 35 Mbit/s data rate difference appears in the cable binder with the lengths ranging from 0.3 km to 0.5 km. We divide 21 lines into two groups: lines 1 to 14 having required data rate of 40 Mbit/s and lines 15 to 21 having the required data rate of 25 Mbit/s.

The required data rates and the data rates obtained by the ordinary partial cancellation with 40% complexity are shown in Figure 8.4. In the ordinary partial cancellation, the number of the cancelled crosstalk interference components is 168. It can be observed that 8 out of 21 lines are not satisfied with the achieved data rates and some lines, e.g., lines 9 and 12 obtain the data rates quite far from the required ones. However, when the QoS-based partial cancellation is applied, those gaps are filled up.

The crosstalk components considered in the cancellation are listed in Table 8.2. It can be seen that the overall required computation complexity in the QoS-based cancellation is nearly identical to that of the ordinary one.

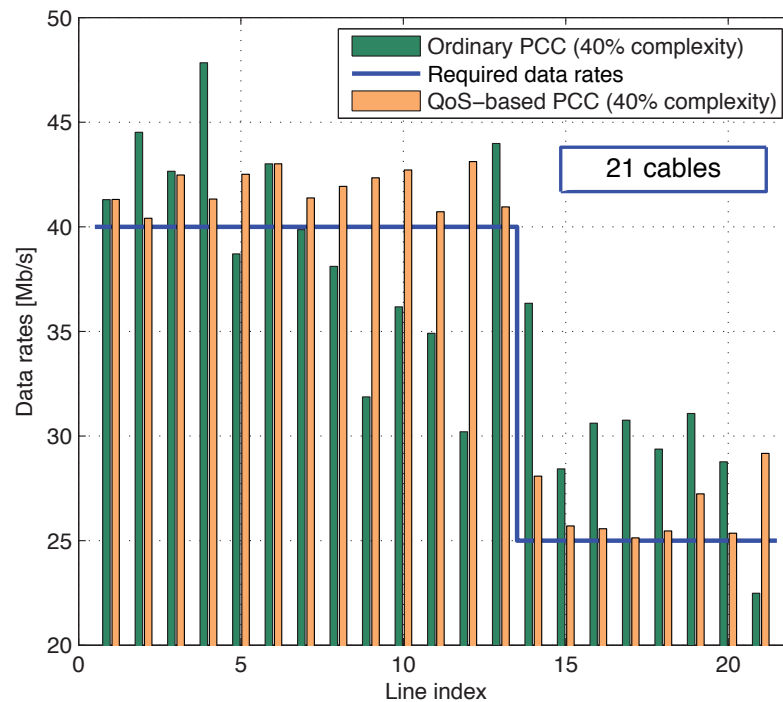


Figure 8.4: Data rate comparison between the ordinary PCC and QoS-based PCC

Figure 8.5 shows the data rate performance comparison with 25% computation complexity. The required data rate for lines 1 to 18 is given as 30 Mbit/s and rate for lines 19 to 21 is defined as 20 Mbit/s. Similar observation can be made in Figure 8.5 that the overshoot in some lines are reduced and the performance of each line is successfully tailored to fulfill its own data rate requirement. Furthermore, as shown in Table 8.3, the overall computation complexity need in the QoS-based partial cancellation remain nearly the same as in the ordinary one but different portions of overall computation resource are allocated to different lines.

As a summary, the proposed QoS-based partial crosstalk cancellation scheme considers the QoS criterion of each line to be fulfilled in the cable binder. The line-wise crosstalk selection algorithm dynamically adapts to the users' QoS requirements and distributes the total computation complexity into individual lines based on the QoS criteria.

8.3. CROSSTALK CANCELLATION FACING DYNAMIC SITUATIONS

Table 8.2: Crosstalk component number eliminated by the QoS-based partial cancellation with 40% complexity in the binder with the cable length ranging from 0.3 km to 0.5 km

Line i	1	2	3	4	5	6	7	8	9	10	11
q_i	8	6	8	6	10	8	9	10	12	11	10
Line i	12	13	14	15	16	17	18	19	20	21	Σq_i
q_i	13	7	4	7	5	5	6	7	6	9	167

Table 8.3: Crosstalk component number eliminated by the QoS-based partial cancellation with 25% complexity in the binder with the cable length ranging from 0.3 km to 0.5 km

Line i	1	2	3	4	5	6	7	8	9	10	11
q_i	1	0	2	1	4	3	3	4	7	5	6
Line i	12	13	14	15	16	17	18	19	20	21	Σq_i
q_i	9	4	6	9	8	8	9	5	4	8	106

8.3 Crosstalk Cancellation Facing Dynamic Situations

In the previous two sections, the QoS-based partial crosstalk cancellation scheme is introduced and its performance is evaluated with predefined data rate of each line or user. However, in a real world things are always changing. Some users might switch on or off their modems, starting or terminating the data transmission. In the case of transmission terminated, the interference level is reduced whereas in the case of new line starting transmission there might be severe impact on the performance of the existing running lines. Nowadays, new applications, such as triple play of voice, data and video require high QoS. Such dynamic situation might cause the unpleasant or non-acceptable latency in two-way communications, either by voice or video. It can also very easily upset the smooth flow of online TV video and cause the visible damage of pictures. Therefore, it is very important to handle such situation properly in VDSL2 systems.

Conventionally, certain noise margin is operated in the systems to avoid unacceptable error rate in the event of minor increase in crosstalk noise and to ensure the reliable operation [GDJ06]. Typically, the noise margin is at least 5dB or 6dB. However, in the addressed dynamic situation, the sudden appearance of crosstalk interference might be so severe that the QoS is damaged. So the noise margin shall further be increased in the system de-

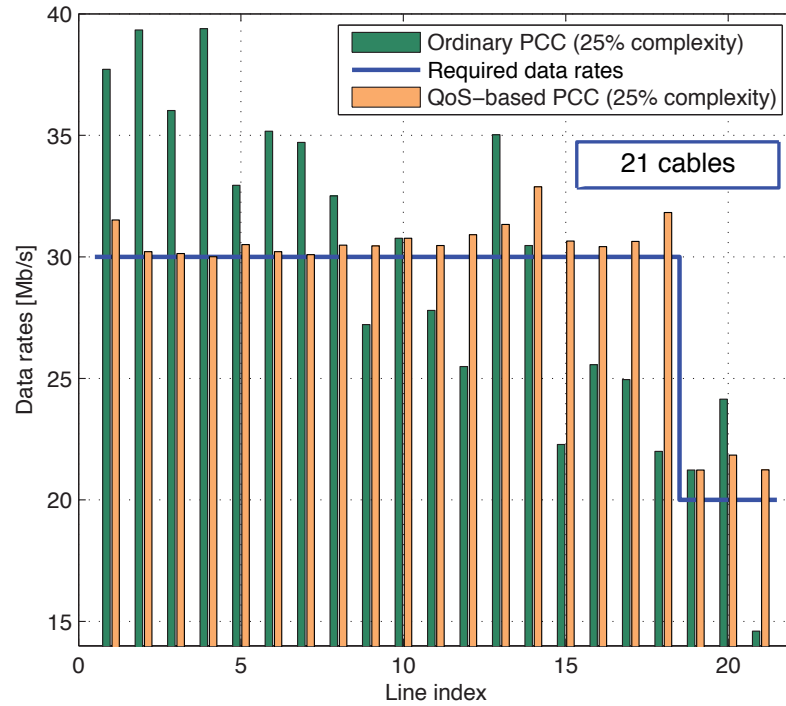


Figure 8.5: Data rate comparison between the ordinary PCC and QoS-based PCC

sign phase to provide a sufficient tolerance of the system. In this case, the system capacity can not be fully explored and the achievable data rates in the system are relatively low.

On the contrary to the conventional passive method, here we explore the dynamic features of the system and present a successive cancellation scheme suitable for the dynamic scenario [RDR11].

8.3.1 Successive cancellation for the dynamic scenario

Before the dynamic scenario happens, the transmission of the existing $M+1$ running lines can be described analytically for each single subcarrier as

$$\mathbf{Y}' = \mathbf{H}'\mathbf{X} + \mathbf{Z}', \quad (8.2)$$

where \mathbf{X} , \mathbf{Y}' and \mathbf{Z}' denote the transmit signal vector, received signal vector and noise vector of all existing running lines, respectively and \mathbf{H}' is an $(M+1)$ -by- $(M+1)$ matrix containing the channel transfer factors of all existing running lines.

8.3. CROSSTALK CANCELLATION FACING DYNAMIC SITUATIONS

We assume that before new users or cable line starting to transmit their signals, the QoS-based partial crosstalk cancellation has been applied within the cable binder and the QoS requirements of all existing running lines are fulfilled. In this case, letting the set Ω'_i denote the indices of the lines which generate the most significant crosstalk components being cancelled in the QoS-based cancellation procedure before new lines are activated and index set $\bar{\Omega}_i$ denote the other lines being neglected in the procedure, the achieved SINR for each line i can be expressed as:

$$\text{SINR}_i^{\text{old}} = \frac{\sigma_s^2}{\left\| \boldsymbol{\alpha}'^i \bar{\mathbf{T}}'^i \right\|^2 \sigma_s^2 + \left\| \boldsymbol{\alpha}'^i \right\|^2 \sigma_z^2} \quad (8.3)$$

according to equation (7.8), where the partial cancellation coefficients $\boldsymbol{\alpha}'^i$ for each line i as well as the matrix $\bar{\mathbf{T}}'^i$ including all the crosstalk transfer factors being neglected in the partial cancellation procedure are defined similarly to equations (7.3) and (7.6) as

$$\boldsymbol{\alpha}'^i = \left((\mathbf{T}'^i)^{-1} \right)_{\text{row } 1} \quad (8.4)$$

$$\text{with } \mathbf{T}'^i = \begin{pmatrix} H'_{ii} & (\mathbf{H}')_{\text{row } i, \text{cols } \Omega'_i} \\ (\mathbf{H}')_{\text{rows } \Omega'_i, \text{col } i} & (\mathbf{H}')_{\text{rows } \Omega'_i, \text{cols } \Omega'_i} \end{pmatrix} \quad (8.5)$$

and

$$\bar{\mathbf{T}}'^i = \begin{pmatrix} (\mathbf{H}')_{\text{row } i, \text{cols } \bar{\Omega}_i} \\ (\mathbf{H}')_{\text{rows } \bar{\Omega}_i, \text{cols } \bar{\Omega}_i} \end{pmatrix}. \quad (8.6)$$

Once new lines are activated and start to transmit signals, assuming that the vector $\mathbf{S} \triangleq (\mathbf{X}^T, \mathbf{U}^T)^T$ contains all transmit signals of $M+1$ running lines and the transmit signals of N newly activated lines $\mathbf{U} \triangleq (U_1, U_2, \dots, U_N)^T$, the overall received signals \mathbf{R} for all $M+N+1$ lines after new lines activated can be formulate as:

$$\mathbf{R} = \mathbf{H}\mathbf{S} + \mathbf{Z} \quad (8.7)$$

$$\text{with } \mathbf{H} \triangleq \begin{pmatrix} \mathbf{H}'_{(M+1) \times (M+1)} & \mathbf{A}_{(M+1) \times N} \\ \mathbf{B}_{N \times (M+1)} & \mathbf{H}''_{N \times N} \end{pmatrix}. \quad (8.8)$$

The matrix \mathbf{H} is now defined as the overall channel transfer matrix in the dynamic scenario. The element $H''_{ij} \triangleq (\mathbf{H}'')_{i,j}, \forall i, j \in \{1, 2, \dots, N\}$ is the channel transfer factor from

the transmitter j to receiver i among the new active lines. Similarly, the elements $A_{ij} \triangleq (\mathbf{A})_{i,j}, \forall i \in \{1, 2, \dots, M+1\}$ and $j \in \{1, 2, \dots, N\}$ and $B_{ij} \triangleq (\mathbf{B})_{i,j}, \forall i \in \{1, 2, \dots, N\}$ and $j \in \{1, 2, \dots, M+1\}$ describe the channel transfer factors from the j -th new active line to the i -th running line and the j -th running line to the i -th new active line, respectively. The vector $\mathbf{Z} \triangleq ((\mathbf{Z}')^T, (\mathbf{Z}'')^T)^T$ contains all white noise components for $M+1$ running lines and N new active lines.

Specifically, the crosstalk impact from the newly activated lines to the existing running line is illustrated in Figure 8.6. The n -th column $\mathbf{A}_n = (A_{1,n}, A_{2,n}, \dots, A_{M+1,n})^T, \forall n \in \{1, 2, \dots, N\}$ of the crosstalk matrix \mathbf{A} describes the crosstalk interference from the new active line n to all existing $M+1$ running lines.

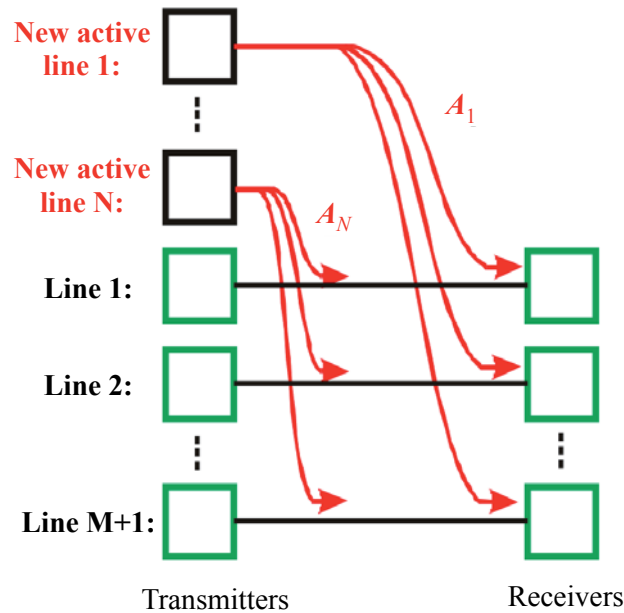


Figure 8.6: Crosstalk impact from new active lines to the existing running lines

It is assumed that the QoS requirements are satisfied for all running lines before the dynamic situation happens. However, whenever a new line starts to transmit data, the QoS of the existing running lines might not be maintained due to the crosstalk interference generated from the new line. Therefore, the influence of those crosstalk interference components coming from the new active lines have to be evaluated.

The received signals of $M+1$ existing running lines after new line activation will change to be:

8.3. CROSSTALK CANCELLATION FACING DYNAMIC SITUATIONS

$$\mathbf{Y} = \begin{pmatrix} \mathbf{H}' & \mathbf{A} \end{pmatrix} \mathbf{S} + \mathbf{Z}' \quad (8.9)$$

$$= \mathbf{Y}' + \mathbf{A}\mathbf{U}, \quad (8.10)$$

each of which is the summation of the received signal before new line activating and the crosstalk interference generated by the new lines.

Correspondingly, the performance degradation of each existing running line is represented by the SINR loss on each tone. If the cancellation scheme remains unchanged, the SINR for each existing line i can be predicted as

$$\text{SINR}_i^{\text{pred}} = \frac{\sigma_s^2}{\left(\left\| \boldsymbol{\alpha}^{i'} \bar{\mathbf{T}}^{i'} \right\|^2 + \left\| \boldsymbol{\alpha}^{i'} \mathbf{A}^i \right\|^2 \right) \sigma_s^2 + \left\| \boldsymbol{\alpha}^{i'} \right\|^2 \sigma_z^2} \quad (8.11)$$

$$\text{with } \mathbf{A}^i = \begin{pmatrix} (\mathbf{A})_{\text{row } i} \\ (\mathbf{A})_{\text{rows } \Omega'_i} \end{pmatrix}, \quad (8.12)$$

and the SINR loss in decibel on the existing running line i can be further calculated as

$$\left(\text{SINR}_i^{\text{loss}} \right)_{\text{dB}} = 10 \lg \left(1 + \left\| \boldsymbol{\alpha}^{i'} \mathbf{A}^i \right\|^2 \text{SINR}_i^{\text{old}} / \sigma_s^2 \right). \quad (8.13)$$

Note that "1" in the formula ensures the positive degradation due to new line joining.

As SINR degradation can be predicted on each line for each tone, the total data rate loss for the line can be predicted as well. If the QoS requirement of the line is no longer fulfilled, a successive cancellation procedure adapting to the new active lines will be carried out. Otherwise, the cancellation scheme remains unchanged for the line. The procedure is illustrated in Figure 8.7 and the complete algorithm is explained as following:

1. Estimate the impact from new active lines to the existing running lines: predict the SINR loss as well as data rate loss for each line $i, \forall i \in \{1, 2, \dots, M+1\}$.
2. Select victim running lines by comparing the current remaining data rate of each line with its QoS requirement. Let the Φ denote the set of indices of the victim lines whose QoS requirements are no longer fulfilled.
3. Keep cancellation unchanged for the non-victim lines, i.e. the cancellation vector $\boldsymbol{\alpha}^{i'}$ is applied in the cancellation for line $i, \forall i \in \{1, 2, \dots, M+1\} \setminus \Phi$.

4. Regarding the victim lines, sort and rank the crosstalk inference components for the individual lines and tones.
5. Calculate the gaps between the current data rate and the required data rate for all victim lines: $G_i = R_i^{\text{required}} - R_i^{\text{current}}, \forall i \in \Phi$.
6. For each victim line $i, \forall i \in \Phi$, cancel the largest *remaining* crosstalk signal on all tones if the gap $G_i > 0$.
7. Update the data rate gap G_i for each victim line $i, \forall i \in \Phi$ with the current data rate R_i^{current} .
8. Repeat steps 5 to 7 until $G_i \leq 0$ for $\forall i \in \Phi$, i.e., all victim lines achieve their required data rate again.

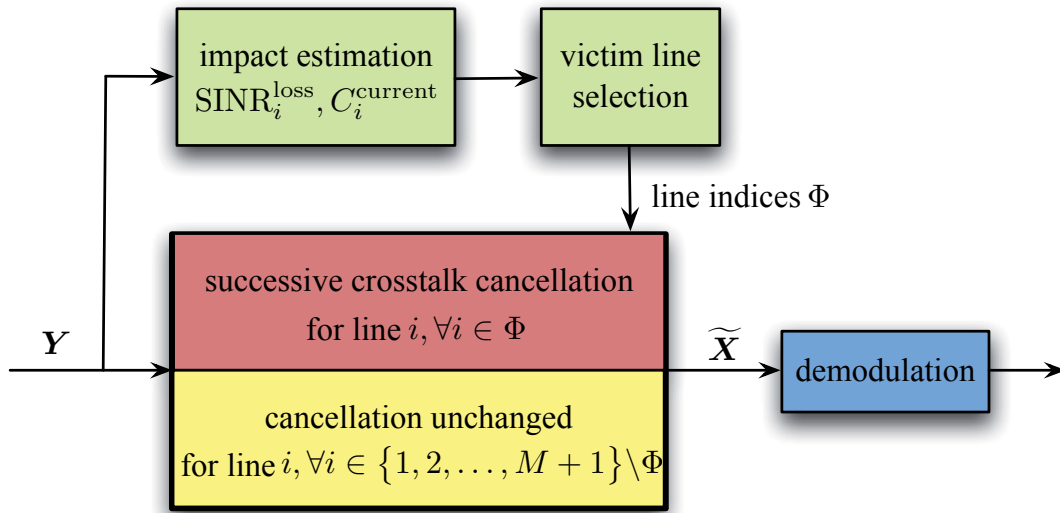


Figure 8.7: The crosstalk cancellation procedure for the existing running lines

During the iteration procedure, the considered crosstalk interference components for each victim line are coming from the existing running lines as well as new active lines. As the set Ω_i denoting the indices of the major crosstalk interferers to be cancelled for the victim line $i, \forall i \in \Phi$, Ω_i is the subset of $\{1, 2, \dots, M + N + 1\} \setminus i$ which is similar as that defined in the ordinary partial crosstalk cancellation schemes in Section 7.1.1. All received signals shall be available for the crosstalk cancellation. The sub-crosstalk matrix T^i and the partial cancellation coefficients α^i for the victim line are selected and calculated in the same way as introduced in the ordinary partial cancellation schemes. The SINR and the current data rate R_i^{current} for victim line i can be calculated as in steps 5 and 6.

8.3. CROSSTALK CANCELLATION FACING DYNAMIC SITUATIONS

As to the new active lines, QoS-based partial crosstalk cancellation scheme can be directly applied on them.

During the partial cancellation procedure, for each new active line $n, \forall n \in \{1, 2, \dots, N\}$, the indices of the lines which generate the crosstalk interference to be cancelled can still be denoted as the set Ω_i , and $\Omega_i \subseteq \{1, 2, \dots, M + N + 1\} \setminus i$. Here, $i = M + 1 + n$ is the index of the n -th new active line considered in the overall $M + N + 1$ cable lines. Therefore, the sub-crosstalk matrix T^i containing only the most significant crosstalk interference components on the n -th new active line and the partial cancellation coefficients α^i as the first row elements of the sub-crosstalk matrix inverse $(T^i)^{-1}$ can be obtained according to equations (7.1) and (7.3).

In summary, when the dynamic situation happens, the performance degradation of the existing running lines is predicted and a line-wise successive partial crosstalk cancellation is performed for those existing running lines which are severely influenced by the new active lines as well as for the new active lines. The algorithm will be stopped if the QoS requirements are fulfilled again. By this means, the QoS requirements can always be maintain in the dynamic scenario. The proposed cancellation scheme is described in the upstream transmission. However, a similar procedure can be also applied in the downstream.

8.3.2 System performance in the dynamic scenario

In this section the system performance obtained by the proposed successive partial cancellation scheme is presented. The cable binder being considered in the dynamic scenario is still the one mentioned in Section 8.1

We assume that there are 15 existing running lines before the dynamic situation happens. Figure 8.8 depicts the achieved data rates of these 15 running cable lines in the stationary scenario. These 15 cable lines are randomly selected to be active among the total 21 lines.

The required data rates for the individual running lines are also shown in Figure 8.8. The QoS demands of all running lines are guaranteed by the QoS-based partial crosstalk cancellation. The cable lengths and the number of crosstalk contributions cancelled for each running line i are listed in Table 8.4. In total, 65 crosstalk signals are eliminated in the

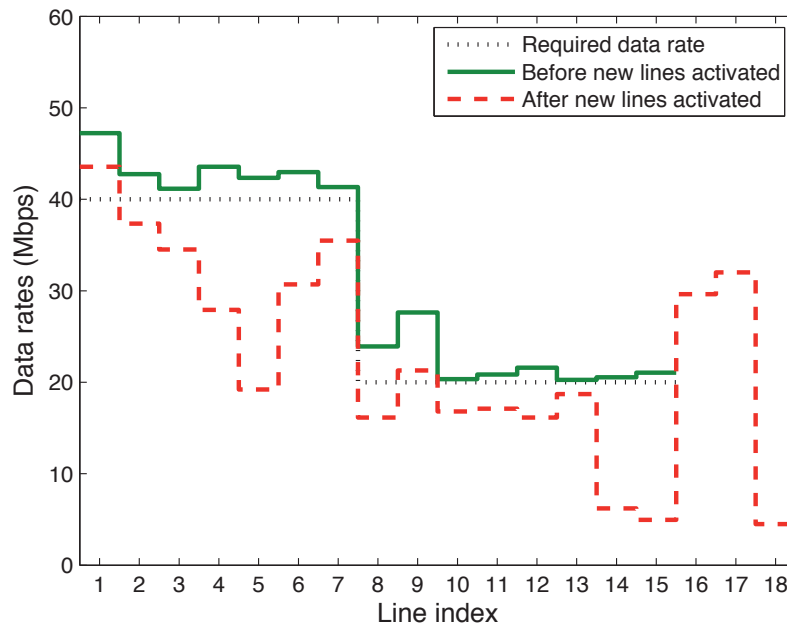


Figure 8.8: The achieved data rates of the existing running lines before dynamic situation happens and the predicted rates of all lines after new lines activate

QoS-based partial cancellation, which is about 31% computation complexity respected to the full crosstalk cancellation scheme.

Table 8.4: Crosstalk component number eliminated for each existing running line

Line i	1	2	3	4	5	6	7	8
Length (m)	300	325	400	425	450	500	525	550
q_i	1	0	3	4	3	8	6	2
Line i	9	10	11	12	13	14	15	Σq_i
Length (m)	600	625	650	700	725	775	800	
q_i	2	3	4	5	7	8	9	65

Next, the dynamic scenario appears and three new lines start to transmit signals. The performance impact to those 15 existing running lines is predicted and the resulting data rates of the existing running lines as well as the predicted data rates of the new coming lines are also shown in Figure 8.8 . It can be observed that in this case only 2 of 15 existing running lines still fulfill their QoS requirements. The rest are all strongly disturbed and some of them even lose more than half of their data rates. In Figure 8.8 the predicted data

8.3. CROSSTALK CANCELLATION FACING DYNAMIC SITUATIONS

rates of the new active lines (line 16, 17 and 18) without considering crosstalk cancellation are also plotted.

With predicted data rate loss, the line-wise successive crosstalk cancellation scheme is applied to the new lines and those existing running lines which are strongly affected. Figure 8.9 shows the achieved data rates of all 18 cables. Obviously, after applying the proposed cancellation scheme the QoS requirements of those victim lines are fulfilled again. Meanwhile, the new active lines also achieve their QoS targets.

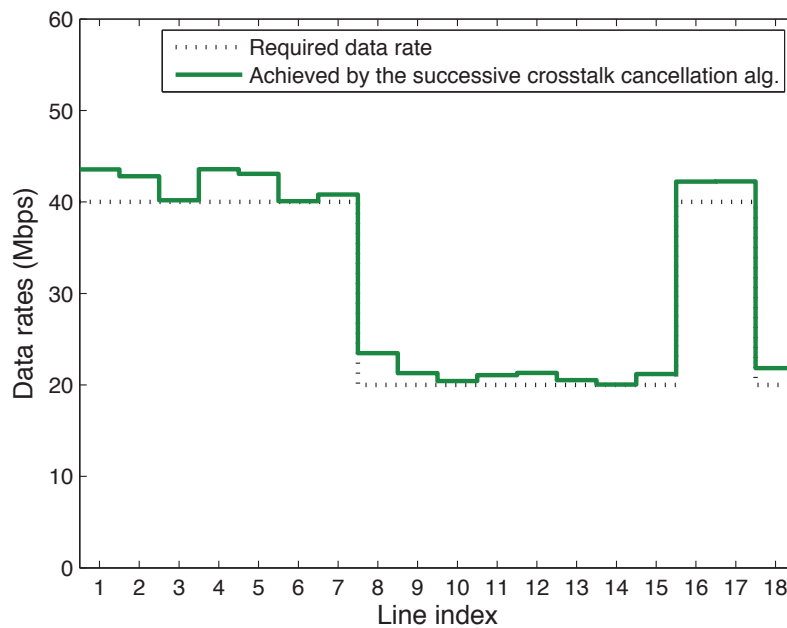


Figure 8.9: The achieved data rates of all cable lines by applying successive cancellation

The additional number of crosstalk signals cancelled for each existing running line as well as for the new active lines is denoted as Δq_i and listed in Table 8.5. The individual cable length is also shown in the table. It can be observed that among the three new coming lines, two of them have relatively strong influence to the existing running lines due to the short cable lengths in the upstream transmission. As shown in the table, in most cases only 1 or 2 new crosstalk interference components need to be dealt with to achieve the rate requirements again. So the proposed algorithm adapts to the new crosstalk situation quite well. In total 98 crosstalk signals are cancelled for 18 lines resulting in about 32% complexity which is similar as that in the stationary scenario.

Table 8.5: Additional number of crosstalk components cancelled after new line activation

Line i	1	2	3	4	5	6	7	8	9	10
Length (m)	300	325	400	425	450	500	525	550	600	625
Δq_i	0	1	2	1	2	1	2	1	0	1
Line i	11	12	13	14	15	16	17	18	Σq_i	
Length (m)	650	700	725	775	800	350	375	675		
Δq_i	2	1	1	2	3	4	3	6	33	

In this chapter, the partial crosstalk cancellation schemes being aware of the QoS requirements of the lines or users are developed. In the QoS-based partial cancellation schemes, the crosstalk interference components are cancelled in a step-by-step and line-by-line procedure until the individual QoS requirements are fulfilled. It is shown that with such cancellation schemes, the crosstalk selection algorithms dynamically adapt to the users' QoS requirements and the performance of each line or user is successfully tailored to fulfill its own requirement. In this case, the overall computation complexity of the system remains low and is distributed to the different lines or users more wisely.

Furthermore, as the computation complexity is only spent to the running lines for fulfilling their QoS requirements, whenever new lines become active, further computation complexity need to be spent to the existing running lines whose QoS are severely impacted as well as to the new active lines. Therefore, the successive partial cancellation scheme facing such dynamic situation is proposed. The performance degradation due to newly activated lines is first estimated in the proposed cancellation scheme and then a line-wise partial crosstalk cancellation considering the computation complexity and the QoS figures is organized in a successive way for those significantly influenced cable lines. It is shown that the proposed algorithm can properly react to the dynamic situation and guarantee the QoS requirements of the victim lines as well as the new active lines.

9 Power Allocation for Crosstalk Cancellation

In chapters 5, 7 and 8 the details of the subcarrier-based signal processing for completely eliminating or partially removing crosstalk interference in VDSL2 systems are discussed. In such crosstalk cancellation techniques, signal level coordination is needed either at the transmitters or at receivers. However, this is not always possible either to the run-time complexity of DSL modems or the deployment of the transceivers. In such case, some crosstalk interference components remain in the systems and the transmission power of those crosstalk signals will affect the performance figures. Therefore, global signal processing techniques like power allocation are considered in this chapter to optimize the system performance.

9.1 State of the art

9.1.1 Water-filling (WF) and iterative water-filling (IWF)

In a single-line DMT transmission system which has multiple parallel subchannels in the transmission band, the optimal solution of distributing a certain amount of power among the plurality of parallel non-interactive channels is well-known as the so-called water-filling principle [CTW⁺91], [Gal68].

For a bank of K parallel subchannels, the water-filling principle provides the optimal solution to two problems: to maximize the data rate R with a fixed transmit power P and to minimize the transmit power P with a fixed data rate.

For the first problem, the maximization is achieved when the sum of the number of bit b_k being loaded on individual subchannel k is maximized, subject to a total power constraint:

$$\max_{b_k, P_k} \{R\} \triangleq \max \left\{ \sum_{k=0}^{K-1} \log_2 \left(1 + \frac{1}{\Gamma} \cdot \frac{|H_k|^2 P_k}{\sigma_z^2} \right) \right\}, \quad (9.1)$$

$$\text{subject to } \sum_{k=0}^{K-1} P_k \leq P. \quad (9.2)$$

Using Lagrange multipliers, the cost function to maximize (9.1) subject to the constraint in (9.2) becomes

$$\frac{1}{\ln 2} \sum_k \ln \left(1 + \frac{1}{\Gamma} \cdot \frac{|H_k|^2 P_k}{\sigma_z^2} \right) + \lambda \left(\sum_k P_k - P \right). \quad (9.3)$$

Differentiating with respect to P_k , it can be obtained that the optimum water-filling transmit power satisfies

$$P_k + \Gamma \cdot \frac{\sigma_z^2}{|H_k|^2} = \mu = \text{constant}. \quad (9.4)$$

As transmit power can only have positive values in practice, the power level of each subchannel is defined as

$$P_k = \begin{cases} \mu - \frac{\Gamma \sigma_z^2}{|H_k|^2} & \text{if } \frac{\Gamma \sigma_z^2}{|H_k|^2} < \mu \\ 0 & \text{if } \frac{\Gamma \sigma_z^2}{|H_k|^2} \geq \mu \end{cases} \quad (9.5)$$

and the constant threshold μ is determined by solving a set of linear equations which has the water-filling distribution as its solution:

$$\mu = \frac{P + \Gamma \cdot \sum_{k'=1}^{K'} \frac{\sigma_z^2}{|H_{k'}|^2}}{K'}, \quad (9.6)$$

where K' is the total number of loaded subchannels with transmit power larger than zero.

Similarly, for the second optimization problem, the total transmit power P is to be minimized subject to a given fixed data rate R :

$$\min_{b_k, P_k} \{P\} \triangleq \min \left\{ \sum_{k=0}^{K-1} P_k \right\}, \quad (9.7)$$

$$\text{subject to } f_s \sum_k \log_2 \left(1 + \frac{1}{\Gamma} \cdot \frac{|H_k|^2 P_k}{\sigma^2} \right) = R. \quad (9.8)$$

$$=0 \qquad z$$

After correct differentiation the solution to the transmit power minimization problem is again the water-filling solution given by equation (9.4).

The optimal water-filling solution is based on the assumption that a continuous rate is possible. However, in practice, bit loading with fractional values can not be implemented and typically there is only a set of discrete rates: 1-15 bits per subcarrier. Therefore, sub-optimal loading algorithms to approximate the water-filling solution are proposed according to the two objectives: maximize the data rate subject to a fixed power constraint and minimize the transmit power subject to a fixed data rate constraint. For example, there are two well-known algorithms: Chow's bit loading algorithm [CCB95] computing a bit distribution by rounding of approximate water-filling results and Levin-Campello algorithm [Cam98], [SSCS03] using the greedy optimization method.

For multiple-line DMT transmission systems, power distribution among all lines and all subcarriers is much more complicated. The performance of each line depends not only on its own power allocation, but also on the power allocation of the other lines. In particular, when transmitters or receivers are located in different distances trying to communicate with the same central office at the same time, the interference from the closer transmitters might even overwhelm the signals from the farther transmitters.

Iterative water-filling as an extension of optimal water-filling solution in a single line transmission system is proposed in [YGC02]. The power control algorithm is based on the formulation of the multiuser environment as a noncooperative game and specifically considering the frequency-selective nature of the DSL channels. Starting from any initial given total power P_i of line i , each line independently maximizes its own data rate R_i by water filling over the noise and interference from other other lines:

$$\max_{P_{k,i}} \{R_i\} \triangleq \max \left\{ \sum_{k=0}^{K-1} \log_2 \left(1 + \frac{1}{\Gamma} \cdot \frac{|H_{i,i,k}|^2 P_{k,i}}{\sum_{j=1, j \neq i}^M |H_{i,j,k}|^2 P_{k,j} + \sigma_z^2} \right) \right\}, \quad (9.9)$$

$$\text{subject to } \sum_{k=0}^{K-1} P_{k,i} \leq P_i, \text{ and} \quad (9.10)$$

$$P_{k,i} \geq 0. \quad (9.11)$$

The iterative water-filling algorithm contains two stages. The inner stage takes a set of power constraints for each line as input to derive optimal power allocation and its corresponding data rate; the outer stage finds the optimal total power constraint for each line for achieving its target data rate. In other words, in the inner stage, with a fixed total power constraint for each user, the lines sequentially update their power allocation according to water-filling principle while regarding the interference from other lines as noise until the

process converges; and in the outer stage, the total power of each line is increased or reduced by a small amount depending on whether the data rate achieved in the inner stage is below or much above the corresponding target data rate of the line. It is concluded in [YGC02] that the iterative process converges from any initial spectrum to a unique point in DSL lines.

To implement the iterative water-filling algorithm, each user must know its target data rate a priori. Therefore, a centralized agent is needed to determine the set of achievable target rates. This shall be done in the loop planning stage.

9.1.2 Optimal spectrum balancing (OSB)

In a cable binder with different length cables, long lines are typically experience large attenuation at high frequencies and they are only active on low frequencies. In contrast, short lines experience relatively flat attenuation with frequency. So it might be wise to switch off the low frequency subcarriers of the short lines and transmit only in high frequencies, which are not used by the long lines. In such case, short lines can still achieve good data rate and meanwhile, the crosstalk interference from short lines to long lines is reduced.

However, the above-addressed iterative water-filling algorithm can not follow this approach as short lines experiencing low crosstalk interference are always assigned relatively flat transmission PSDs and the low frequencies are not switched off. This leads to poor performance of the long lines.

Additionally, although the iterative water-filling algorithm converges to a unique point, it does not guarantee any optimality. The multiple-lines DSL channel without signal level coordination is an example of an interference channel in multiuser information theory. To achieve the boundary of the capacity region for the interference channel is a long-standing problem in multiuser information theory. Restricting to two user case, the problem can be defined as

$$\max_{P_{k,1}, P_{k,2}} \{R_2\}, \quad (9.12)$$

$$\text{subject to } R_1 \leq R_1^{\text{target}}, \quad (9.13)$$

$$\text{and } \sum_{k=0}^{K-1} P_{k,i} \leq P_i, \quad i = 1, 2. \quad (9.14)$$

An extension to more than two users follows naturally. The rate region is a plot of all possible operating points or rate combinations that can be obtained in a multiuser channel.

The main difficulty for the optimal design is the computational complexity associated with the optimization problem. An exhaustive search leads to a complexity exponentially increasing with the number of subcarriers K and the number of users in the systems. In a discrete bit loading case, maximum $b_{\max} = 15$ bits can be loaded on each subcarrier. I.e., there are $b_{\max} + 1$ possibilities of bit loading per subcarrier, corresponding to $b_{\max} + 1$ possibilities of power distributions on each subcarrier. The resulting complexity is $\mathcal{O}((b_{\max} + 1)^{MK})$. This leads to a computationally intractable problem.

A method, the so-called optimal spectrum balancing (OSB) which is optimum within the current capacities of DSL modems in a synchronized DMT system is proposed in [CYM⁺06], [YLC04] and [YL06]. It is shown in [CYM⁺06] that solving the original optimization problem of (9.12) with the rate and power constraints of (9.13) and (9.14) is equivalent to maximize the weighted rate sum under the power constraint (9.14):

$$\max_{P_{k,1}, P_{k,2}} \{ \omega R_1 + (1 - \omega) R_2 \}, \quad \omega \in [0, 1]. \quad (9.15)$$

The power constraint (9.14) can be incorporated into the weighted rate-sum optimization by defining the Lagrangian

$$L \triangleq \omega R_1 + (1 - \omega) R_2 - \lambda_1 \sum_k P_{k,1} - \lambda_2 \sum_k P_{k,2}, \quad (9.16)$$

where λ_i is the Lagrangian multiplier for line i which is chosen such that either the power constraint on line i is tight ($\sum_k P_{k,i} = P_i$) or $\lambda_i = 0$. Accordingly, the constrained optimization can be solved by the unconstrained optimization

$$\max_{P_{k,1}, P_{k,2}} \left\{ L(\omega, \lambda_1, \lambda_2, P_{k,1}, P_{k,2}) \right\}. \quad (9.17)$$

Using a technique called dual decomposition [YLC04] the exponential complexity in the number of subcarriers K can be reduced. Defining the Lagrangian on each subcarrier k as

$$L_k \triangleq \omega b_{k,1} + (1 - \omega) b_{k,2} - \lambda_1 P_{k,1}(b_{k,1}, b_{k,2}) - \lambda_2 P_{k,2}(b_{k,1}, b_{k,2}), \quad (9.18)$$

the Lagrangian (9.16) can be decomposed into a sum across subcarriers of L_k :

$$L = \sum_k L_k. \quad (9.19)$$

Thus, the overall optimization can be split into K per-subcarrier optimizations that are coupled only through ω , λ_1 and λ_2 and can be solved by exhaustive M -dimensional search on each subcarrier. This will lead to a linear, rather than exponential, complexity in K and a computationally tractable search.

For the implementation of the OSB technique, three loops are needed: an outer loop that varies ω , an intermediate loop that searches for λ_1 , and an inner loop that searches for λ_2 . The bisection method can be used in each loop of searching. The OSB technique can be extended to more than two users' case in a straightforward way.

9.2 Sequential power allocation (SPA)

The OSB technique overcomes the exponential complexity in the number of subcarriers K through the use of dual decomposition. However, the computational complexity associated with the overall optimization, although linear in K , is still exponential in the number of lines M . Here, we propose a sequential power allocation (SPA) method as a heuristic method to further reduce the computation complexity.

As its name indicates, a sequential procedure is applied in the method. The idea of the sequential power allocation is starting with the line having the best channel condition, to perform the data rate maximization of this line and then to reduce its target data rate while maximizing the data rate of the line with the second best channel condition. The procedure continues sequentially until the line with the second worst channel condition obtains its target data rate and the line with the worst channel condition achieves the maximum data rate it can get under the power distribution condition of all other lines.

As an example, Figure 9.1 illustrates this idea. Assuming lines 1 to 3 are sequenced according to their channel condition and starting with line 1 having the best channel condition, its data rate can be maximized:

$$\max_{P_{k,1}} \{R_1\}, \text{ subject to } \sum_k P_{k,1} \leq P_1. \quad (9.20)$$

As shown in the figure, the point $(R_1^{\max}, 0, 0)$ is achieved.

Then, considering the target data rate R_1^{target} of line 1, the data rate of line 2 having the second best channel condition can be maximized while reducing the maximum data rate R_1^{\max} of line 1 to its target data rate R_1^{target} :

$$\max_{P_{k,2}} \{R_2\}, \quad (9.21)$$

$$\text{subject to } \Delta R_1 = R_1^{\max} - R_1^{\text{target}}, \quad (9.22)$$

$$\text{and } \sum_k P_{k,2} \leq P_2. \quad (9.23)$$

Accordingly, the point $(R_1^{\text{target}}, R_2^{\max}, 0)$ is achieved.

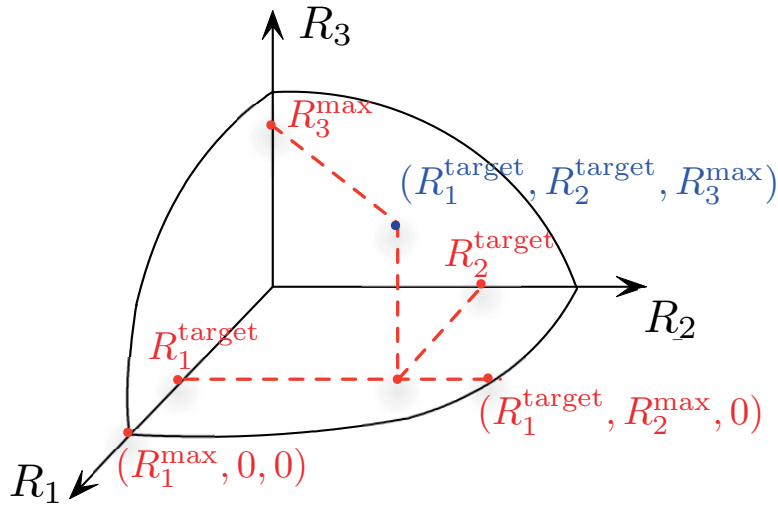


Figure 9.1: Data rate regions in the upstream VDSL2 system with 2 cable lines

Fixing the power distribution of line 1, the data rate of line 3 can be maximized while reducing the maximum data rate R_2^{\max} of line 2 to its target data rate R_2^{target} , similar as the maximization of the data rate of line 2.

Assuming lines 1 to M are sequenced according to their channel condition, the sequential power allocation algorithm can be described as two steps:

1) The step of the initialization as defined in (9.20).

Defining the Lagrangian to incorporate the power constraint

$$L_1 \triangleq R_1 - \lambda_1 \sum_k P_{k,1}, \quad (9.24)$$

it is to solve the unconstrained optimization

$$\max_{P_{k,1}} \left\{ L_1(\lambda_1, P_{k,1}) \right\}. \quad (9.25)$$

Similar as in the OSB technique, the dual decomposition technique can also be applied here to reduce the exponential complexity in the number of subcarriers K :

$$L_{k,1} \triangleq b_{k,1} - \lambda_1 P_{k,1}. \quad (9.26)$$

Thus, 1-dimensional exhaustive search is applied in each subcarrier.

2) The step of allocating power for line $i, i = 2, 3, \dots, M$ sequentially while reducing the maximum data rate R_{i-1}^{\max} of line $i - 1$ to its target data rate R_{i-1}^{target} :

$$\max_{P_{k,i}} \{R_i\}, \quad (9.27)$$

$$\text{subject to } \Delta R_{i-1} = R_{i-1}^{\max} - R_{i-1}^{\text{target}}, \quad (9.28)$$

$$\text{and } \sum_k P_{k,i} \leq P_i. \quad (9.29)$$

Similar as in step 1), the Lagrangian for the optimization of line i as well as dual decomposition can be applied, and the Lagrangian on each subcarrier k can be defined as

$$L_{k,i} \triangleq b_{k,i} - \lambda_i P_{k,i}. \quad (9.30)$$

So, if considering the objective (9.27) and the power constraint (9.29) only, it is to maximize $L_{k,i}$ on each subcarrier k for each line i :

$$\max_{P_{k,i}} \{L_{k,i}(\lambda_i, P_{k,i})\}. \quad (9.31)$$

When further taking the rate constraint (9.28) into account, we can define a value of efficiency:

$$v_{k,i} = \Delta b_{k,i} - \lambda_i \Delta P_{k,i}, \quad (9.32)$$

where the penalty $\Delta P_{k,i}$ is the additional power allocation of line i on subcarrier k and the gain $\Delta b_{k,i}$ is the bit increase of line i on subcarrier k due to its power increase $\Delta P_{k,i}$.

For a certain λ_i of line i , the maximum value $v_{k,i}^{\max}$ on each subcarrier k is calculated and the corresponding bit reduction of line $i - 1$ is denoted as $\Delta b_{k,i-1}$. For each line i , we sequentially find out the subcarrier with the biggest value $v_{k,i}^{\max}$ among all subcarriers and allocate the corresponding power on the subcarrier until the maximum data rate R_{i-1}^{\max} of $i - 1$ is reduced to its target data rate R_{i-1}^{target} : $\sum_k f_s \Delta b_{k,i-1} = \Delta R_{i-1}$.

In this step, 2-dimensional search on each tone for each line is performed. Therefore, the M -dimensional search in the OSB technique is simplified in the sequential power allocation. Considering the complexity of the bisection search, in the sequential power allocation, $\log_2(1/\epsilon_\lambda)$ iterations is required for each line, where ϵ_λ is an accuracy required by all λ_i and typically set as 10^{-10} . This results in a computation complexity

$$V_{\text{SPA}} = \mathcal{O}(KM(b_{\max} + 1)^2 \cdot 33)$$

for the method of sequential power allocation. In contrast, in the OSB method, as bisection is done on λ_1 to λ_M such that the power constraints on all M users become tight, the resulting computation complexity is

$$V_{\text{OSB}} = \mathcal{O}(KM(b_{\max} + 1)^M 33^M),$$

9.3. SYSTEM PERFORMANCE WITH SEQUENTIAL POWER ALLOCATION

which is much higher than the proposed sequential power allocation method.

The proposed sequential power allocation method can also be easily combined with partial crosstalk cancellation schemes. During the sequential power allocation procedure, whenever the maximum data rate R_i^{\max} of line i is smaller than the target data rate R_i^{target} of line i , partial crosstalk cancellation for line i can be additionally applied to eliminate the crosstalk interference coming from lines 1 to $i - 1$ without affecting the power allocation of those lines. In this case, the sequential power allocation procedure can be started over from line i and further process line $i + 1$, and so on.

9.3 System performance with sequential power allocation

In this section system performance with sequential power allocation is presented. We consider the upstream transmission scenario with different cable lengths as shown in Figure 5.5b. The system parameters are chosen as in Table 5.2 except the transmitter PSD. The mask of the transmit PSD is not applied and the 998 FDD bandplan is used. The maximum transmit power for each line is given as 11.5dBm.

We first consider a very simple scenario with only 2 cable lines, where both of the proposed sequential power allocation scheme and the optimal spectrum balancing technique can be applied, and show the comparison of their achievable data rate region. Then, more cable lines in the binder are considered in the sequential power allocation scheme and the results for different sets of target data rates are shown in comparison with the case that no power allocation is applied. In the end, the results achieved by the sequential power allocation scheme in combination with the partial crosstalk cancellation schemes is presented.

a) 2-line scenario

In the first scenario, a short line of 0.6 km and a long line of 1.2 km are considered. The rate region obtained by the sequential power allocation scheme is plotted in Figures 9.2 in comparison with that of the optimal spectrum balancing. Furthermore, the data rates achieved with/without crosstalk cancellation in the system having flat transmission PSD over all subcarriers are also shown in the figures.

It can be observed that the performance achieved by the sequential power allocation scheme is quite close to that of optimal spectral balancing. In particular, in the lower data rate range of the short line, the achievable data rate of the long line are identical for

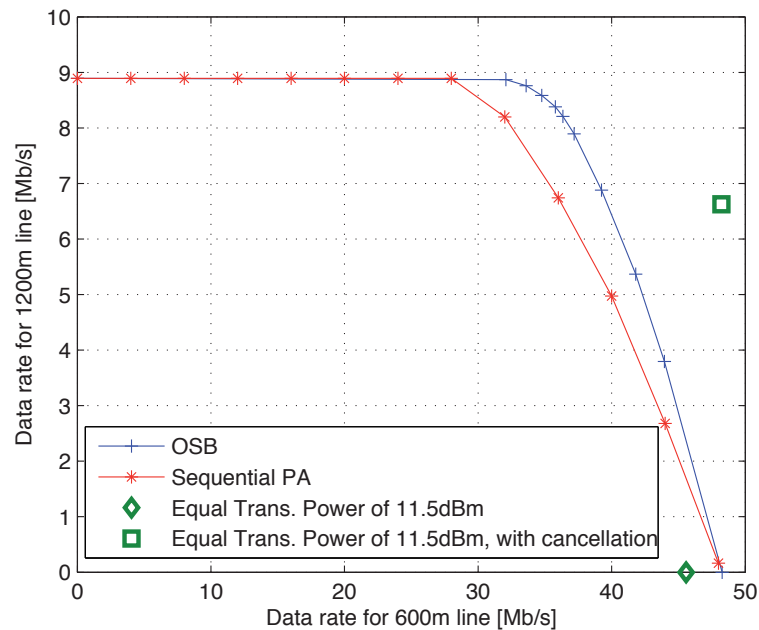


Figure 9.2: Data rate regions in the upstream VDSL2 system with 2 cable lines

both schemes. In the relatively high data rate range of the short line, there exists a small performance gap between the low complexity scheme and the optimal one. Nevertheless, the maximal data rate loss of the long line in the sequential power allocation scheme is less than 25%.

For the detailed analysis of the two schemes, the PSDs of two cable lines corresponding to a rate of 36Mbps transmitted on the short line are depicted in Figures 9.3 and 9.4 for the optimal spectrum balancing and sequential power allocation, respectively.

In Figures 9.3 the PSDs of both cable lines obtained by optimal spectrum balancing are shown. In the high frequency band, the long line is switched off as the attenuation of the long line is very high and the crosstalk interference from short line to the long line is also high. In such case, the transmit PSDs of the short line in the low frequency band are significant reduced so as to also reduce the interference to the long line.

As shown in Figure 9.4, the transmit PSDs of the two cable lines obtained by sequential power allocation behave in a similar way. The short line's transmit PSDs are also reduced to a very low level at the place where the long line is transmitting. However, it can be observed that the low frequency band is not completely assigned to the long cable line in sequential power allocation scheme. The algorithm tends to further increase the power

9.3. SYSTEM PERFORMANCE WITH SEQUENTIAL POWER ALLOCATION

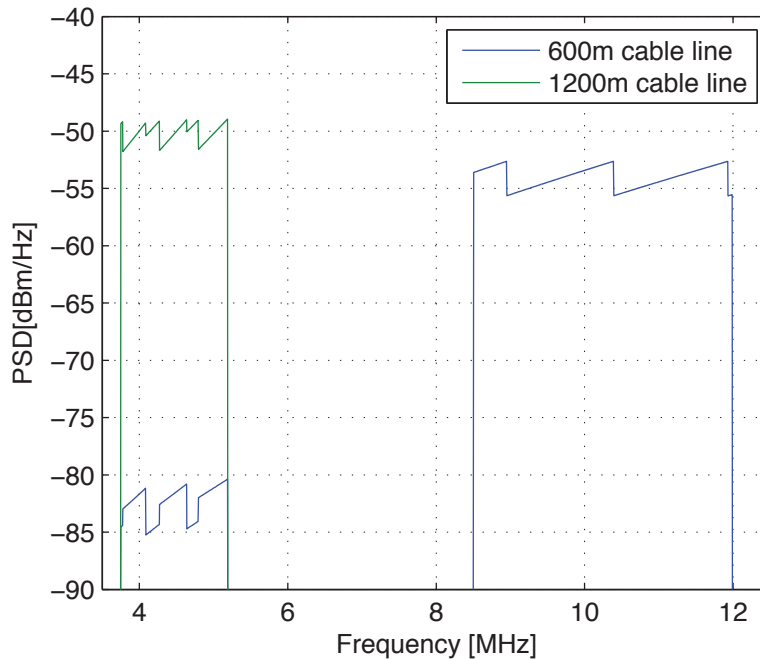


Figure 9.3: Optimal spectrum balancing PSDs

level of the long line at lower frequencies rather than assigning higher frequencies where the cable line has larger attenuation.

b) *scenario with more cable lines*

In this scenario we consider a cable binder with more lines having different cable lengths. The cable lines range from 0.6 km to 1.2 km with 0.1 km increase, indexed from 1 to 7. Two sets of target data rates are considered as shown in Figures 9.5 and 9.6 .

It can be seen in the figures that without applying transmit power allocation, the shortest line obtains extremely high data rate whereas the longer lines, e.g. lines 5 - 7 can hardly maintain their transmission.

The first set of target data rates as shown in Figure 9.5 is set to maintain relatively high transmit rates for shorter lines and meanwhile enable the transmission of the longer lines. The second set of target data rates shown in Figure 9.6 reduces the transmit rate of the shortest line to a moderate level and providing the longer lines considerable transmit rates in view of their channel conditions. It can be seen that after applying sequential power allocation among the cable binder, in both cases, the achieved data rates of all ca-

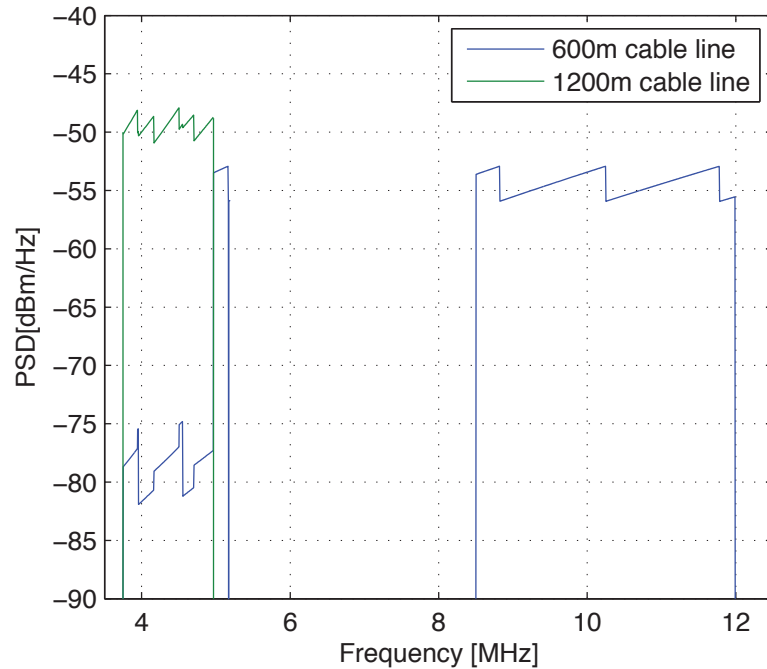


Figure 9.4: Sequential power allocation PSDs

ble lines are shaped according to the targets. Furthermore, the line 7 having the worst channel condition can also obtain a relatively high data rate.

c) scenario with QoS-based partial crosstalk cancellation applied

In this scenario, we still consider the cable binder with 7 lines ranging from 0.6 km to 1.2 km with 0.1 km increase. Sequential power allocation is applied in combination with the QoS-based partial crosstalk cancellation scheme. The achievable data rates are presented in Figure 9.7 in comparison with the data rates obtained by partial crosstalk cancellation with equal transmit power for each lines. The data rates obtained in the case without crosstalk cancellation and power allocation is also plotted as reference.

To achieve the given target data rates as shown in Figure 9.7, QoS-based partial crosstalk cancellation is first applied. The achieved data rates is shown in the figure with black dash-dot line. The corresponding number of crosstalk interference components q_i cancelled for each cable line is shown in Table 9.1. Indeed, due to the bad channel condition of line 7, it is not possible to achieve its target data rate even if all crosstalk interference has been cancelled out. Moreover, as power allocation is not applied in this case, all subcarriers

9.3. SYSTEM PERFORMANCE WITH SEQUENTIAL POWER ALLOCATION

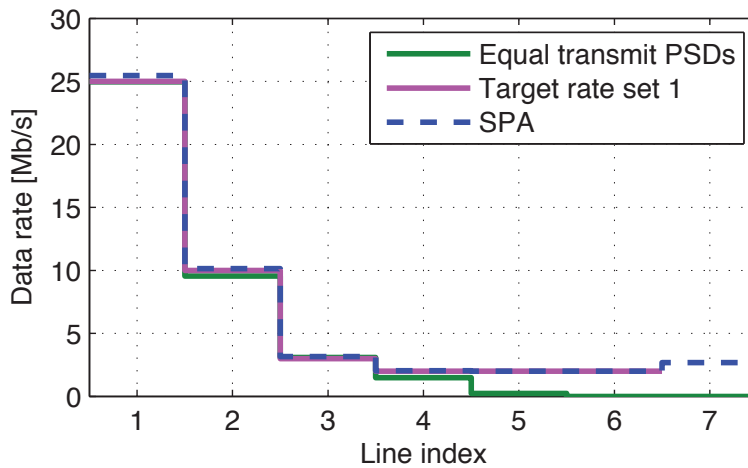


Figure 9.5: Data rates achieved by sequential power allocation with target data rate set 1

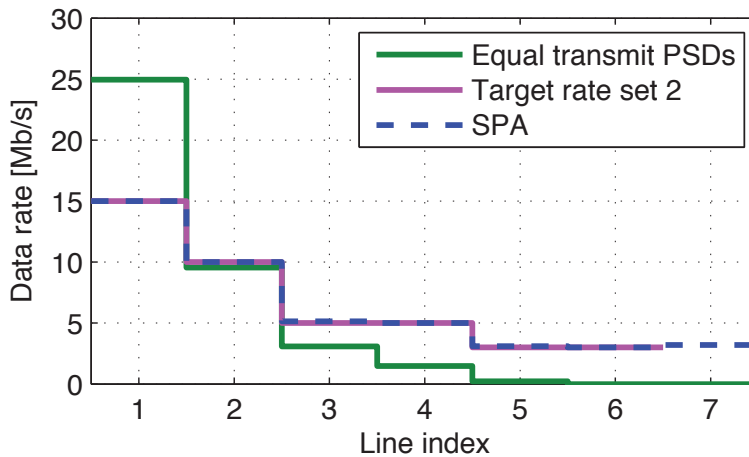


Figure 9.6: Data rates achieved by sequential power allocation with target data rate set 2

are used with the same power for the transmission and crosstalk cancellation need to be applied for all subcarriers, namely 1147 subcarriers in the upstream transmission.

Then, sequential power allocation is applied in combination with the QoS-based partial crosstalk cancellation scheme. The achievable data rates are shown in Figure 9.7 with blue dash line and the corresponding number of crosstalk interference components q_i cancelled for each cable line is shown in Table 9.2.

It can be observed that when the sequential power allocation scheme is applied in addition, the number of crosstalk interference components to be cancelled for longer lines is reduced. This is due to the fact that in sequential power allocation the longer lines stop

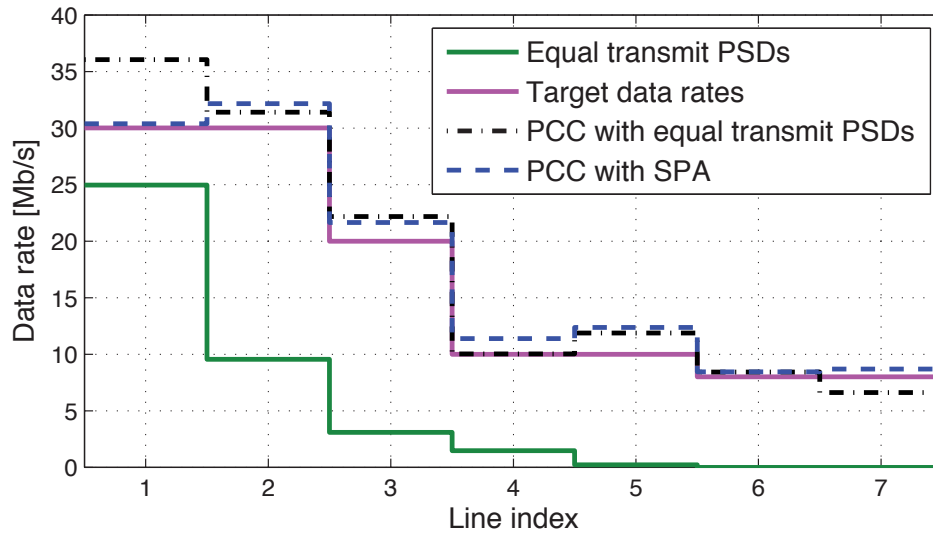


Figure 9.7: Data rates achieved by sequential power allocation with QoS-based PCC

Table 9.1: Crosstalk component number eliminated by the QoS-based partial cancellation without sequential power allocation

Line i	1	2	3	4	5	6	7	$\sum q_i$
q_i	1	2	2	2	4	5	6	
c_i	1147	1147	1147	1147	1147	1147	1147	25234

transmission in the high frequency band where their attenuation is large and the transmit PSDs of shorter lines in the low frequency band are significantly lowered. Accordingly, the crosstalk interference level of the longer lines is reduced.

For shorter lines, as they "sacrifice" their sweet low frequency band to reducing crosstalk interference to longer lines, they need to cancel higher level crosstalk interference at their transmission bands compared with the case that equal transmit PSDs are applied in the partial cancellation scheme.

However, as shown in Table 9.2, the number of subcarriers c_i where crosstalk cancellation need to be applied in each line i is reduced as not all subcarriers are used for the transmission when sequential power allocation is applied. Consequently, the overall number of crosstalk components cancelled in case that the sequential power allocation is applied in addition, is much smaller than applying partial cancellation only.

9.3. SYSTEM PERFORMANCE WITH SEQUENTIAL POWER ALLOCATION

Table 9.2: Crosstalk component number eliminated by the QoS-based partial cancellation with sequential power allocation

Line i	1	2	3	4	5	6	7	Σq_i
q_i	1	2	2	2	4	5	6	
c_i	854	1050	1004	893	635	352	336	16177

In this chapter, power allocation techniques are considered in VDSL2 systems. Starting from the state of the art different power allocation schemes are addressed and then a heuristic method, namely sequential power allocation scheme is developed. The capacity region achieved by the sequential power allocation scheme in case of two cable lines in a cable binder as well as the data rate performance obtained in the binders with more cable lines are presented.

In the proposed sequential power allocation scheme, as its name indicates, power allocation is performed sequentially from the cable line having the best channel condition to the line in the worst channel condition. In each step of the power allocation procedure, the data rate of the considered line is maximized while the data rate of its previous line is reduced to its target data rate. Comparing with the so-called optimal spectrum balancing technique, the proposed sequential power allocation scheme need much less computation complexity and provides a performance with small data rate reduction.

Furthermore, the proposed sequential power allocation scheme can easily be combined with partial cancellation schemes. It is shown that the run-time cancellation effort can be reduced when sequential power allocation is applied in addition to the QoS-based partial cancellation scheme to achieve certain target data rates.

10 Summary

Crosstalk interference is the major performance limitation in modern DSL systems. Instead of accepting it as performance degradation, this thesis focuses on different crosstalk cancellation techniques to deal with such impairment. More specifically, signal level coordination for crosstalk interference cancellation as well as spectral coordination for reducing crosstalk interference in a cable binder is considered.

Assuming that in the CO the transceivers are co-located and perfect CSI is available, zero-forcing base upstream crosstalk cancellation and downstream channel decomposition based precoding are proposed. Simulation results show that for the short cable lines, the achievable data rates can be doubled or even tripled with crosstalk cancellation techniques and for the long cable lines, data rate performance can be significantly improved. In some special cases, data transmission can be enabled by applying cancellation techniques to those lines which suffer so much from crosstalk interference that they can barely transmit anything.

In case that CSI is not available, channel estimation aspects are considered. It is shown that without perfect CSI there exists tens of Mbit/s data rate loss when applying the crosstalk interference cancellation schemes. Data rate performance can be improved with higher channel estimation accuracies. Reducing MSE by a factor of ten in the estimation, data rates approaching the performance of perfect CSI can be achieved with upstream or downstream crosstalk cancellation.

Based on the proposed crosstalk cancellation schemes, the computation complexity issue is further considered in the systems. The line-wise partial crosstalk cancellation schemes for reducing the computation complexity in upstream and downstream crosstalk cancellation are introduced and it is illustrated that with less than 50% of computation complexity spent in full crosstalk cancellation, most cable lines in a binder can achieve the data rate performance close to that of full cancellation. That's to say, a good trade-off can be provided by the partial crosstalk cancellation schemes between the data rate performance and the computation complexity need to be spent for crosstalk cancellation.

On top of the ordinary partial crosstalk cancellation scheme, a QoS-based partial crosstalk cancellation scheme that provides joint signal processing among adjacent cable lines and meanwhile takes different QoS requirements into account are developed and analyzed. It is shown in the simulations that with the developed QoS-based partial crosstalk cancellation scheme, the performance of each user/line can be successfully tailored to fulfill its own requirement. In contrast, about 30% users/lines would not be satisfied if the ordinary partial crosstalk cancellation is applied instead. Moreover, considering the realistic situation that crosstalk interference levels of individual lines may dramatically change due to the transmission status of new or existing interfering lines, a successive cancellation scheme is proposed and shown to successfully predict the effect of the channel changes and further adapt to meet the QoS demands in such dynamic situation.

Last but not least, spectral coordination for crosstalk interference cancellation is investigated. A heuristic method, namely sequential power allocation is developed and compared with the optimal spectrum balancing technique. The sequential power allocation is shown to have much less computation complexity and provide a performance with relative small data rate reduction. It is also shown that the proposed sequential power allocation scheme can be easily combined with the partial crosstalk cancellation schemes, thereby reducing the run-time computation complexity in the crosstalk cancellation procedure.

It can be concluded that for modern DSL systems, there will be great advantages to perform joint signal processing to eliminate crosstalk interference among adjacent lines in a cable binder. Computation complexity can be dramatically saved in the crosstalk cancellation procedure by partially cancelling the dominant crosstalk interference components and achieve a good trade-off between system performance and complexity. Furthermore, benefitting from the proposed QoS-aware crosstalk cancellation scheme, the computation complexity of crosstalk cancellation can also be spent according to the QoS demands of the users or lines. Additionally, the low complexity sequential power allocation scheme can be further applied in future systems for reducing crosstalk interference.



Bibliography

- [Ala98] S.M. Alamouti. A simple transmit diversity technique for wireless communications. *Selected Areas in Communications, IEEE Journal*, 16(8):1451–1458, 1998.
- [BFH⁺98] R. Burow, K. Fazel, P. Hoher, O. Klank, H. Kussmanna, P. Pogrzeba, P. Robertson, and M. Ruf. On the performance of the DVB-T system in mobile environments. In *Multimedia Applications, Services and Techniques - ECMAST'98*, pages 467–480. Springer, 1998.
- [Bin00] J.A.C. Bingham. *ADSL, VDSL, and Multicarrier Modulation*. John Wiley & Sons, Inc. New York, NY, USA, 2000.
- [CA00] X. Cai and A.N. Akansu. A subspace method for blind channel identification in OFDM systems. In *Communications, 2000. ICC 2000. 2000 IEEE International Conference*, volume 2, pages 929–933. IEEE, 2000.
- [Cam98] J. Campello. Optimal discrete bit loading for multicarrier modulation systems. In *Information Theory, 1998. Proceedings. 1998 IEEE International Symposium*, page 193. IEEE, 1998.
- [CCB95] P.S. Chow, J.M. Cioffi, and J.A.C. Bingham. A practical discrete multitone transceiver loading algorithm for data transmission over spectrally shaped channels. *Communications, IEEE Transactions*, 43(234):773–775, 1995.
- [CEPB02a] S. Coleri, M. Ergen, A. Puri, and A. Bahai. Channel estimation techniques based on pilot arrangement in OFDM systems. *Broadcasting, IEEE Transactions*, 48(3):223–229, 2002.
- [CEPB02b] S. Colieri, M. Ergen, A. Puri, and A. Bahai. A study of channel estimation in ofdm systems. In *Vehicular Technology Conference, 2002. Proceedings. VTC 2002-Fall. 2002 IEEE 56th*, volume 2, pages 894–898. IEEE, 2002.

- [CGM⁺03] R. Cendrillon, G. Ginis, M. Moonen, K. Van Acker, T. Bostoen, and P. Vandaele. Partial crosstalk cancellation exploiting line and tone selection in upstream VDSL. In *Baiona Workshop on Signal Processing in Communications*, 2003.
- [Cio91] J.M. Cioffi. A multicarrier primer. *ANSI T1E1*, 4:91–157, 1991.
- [CKB⁺99] J.W. Cook, R.H. Kirkby, M.G. Booth, K.T. Foster, D.E.A. Clarke, and G. Young. The noise and crosstalk environment for ADSL and VDSL systems. *Communications Magazine, IEEE*, 37(5):73–78, 1999.
- [CL04] J.I.W. Cho and Y.H. Lee. Design of the optimum pilot pattern for channel estimation in OFDM systems. In *Global Telecommunications Conference, 2004. GLOBECOM'04. IEEE*, volume 6, pages 3661–3665. IEEE, 2004.
- [CMV⁺04] R. Cendrillon, M. Moonen, J. Verlinden, T. Bostoen, and G. Ginis. Improved linear crosstalk precompensation for DSL. In *Acoustics, Speech, and Signal Processing, 2004. Proceedings. (ICASSP'04). IEEE International Conference*, volume 4, pages iv–1053–6. IEEE, 2004.
- [CTW⁺91] T.M. Cover, J.A. Thomas, J. Wiley, et al. *Elements of Information Theory*, volume 6. Wiley Online Library, 1991.
- [CYM⁺06] R. Cendrillon, W. Yu, M. Moonen, J. Verlinden, and T. Bostoen. Optimal multiuser spectrum balancing for digital subscriber lines. *Communications, IEEE Transactions*, 54(5):922–933, 2006.
- [DP02] H. Dai and V. Poor. Turbo multiuser detection for coded DMT VDSL systems. *Selected Areas in Communications, IEEE Journal*, 20(2):351–362, 2002.
- [DRR10] M. Dünge, Y. Ruan, and H. Rohling. Crosstalk Cancellation in VDSL Systems. In *Proc. 18th European Signal Processing Conference (EUSIPCO-2010)*, 2010.
- [Dwo79] L.N. Dworsky. *Modern Transmission Line Theory and Applications*, volume 260. Wiley, 1979.
- [ETS03] ETSI. Transmission and Multiplexing (TM); Access transmission systems on metallic access cables; Very high speed Digital Subscriber Line (VDSL); Part 1: Functional requirements. *ETSI TS 101 270-1 v1.3.1*, 2003.
- [FYL07] C.H.F. Fung, W. Yu, and T.J. Lim. Precoding for the multiantenna downlink:



Bibliography

- Multiuser SNR gap and optimal user ordering. *Communications, IEEE Transactions*, 55(1):188–197, 2007.
- [Gal68] R.G. Gallager. *Information Theory and Reliable Communication*, volume 15. Wiley, 1968.
- [GC02] G. Ginis and J.M. Cioffi. Vectored transmission for digital subscriber line systems. *Selected Areas in Communications, IEEE Journal*, 20(5):1085–1104, 2002.
- [GDJ06] P. Golden, H. Dedieu, and K. Jacobsen. *Fundamentals of DSL technology*. CRC Press, 2006.
- [HCS92] M.L. Honig, P. Crespo, and K. Steiglitz. Suppression of near- and far-end crosstalk by linear pre- and post-filtering. *Selected Areas in Communications, IEEE Journal*, 10(3):614–629, 1992.
- [HW98] M.H. Hsieh and C.H. Wei. Channel estimation for OFDM systems based on comb-type pilot arrangement in frequency selective fading channels. *Consumer Electronics, IEEE Transactions*, 44(1):217–225, 1998.
- [ITU] ITU. Very high speed digital subscriber line transceivers 2 (VDSL2) Amendment. *ITU-T Recommendation G.993.2 (2006) Amendment 1*.
- [LCJS98] Y. Li, L.J. Cimini Jr, and N.R. Sollenberger. Robust channel estimation for ofdm systems with rapid dispersive fading channels. *Communications, IEEE Transactions*, 46(7):902–915, 1998.
- [MB00] H. Minn and V.K. Bhargava. An investigation into time-domain approach for ofdm channel estimation. *Broadcasting, IEEE Transactions*, 46(4):240–248, 2000.
- [Nor03] T. Nordstrom. ftw. Cable Measurements. Technical Report FTW-TR-2003-002, Forschungszentrum Telekommunikation Wien (FTW), Austria, February 24, 2003.
- [Pro00] J.G. Proakis. *Digital Communications*. McGraw-Hill Science/Engineering/Math, 2000.

- [RDR08] Y. Ruan, M. Düngen, and H. Rohling. Crosstalk cancellation in VDSL2 systems. In *Proceedings of the 13th International OFDM Workshop (InOWo)*, Hamburg, Germany, August 2008.
- [RDR09] Y. Ruan, M. Düngen, and H. Rohling. QoS-based partial crosstalk cancellation in upstream VDSL systems. In *Proceedings of the 14th International OFDM Workshop (InOWo)*, Hamburg, Germany, September 2009.
- [RDR11] Y. Ruan, M. Düngen, and H. Rohling. Successive crosstalk cancellation facing the dynamic situation in very-high-speed digital subscriber line 2 systems. *Communications, IET*, 5(11):1491–1496, 2011.
- [RGR⁺03] J. Ran, R. Grunheid, H. Rohling, E. Bolinth, and R. Kern. Decision-directed channel estimation method for ofdm systems with high velocities. In *Vehicle Technology Conference, 2003. VTC 2003-Spring. The 57th IEEE Semianual*, volume 4, pages 2358–2361. IEEE, 2003.
- [Roh11] H. Rohling. *OFDM: Concepts for Future Communication Systems*. Springer, 2011.
- [Rua08] Y. Ruan. Partial crosstalk cancellation in VDSL2 systems. Technical Report, Department of Telecommunications, Hamburg University of Technology, October, 2008.
- [SCS99] T. Starr, J.M. Cioffi, and P.J. Silverman. *Understanding Digital Subscriber Line Technology*. Prentice Hall, 1999.
- [Sha48] C.E. Shannon. A mathematical theory of communication. *The Bell System Technical Journal*, 27, 1948.
- [SSCS03] T. Starr, M. Sorbara, J.M. Cioffi, and P.J. Silverman. *DSL Advanced*. Prentice Hall, 2003.
- [Tel99] E. Telatar. Capacity of multi-antenna Gaussian channels. *European transactions on telecommunications*, 10(6):585–595, 1999.
- [TH00] G. Taubock and W. Henkel. MIMO systems in the subscriber-line network. In *Proceedings of the 5th International OFDM Workshop (InOWo)*, pages 18–1, 2000.



Bibliography

- [TJC99] V. Tarokh, H. Jafarkhani, and A.R. Calderbank. Space-time block codes from orthogonal designs. *Information Theory, IEEE Transactions*, 45(5):1456–1467, 1999.
- [TL07] Z. Tang and G. Leus. Pilot schemes for time-varying channel estimation in OFDM systems. In *Signal Processing Advances in Wireless Communications, 2007. SPAWC 2007. IEEE 8th Workshop*, pages 1–5. IEEE, 2007.
- [TSC98] V. Tarokh, N. Seshadri, and A.R. Calderbank. Space-time codes for high data rate wireless communication: Performance criterion and code construction. *Information Theory, IEEE Transactions*, 44(2):744–765, 1998.
- [TV05] D. Tse and P. Viswanath. *Fundamentals of Wireless Communication*. Cambridge University Press, 2005.
- [vdB98] R.F.M. van den Brink. Cable reference models for simulating metallic access networks. Permanent document TM6 (97) 02 revision 3, ETSI, Luleå, Sweden, June 1998.
- [VdBES⁺95] J.J. Van de Beek, O. Edfors, M. Sandell, S.K. Wilson, and P.O. Borjesson. On channel estimation in ofdm systems. In *Vehicular Technology Conference, 1995 IEEE 45th*, volume 2, pages 815–819. IEEE, 1995.
- [Ver08] J. Verlinden. Crosstalk Channel Model: Text Proposal. *Contribution to ATIS NIPP-NAI-2008-010R1, Alcatel-Lucent*, 2008.
- [WFGV98] P.W. Wolniansky, G.J. Foschini, GD Golden, and RA Valenzuela. V-BLAST: An architecture for realizing very high data rates over the rich-scattering wireless channel. In *Signals, Systems, and Electronics, 1998. ISSSE 98. 1998 URSI International Symposium*, pages 295–300. IEEE, 1998.
- [YGC02] W. Yu, G. Ginis, and J.M. Cioffi. Distributed multiuser power control for digital subscriber lines. *Selected Areas in Communications, IEEE Journal*, 20(5):1105–1115, 2002.
- [YL06] W. Yu and R. Lui. Dual methods for nonconvex spectrum optimization of multicarrier systems. *Communications, IEEE Transactions*, 54(7):1310–1322, 2006.
- [YLC04] W. Yu, R. Lui, and R. Cendrillon. Dual optimization methods for multiuser orthogonal frequency division multiplex systems. In *Global Telecommunica-*



Bibliography

- tions Conference, 2004. GLOBECOM'04. IEEE*, volume 1, pages 225–229. IEEE, 2004.
- [ZDS00] X. Zhuang, Z. Ding, and AL Swindlehurst. A statistical subspace method for blind channel identification in OFDM communications. In *Acoustics, Speech, and Signal Processing, 2000. ICASSP'00. Proceedings. 2000 IEEE International Conference*, volume 5, pages 2493–2496. IEEE, 2000.
- [ZJOP03] H. Zamiri-Jafarian, M.J. Omid, and S. Pasupathy. Improved channel estimation using noise reduction for ofdm systems. In *Vehicular Technology Conference, 2003. VTC 2003-Spring. The 57th IEEE Semiannual*, volume 2, pages 1308–1312. IEEE, 2003.



Lebenslauf

Name	Ruan
Vorname	Yajie
Geburtsdatum	21.08.1979
Geburtsort, -land	Nanjing, China
09.1985 - 07.1991	Grundschule in Nanjing, China
09.1991 - 07.1997	Mittelschule in Nanjing, China
09.1997 - 07.2001	Studium der Control Technology & Instrumentation Universität Südostchinas, Nanjing, China Abschluss: Bachelor of Engineering
08.2001 - 07.2003	Wissenschaftliche Mitarbeiterin im Institut für Instrumentenwissenschaft und -technik Universität Südostchinas, Nanjing, China
10.2003 - 11.2005	Studium der Digital Communications Christian-Albrechts-Universität zu Kiel Abschluss: Master of Science
03.2006 - 02.2010	Wissenschaftliche Mitarbeiterin im Institut für Nachrichtentechnik (Prof. Rohling) Technische Universität Hamburg-Harburg
11.2010 - heute	Patentingenieurin bei der Kanzlei Betten & Resch



